NATIONAL TECHNICAL UNIVERSITY OF ATHENS

SCHOOL OF NAVAL ARCHITECTURE AND MARINE ENGINEERING

DIVISION OF MARINE STRUCTURES

LABORATORY FOR FLOATING STRUCTURES AND MOORING SYSTEMS

MASTER THESIS

« HYDRODYNAMIC ANALYSIS OF AN OFFSHORE MULTI-PURPOSE FLOATING STRUCTURE AND EVALUATION OF THE ANNUAL WAVE ENERGY YIELD AT THREE LOCATIONS IN EUROPE »

ANTONIOS K. VAMIADAKIS

08112042

SUPERVISOR PROFESSOR: Prof. Dr.-Ing. S.A. MAVRAKOS

ATHENS, 2018

Acknowledgements

For the completion of this thesis, many people have contributed during the whole period of its preparation.

Due to the above reason, I would like to express my thankfulness to the professor of the School of Naval Architecture and Marine Engineering, Prof. Dr.-Ing. Spyridon A. Mavrakos, for the supervision of my thesis, the trust he has shown to me with the assignment of the present thesis and all the knowledge he has shared with me.

Secondly, I would like to thank Prof. Dr.-Ing. Andres Cura Hochbaum, professor of the Department of Dynamics of Maritime Systems at Technische Universitaet Berlin, as well as his assistant Dipl.-Ing. Jan Löhrmann, for the partial supervision of my thesis during my move in Berlin in the framework of the European Program Erasmus Plus.

Furthermore, I would like to express my gratefulness to Dr.-Eng T. Mazarakos, Post-Doctoral Research Engineer of the Laboratory for Floating Structures and Mooring Systems, who inspired me to choose this specific field for my thesis and continually helped me to understand and conclude the work of my thesis. In addition, he catered to my questions and needs, throughout the whole process of conducting the research.

Moreover, Dr. D. Konispoliatis, Post-Doctoral Researcher of the Laboratory for Floating Structures and Mooring Systems, had an especially important part in the completion of my thesis and I would like to express my gratitude to him as well. Mr. Jason Jonkman, Senior Engineer-Wind Turbine Multi-Physics Engineering Modeling/ Golden, Colorado Laboratories and Offices, National Renewable Energy Laboratory (NREL) also contributed notably enough, by communicating with Dr. Mazarakos and supplying us with useful information.

Concluding, I would like to convey special thanks to my family, for the courage, the support and the help they have showed to me, during the preparation of my thesis, as well as during the entire period of my studies.

Abstract

The present thesis titled “Hydrodynamic analysis of an offshore multi – purpose floating energy platform and evaluation of the annual wave energy yield at three locations in Europe” aims at the calculation of the produced power of an offshore structure, consisting of three oscillating water columns and a floating 10 MW wind turbine (WT) mounted on deck of the floater. Power was calculated for the operation conditions of the configuration at three different locations in Europe; one in the North See and two in the Mediterranean Sea. For the exact calculation of the power, a JONSWAP spectrum was used in combination with an analytical program, named HAMVAB (Hydrodynamic Analysis of Multiple Vertical Axisymmetric Bodies), in Fortran programming environment, which calculates the absorbed Power of a specific configuration. In addition, the bivariate frequency of H_s - T_p at these three locations was taken into consideration for the final calculation of the power per year.

A validation of program HAMVAB was also made. The validation was referring to the numerical results produced by HAMVAB software in the framework of POSEIDON (www.aristeia-poseidon.naval.ntua.gr) program with the corresponding experimental measurements that took place in the Laboratory for Ship and Marine Hydrodynamics in the School of Naval Architecture and Marine Engineering at the National Technical University of Athens. It has to be mentioned that the POSEIDON program was dealt with a multi – purpose floating structure, similar to the one investigated in the present Diploma Thesis, with the difference that it were designed to support a 5MW wind turbine (WT).

Naturally, reference was made to renewable energy sources, offshore structures and their mooring systems, the wave energy converter devices, emphasizing on the oscillating water columns and their historical background. Furthermore, a study on the formulation of the hydrodynamic problem was conducted, considering the configuration, with three oscillating water columns and a floating wind turbine.

Finally there is a presentation of the final results and conclusions, as well as suggestions on further research.

Περίληψη

Η παρούσα διπλωματική εργασία, με τίτλο “Hydrodynamic analysis of an offshore multi – purpose floating energy platform and evaluation of the annual wave energy yield at three locations in Europe” («Υδροδυναμική ανάλυση μιας πλωτής πολύ-χρηστικής υπεράκτιας ενεργειακής πλατφόρμας σύμμικτης εκμετάλλευσης υπεράκτιου αιολικού και κυματικού ενεργειακού δυναμικού και ανάλυση της κυματικής ενεργειακής απόδοσής της σε τρεις περιοχές εγκατάστασής της στην Ευρώπη») στοχεύει στον υπολογισμό της παραγόμενης ενέργειας μιας πλωτής κατασκευής αποτελούμενης από τρεις μηχανισμούς ανάκτησης κυματικής ενέργειας και μια πλωτή ανεμογεννήτρια ισχύος 10MW. Η ενέργεια υπολογίστηκε για λειτουργία της κατασκευής σε τρεις διαφορετικές τοποθεσίες στην Ευρώπη, εκ των οποίων η μία στην Βόρεια Θάλασσα και οι δύο στην Μεσόγειο θάλασσα. Για τον ακριβή υπολογισμό της ενέργειας, χρησιμοποιήθηκε το φάσμα του JONSWAP σε συνδυασμό με το πρόγραμμα HAMVAB (Hydrodynamic Analysis of Multiple Vertical Axisymmetric Bodies) σε προγραμματιστικό περιβάλλον Fortran, που υπολογίζει την απορροφούμενη ενέργεια μιας συγκεκριμένης κατασκευής. Επιπλέον για τον υπολογισμό της τελικής ετήσιας ενέργειας λαμβάνεται υπόψιν η συχνότητα εμφάνισης του κάθε κύματος στις 3 αυτές περιοχές με συγκεκριμένο ύψος κύματος και περίοδο κορυφής.

Στην παρούσα διπλωματική εργασία, έγινε αρχικά επιβεβαίωση των αποτελεσμάτων του προγράμματος HAMVAB που είχε αναπτυχθεί στο Εργαστήριο Πλωτών Κατασκευών και Συστημάτων Αγκύρωσης του ΕΜΠ, μέσω σύγκρισή τους με αντίστοιχα πειραματικά αποτελέσματα που είχαν παραχθεί κατά την εκτέλεση πειραμάτων υπό κλίμακα στα πλαίσια του προγράμματος ΠΟΣΕΙΔΩΝ(www.aristeia-poseidon.naval.ntua.gr) στην Πειραματική Δεξαμενή του Εργαστηρίου Ναυτικής και Θαλάσσιας Υδροδυναμικής της Σχολής Ναυπηγών Μηχανολόγων Μηχανικών του ΕΜΠ. Σημειώνεται ότι στα πλαίσια του προγράμματος ΠΟΣΕΙΔΩΝ μελετήθηκε πλωτή υπεράκτια πολύ-χρηστική πλατφόρμα παρόμοια με αυτή που εξετάζεται στα πλαίσια της παρούσας διπλωματικής εργασίας, με την διαφορά ότι η πλωτή ενεργειακή πλατφόρμα που μελετήθηκε στα πλαίσια του ΠΟΣΕΙΔΩΝ αναφερόταν σε Α/Γ 5MW.

Γίνεται σχετική αναφορά στις ανανεώσιμες πηγές ενέργειας, τις παράκτιες κατασκευές και τα συστήματα αγκύρωσής τους, τους μηχανισμούς ανάκτησης κύματος, με έμφαση στην παλινδρομούσα στήλη νερού και το ιστορικό της μέχρι σήμερα.

Τέλος, παρουσιάζονται τα τελικά αποτελέσματα και συμπεράσματα σχετικά με τη διάταξη αυτή, καθώς και προτάσεις για μελλοντική έρευνα.

Contents

1. Renewable Energy Sources

1.1 Introduction

Due to the continuing incensement in the population of our planet and the increasing demand of energy, people have been forced to search for new ways of energy production in the last few decades. So this need to serve human needs and demands has led countries from all over the world to exploit the sun, the wind and the waves to produce energy from them, the so-called ‘green’ energy.

1.2 Historical background

People used to invent ways of producing energy by exploiting natural resources from the very past years. Exploiting the power of water and air in watermills, windmills and sailing were some of these ways. With the discovery of mineral resources in particular oil fields, the above ways stopped to find application to the high energy demands of industry. In the late decades, the need for a more eco-friendly society has bring back the application and development of renewable energy resources to a very significant degree. In addition, the constant reduction in fossil fuel reserves results in an increase in the cost of using these, which makes renewable energy sources also economically efficient. (www.britannica.com)

Figure 1. Mill Wheel at Path Head Water Mill [www.gatesheadmill.co.uk]

1.3 Types of Renewable Energy

1.3.1 Solar Energy

Solar Energy is called the exploitation of electromagnetic radiation and the emitted heat of the sun. There plenty ways that this energy can be collected. Some of them can be solar water heating or photovoltaic cells (www.altenergy.org).

Figure 2. Solar park at Charanka India, over 210 MW capacity [www.urvishdave.wordpress.com]

1.3.2 Wind Power

This type of energy is related to the movement of the atmosphere due to differences among the temperatures at the Earth's surface. As a result, the kinetic energy from the wind turns into electrical or directly exploitable mechanical energy (www.altenergy.org).

Figure 3. Wind farm in Xinjiang China, produced 22 000 Gwh in 2016 [www.wikipedia.org]

1.3.3 Ocean Energy

This type of energy is divided into three smaller categories (www.altenergy.org):

1. Energy that comes from the waves and their kinematic energy.
2. Energy that comes from the tides. This energy is stored as it goes up and is forced to go through a turbine to produce electricity as it goes down again.
3. Energy that comes from the ocean because of the different temperatures that exists at the different layers of it, using thermal cycles.

Figure 4. Wave energy [www.cmheavyindustries.com]

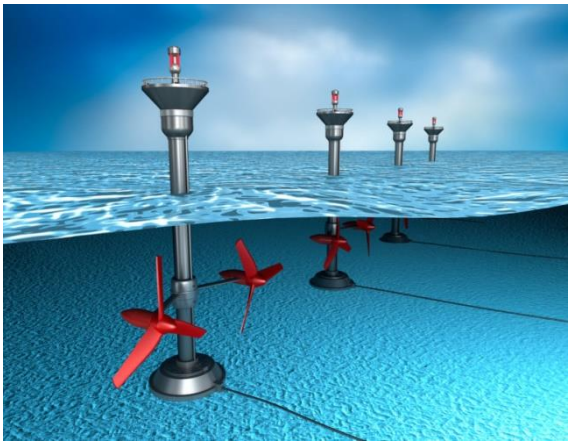

Figure 5. Tidal Energy [www.woodharbinger.com]

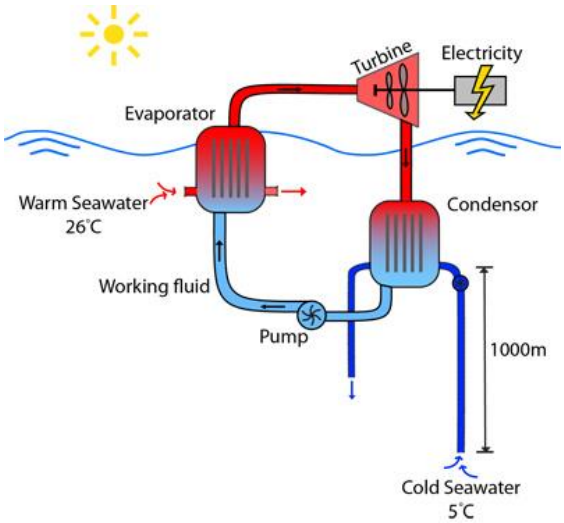

Figure 6. Ocean thermal energy [www.takvera.blogspot.gr]

1.3.4 Biomass

Biomass is the energy that comes from the plants and the carbohydrates they contain. Usually these plants are found in municipal waste and waste from sugar, wood and food industry. All these plants contain energy which was absorbed through photosynthesis and remained at them (www.altenergy.org).

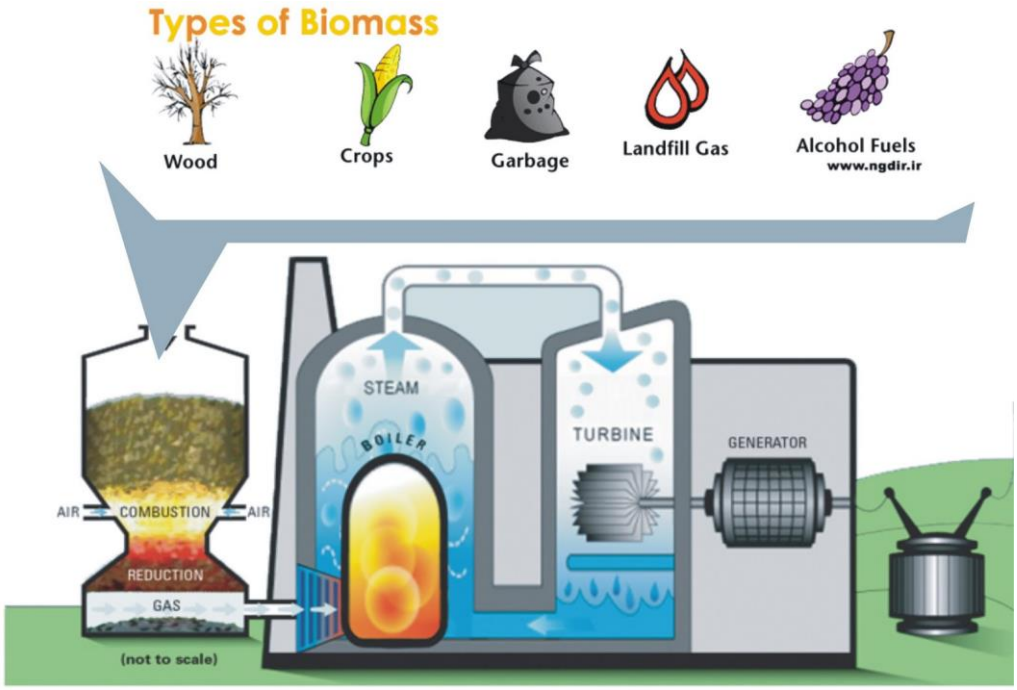

Figure 7. Types of Biomass [www.emaze.com]

1.3.5 Geothermal Power

It is the thermal energy that comes from the interior of the earth. This type of energy is contained in natural vapors, in surface or underground warm waters and hot dry rocks (www.altenergy.org).

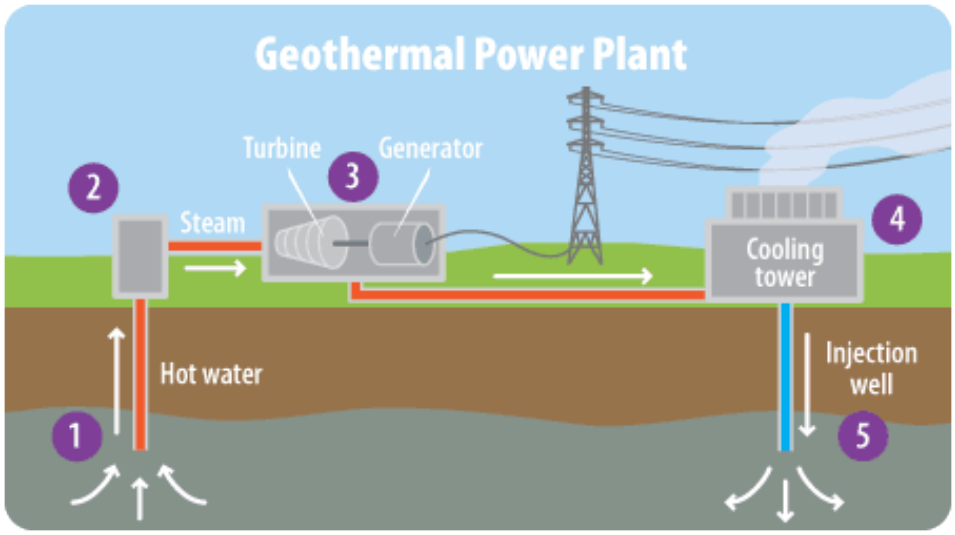

Figure 8. Geothermal Power Plant [www3.epa.gov]

2. Offshore Structures

2.1 Introduction

The development of technology and the need for people to exploit the seas has led recently to the development and installation of a wide range of marine structures and shipbuilding. Efforts in particular to export and exploit hydrocarbons from the marine environment have resulted in the development of Offshore technology. Due to the importance of having reliable and efficient offshore platforms, oil companies have invested a lot of money in the research and development of floating structures. Usually mobile platforms with special drilling systems initially go to a potential hydrocarbon location and if they find sufficient quantity, they remain at the source until a permanent production platform is built. (www.aoghs.org)

2.2 Historical background

The first attempts at offshore drilling for oil happened in America. Off the coast of Summerfield, California, just south of Santa Barbara in 1896 people started to construct a platform using the knowledge and the technics they had from the inshore construction industry, with pounding 150 meters below the seabed. Unfortunately these attempts brought a really bad image of the area with their completion. Dirty coasts full of oil gas, abandoned piers and mining platforms were left there after the offshore drilling was over. Since then the offshore industry has been significantly developed and so far there are really strong offshore platforms in very distant points from the coast, capable of withstanding very bad weather conditions and loads. Despite this development, there is still need for qualified offshore structural personnel, as the oil industry is getting into deeper water in order to find more oil and gas supplies. At the same time technology is emerging for the development of new projects and ideas for offshore platforms. (National Commission on the BP Deepwater Horizon Oil Spill and Offshore Drilling, 2010)

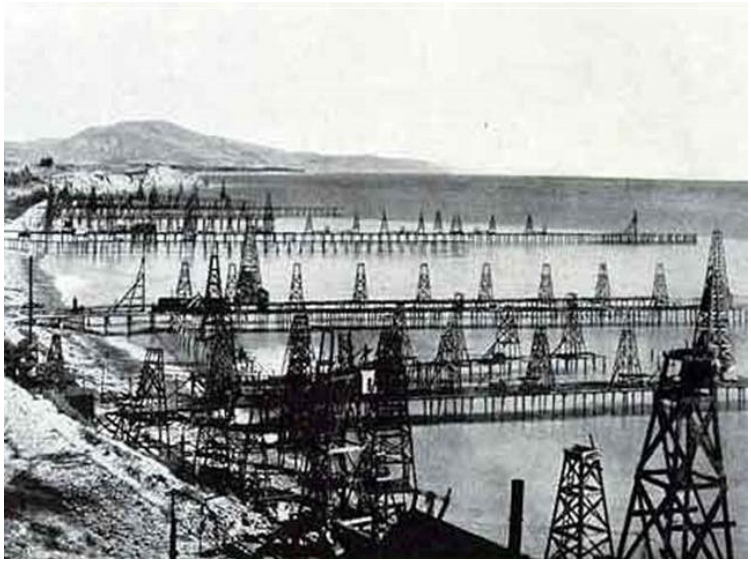

Figure 9. .First submerged oil wells drilled in California [www.aoghs.org]

2.3 Types of Offshore Platforms

Some of the greatest structures that man ever built are the offshore platforms. There are two main categories of offshore platforms:

2.3.1 Floating Platforms

Floating platforms have the ability to move from one place to the other as they float in the free surface. Some examples of these structures are (www.lshipdesign.blogspot.de):

2.3.1.1 Semi-submersible Platforms

The need for a platform with greater freedom of movement in the deeper and more harsh environment of the Gulf of Mexico led Shell Oil to convert a submersible platform to the first semi-submersible platform. This happened in the beginning of 1960s and a few years later ODECO created the first new building semi-submersible platform with the name Ocean Driller. This unit was designed for a depth of approximately 100 m and had the ability to operate also as submersible platform. Their position is maintained by a mooring system. These platforms can move from one location to another by special ships called Heavy Lift ships. (www.lshipdesign.blogspot.de)

Figure 10. Semi-submersible platform in the North Sea [www. wikipedia.org]

2.3.1.2 Spar Platforms

These structures have a large diameter cylindrical deck supporting the main deck. There are three types of Spars:

i. The one-piece cylindrical hull
ii. The Truss Spar with characteristic the midsection that is composed of truss elements connecting the upper hull with the bottom tank using permanent ballast, and
iii. The Cell Spar that is a configuration with multiple vertical cylinders.

The deep draft design of these structures gives them the advantage of withstanding at strong winds and waves. Another characteristic of the vertical cylinder of Spars is that they are surrounded by helical strakes in order to avoid vortex-induced vibrations. (www.strukts.com)

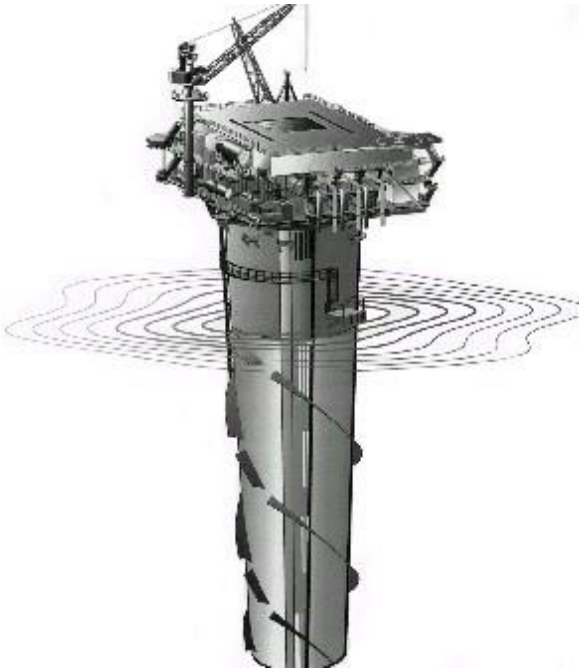

Figure 11. One-piece cylindrical hull Spar Platform [www.marinetalk.com]

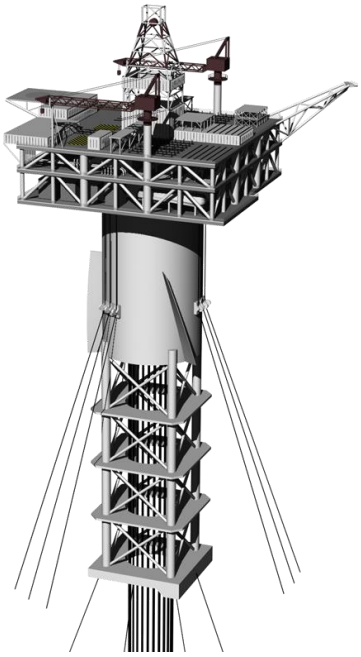

Figure 12. Truss Spar Platform [www.stoprust.com]

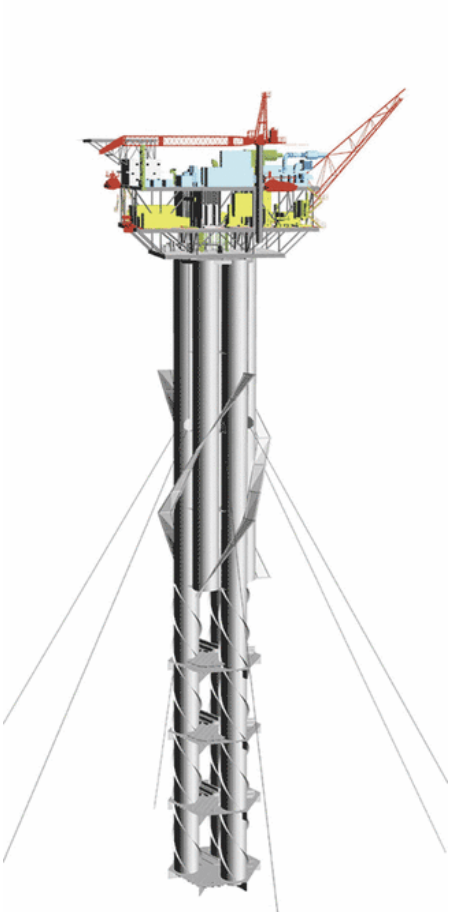

Figure 13. Cell Spar Platform [www.offshore-mag.com]

2.3.1.3 Drill Ships

They are ships with a special installation on them in order to explore and drill of oil and gas resources mainly for scientific exploratory purposes. The first drill ship was designed from Robert F. Bauer in 1955. A usual problem with these vessels is that they are extremely sensitive to waves, resulting in motions like rolling, heaving and pitching, making it difficult to operate. (www.lshipdesign.blogspot.de)

Figure 14. Drill Ship Deepsea Metro 1 [www.northcoastcourier.co.za]

2.3.1.4 FPSOs

The name of this category of structures comes from Floating, Production, Storage and Offloading and they are large ships equipped with a special installation and processing facilities in order for the ship to have the ability to produce, storage and offload oil and other hydrocarbon resources. These ships are moored and sometimes apart from new buildings they come from converted oil tanker ships. It is very usual FPSOs to be buoyed to a vicinal drilling platform. Apart from FPSOs, there are also FSOs (Floating Storage and Offloading) and FSUs (floating storage unit) ships that operate in a similar way. (www.lshipdesign.blogspot.de)

Figure 15. FPSO ship [www.energyindustryonline.com]

2.3.2 Fixed Platforms

Are the type of platforms that are fixed permanently to one place with steel legs anchored onto the seabed. These structures are stronger and more stable than the floating ones, although their installation is irreversible as they cannot be relocated. Some examples of these structures are (www.lshipdesign.blogspot.de):

2.3.2.1 Jacket Platforms

The deck of these platforms is supported by a steel tubular structure called jacket and it has its feet on the seabed. The pipes of the structure have a diameter of between 1 and 2 meters and they can have a penetration of about 100 m as maximum depth (www.lshipdesign.blogspot.de).

Figure 16. Jacket platform at the gulf of Thailand [www.dlubal.com]

2.3.2.2 Gravity Platforms/Concrete Platforms

In the early 1970s, a new type of stationary platforms emerged, gravity platforms. A gravity platform is considered the safest mode of offshore industrial operations. They are based on a submerged solid structure on the sea-bed reducing the risk of problems from bad sea conditions (www.lshipdesign.blogspot.de).

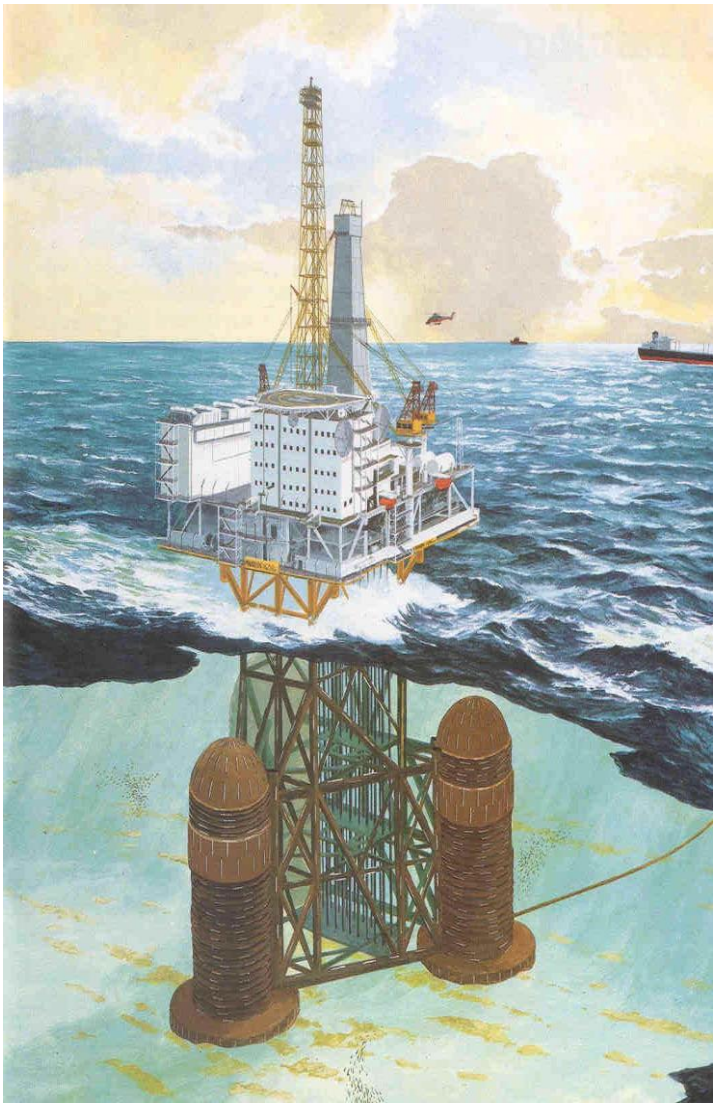

Figure 17.Gravity based Offshore Structure [www.lshipdesign.blogspot.gr]

2.3.2.3 Compliant Towers Platforms

These platforms consist of narrow, flexible towers of 2 to 7 metres in diameter and a piled foundation that is supporting a deck suitable for drilling and production operations. Compliant towers are designed in order to be strong enough for significant lateral deflections and forces. The water depth that they usually operate is between 400 and 900 meters and they can withstand high tides and really difficult sea conditions (www.lshipdesign.blogspot.de).

Figure 18. Compliant Tower [www.writeopinions.com]

2.3.2.4 Jack-up Platforms

As can be easily understood from the name, these platforms have the ability to jack up above the sea. A jack-up platform penetrates its legs, that are made of steel and they are usually three or four, into the sea-bed in order to support deep sea drilling operations. Although, they usually operate in low depth water and they have the ability to move from one location to another and then anchor themselves anytime by deploying the legs that they work like jacks (www.lshipdesign.blogspot.de).

Figure 19. Jack-Up Platform [www.lshipdesign.blogspot.gr]

2.3.2.5 Tension-Leg platforms

These structures use some specialized steel tubes in order to stay afloat and remain in position. These tubes are called tethers or tendons and they work as legs of the floating platform. With these legs the limitation of the vertical movement of the structure is achieved. Tension-Leg platforms can operate for depths up to 1200 meters and they have limited or no storage facility. For the whole installation the equation applies: Tension = Buoyancy – Weight (www.lshipdesign.blogspot.de).

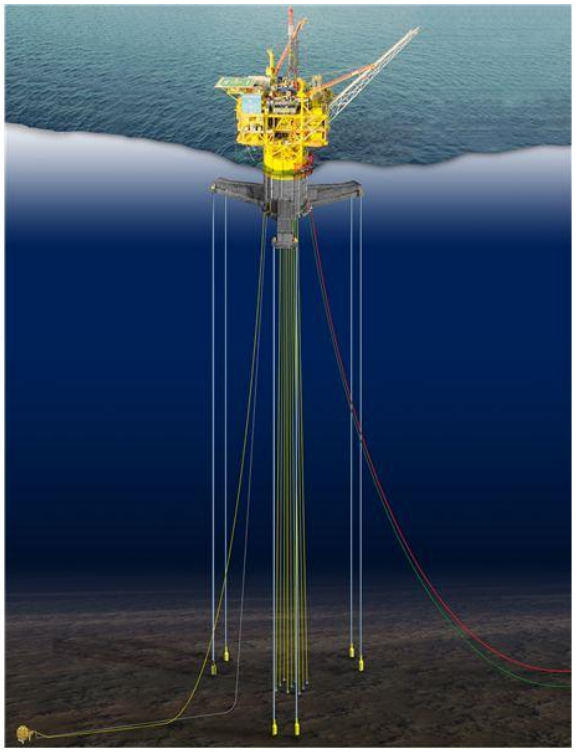

Figure 20. Tension Leg Platform [www.drillingformulas.com]

2.4 Loads of Offshore Structures

For the reliable design and construction of an offshore structure it is necessary to undertake a detailed and analytical study of the environmental conditions prevailing at the site of its installation and operation. There are two big categories of loads, the environmental loads and the functional loads. They can also be divided as following (Mavrakos, 1999):

2.4.1 Environmental Loads

As environmental loads we can assume the following loads (Mavrakos, 1999, DNV, 2011):

2.4.1.1 Wind Loads
At this category belongs all the loads due to the wind at all exposed areas of the structure. (Mavrakos, 1999)

2.4.1.2 Wave Loads
All the loads that are related to the waves, belong to this category. (Mavrakos, 1999)

2.4.1.3 Current Loads
Ocean currents can usually cause drag loads on the structure. In combination with the motion of the waves, dynamic loads are generated. (Mavrakos, 1999)

2.4.1.4 Tidal Loads
These loads come from the tides that exist at the location where the structure is installed. (DNV, 2011)

2.4.1.5 Ice Loads
Ice loads appears in polar regions or cold countries, in cases that ice sheets hit the offshore structure. (DNV, 2011)

2.4.1.6 Mud Loads
Mud flow can occur loads at the structure, if the structure is located in the vicinity of the river mouth.

2.4.1.7 Earthquake Loads
This category of loads can take place at any structure when an earthquake appears close to them, as a result of the waves and the currents that will appear after the end of the earthquake. (Mavrakos, 1999)

2.4.2 Functional Loads

Functional loads can be divided at the following categories (Mavrakos, 1999, DNV, 2011):

2.4.2.1 Dead Loads

Dead loads are defined as all the loads that are relatively constant over time. The weight of the structure itself belongs to this category as well as the immovable fixtures.

2.4.2.2 Fluid Loads

Fluid loads are referring to the weight of the water on the platform, while it is operating.

2.4.2.3 Live Loads

The characteristic of live loads is that they are assumed as movable loads. These loads appears at storage areas and other open areas, such as walkways, helipad etc.

2.4.2.4 Drilling Loads

Drilling loads appear at places where the drill rig is placed. (Mavrakos, 1999)

3. Wave Energy Converter devices

3.1 Introduction

As we already referred, the limited supplies of fossil fuels from nature and the needs in finding new resources of energy, have leaded the research and the market to the renewable energy technology. An important category of these resources are the Wave Energy Converter devices (WEC) which exploit energy from the waves.

3.2 Advantages of Wave Energy Converter devices

- Possible noise pollution is negligible.
- The visual noise is minimal in contrast with other offshore WECs (such as floating wind turbines), so they can be installed and operated closer to the coastline. Because of this, easier maintenance accessibility is achieved and the cost of cable transport to the coast is also lower.
- They have the highest density and power availability per unit area compared to other Renewable Energy Sources. (Drew B. et al., 2009)

3.3 Disadvantages of Wave Energy Converter devices

- The difficulty of storing surplus energy when the market demand is low.
- The conversion of the energy of irregular and low frequency waves to the required constant frequency of electricity.
- The extremely unfavorable conditions to which these devices and their mooring lines are subject due to the waves
- Complexity in designing optimal energy absorption mechanisms due to undefined angles of incident, phases and frequencies of waves. (Drew B. et al., 2009)

3.4 Types of Wave Energy Converter devices

- Point absorbers
- Oscillating Wave Surge Converter
- Overtopping Device
- Attenuator
- Submerged Pressure Differential
- Oscillating Water Column Device

3.4.1 Point absorbers

A floating buoy is connected to a number of components that are located beneath the surface and the energy is derived from the relative motion of the buoy with them. This system is called Point Absorber wave energy converter. (Drew B. et al., 2009)

Figure 21. Point Absorber [www.beachapedia.org]

3.4.2 Oscillating Wave Surge Converter

This term in essence refers to a paddle, rotating around a fixed seabed mounting. As a result of the waves following a surge motion, the paddle is subject to rotation while compressing water, via an onshore hydro power turbine. (Drew B. et al., 2009)

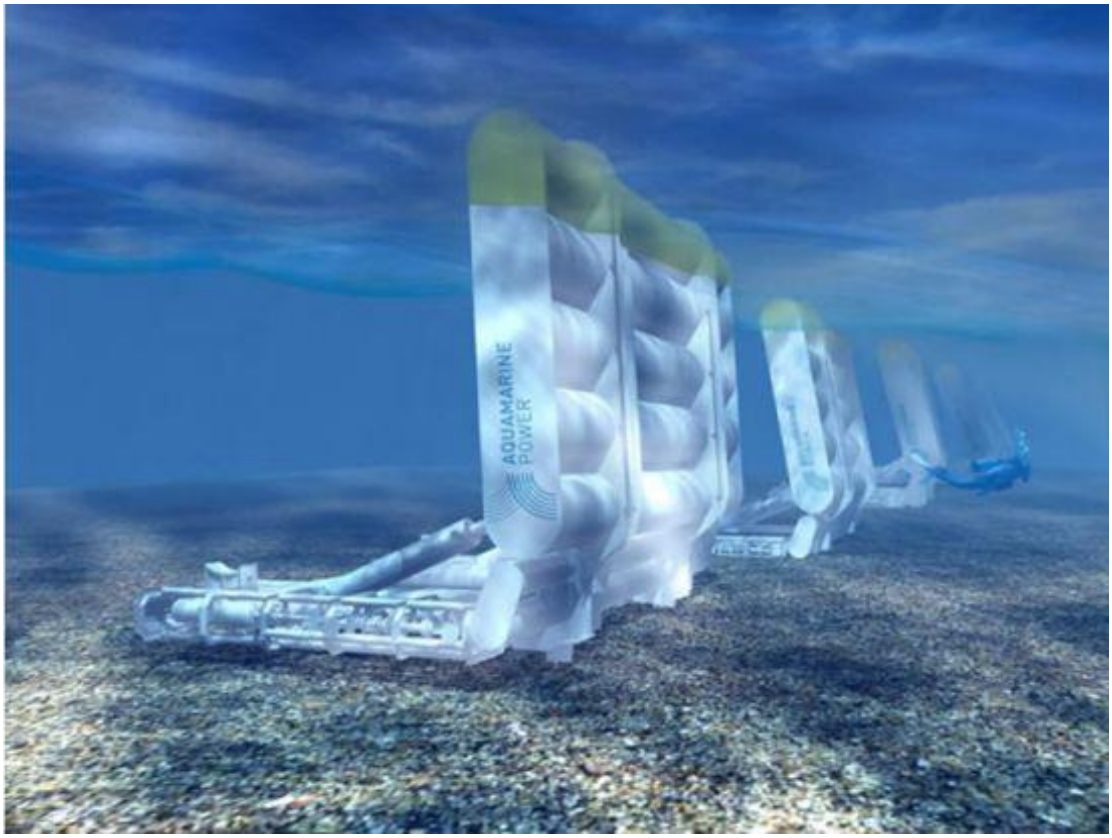

Figure 22. Oscillating Wave Surge Converter [www.drprem.com]

3.4.3 Overtopping Device

Overtopping Device operates according to a principle similar to hydro power. Waves are driven into a raised deposit, to be subsequently returned to the sea, activating the

movement of an installed hydro power turbine located at the bottom of the tank. Thus, electricity is produced. (Drew B. et al., 2009)

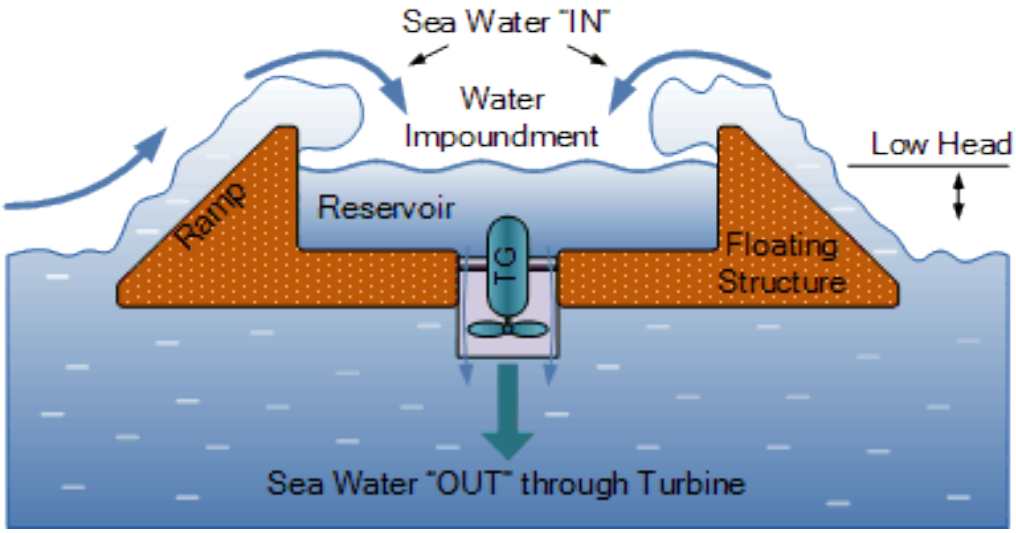

Figure 23. Overtopping Device [www.alternative-energy-tutorials.com]

3.4.4 Attenuator

An attenuator is a device consisting of a series of longitudinal components oriented to the direction of the waves. The joints between the components compress hydraulic oil by means of two pistons that eventually produce power with an electric generator. (Drew B. et al., 2009)

Figure 24. Attenuator [www.coastalenergyandenvironment.web.unc.edu]

3.4.5 Submerged Pressure Differential

This mechanism produces electricity, by taking advantage of the pressure differential, caused by the movement of the waves. Power is produced by the means of a device through which fluid is pumped due to the aforementioned differential. (Drew B. et al., 2009)

Figure 25. Submerged Pressure Differential [www.awsocean.com]

3.5 Oscillating Water Column

The Oscillating Water Column (OWC) concept is probably unique among all the WEC systems and the most promising. A big number of several designs of these devises has been already presented in the literature. The majority of these designs refers to onshore devices. The last years some attempts have been made for the design of free floating or moored devices in the open sea. (Konispoliatis, 2014)

3.5.1 How OWC works

An OWC system is based on two main parts. Chamber is one of these two parts. The function of the chamber is to take power from the motion of the waves and transfer it to the air that already exists inside the chamber. The second main part is a Power Take Off system (PTO), which has the ability to convert the pneumatic power into electricity or other forms. The PTO system is usually a Wells air turbine (Mazarakos et al., 2015) that turns only in one direction, either if the collector is pressurized as the water column goes up or if the collector is decompressed as the water column goes down. Due to this movement of the turbine, a generator is activated to generate electricity, taking advantage of its kinetic energy. The above collector usually is a blow hole in which the air escapes from the chamber. (Mazarakos et al., 2015)

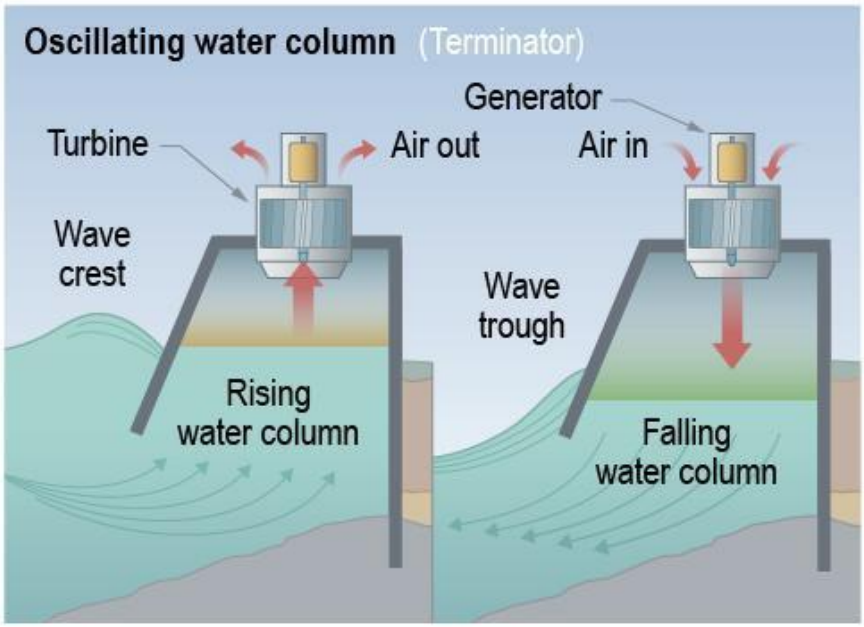

Figure 26. Partially Submerged Oscillating Water Column [www.energy.gov]

3.5.2 History

The first mechanism of OWC was noticed in the nineteenth century, as a device for navigation aid. It used to be a warning device that was whistling. Creator of this device was J. M. Courtney at New York. (Heath, 2012)

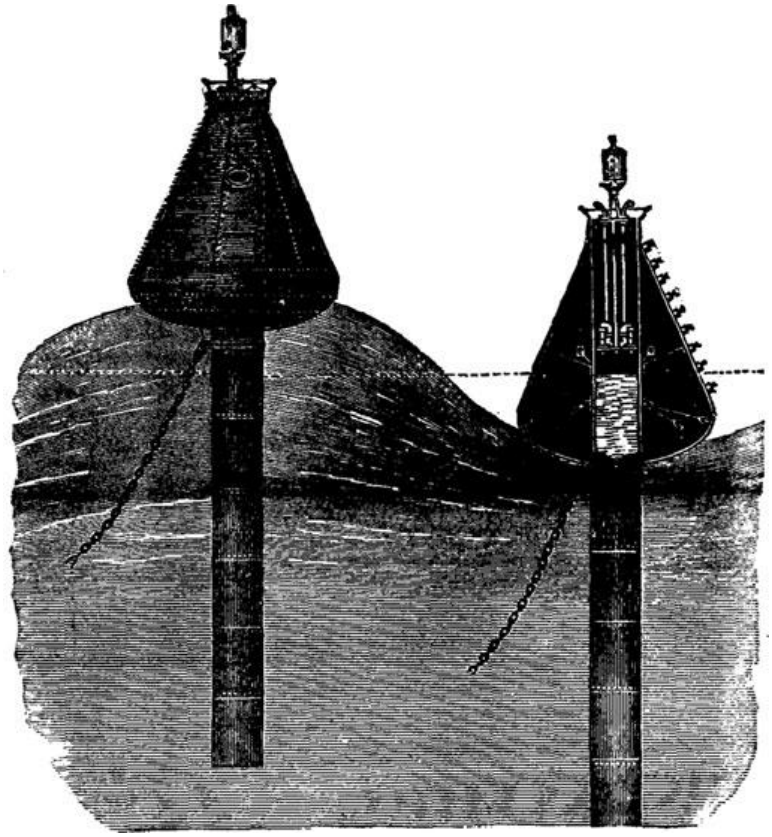

Figure 27. Courtney's whistling buoy [Heath, 2011]

An OWC was used for first time as a device that produces electricity from Masuda (Heath, 2012), in Japan, when in 1947, he created a mechanism driving an impulse turbine in order to produce electricity. The purpose of this device was again the navigation, as navigation light was produced from the electricity, in Osaka Bay. In the following years, many different devices were developed and installed around the world, mainly at shorelines.

One important theory about a fixed OWC device under linear wave theory was developed by Evans in 1978 (Martins-rivas et al., 2009). Two years before, Evans published the 'Theory of wave power absorption by oscillating bodies'. In 1978 he took into account the free surface inside the chamber of OWC as a weightless piston. Finally he managed to develop a theory in which, the free surface was allowed to oscillate under the application of a uniform pressure. Sarmento & Falcao (1985) made a research about the effect of air compressibility that exist inside the chamber of OWC and the same year(1985) Falnes & McIver studied about the 'Surface wave interactions with systems of oscillating bodies and pressure distributions'. They worked on a theory for floating OWC device taking into consideration the interactions between the several devices.

Some characteristic examples of Oscillating Water Columns are the following:

- Wavegen (www.owcwaveenergy.weebly.com/wavegen)
- Oceanlinx (www.oceanlinx.com)
- Ocean Energy Buoy (www.oceanenergy.ie)

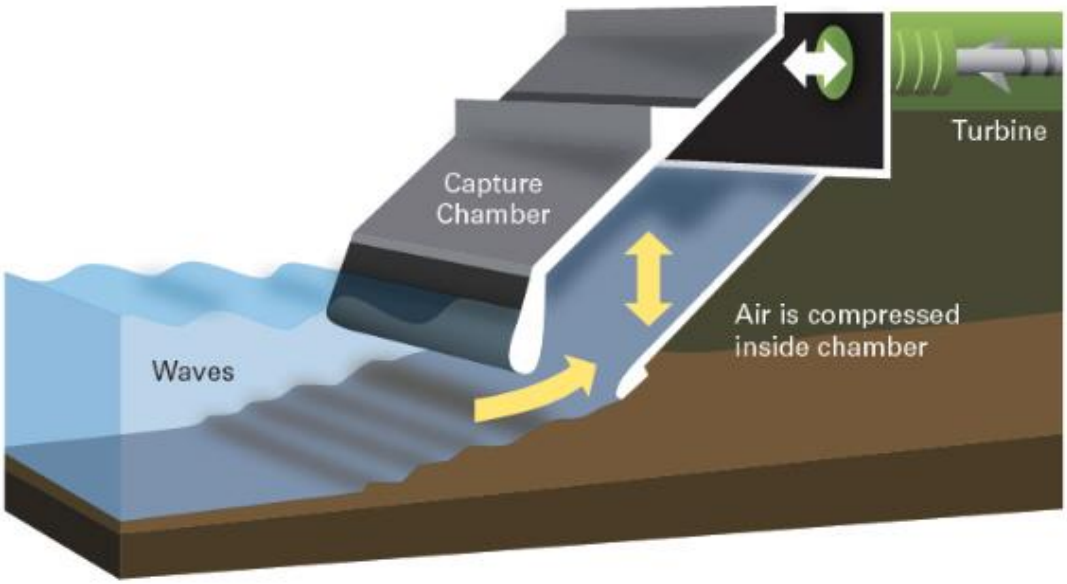

Figure 28. Wavegen onshore OWC [www.esru.strath.ac.uk]

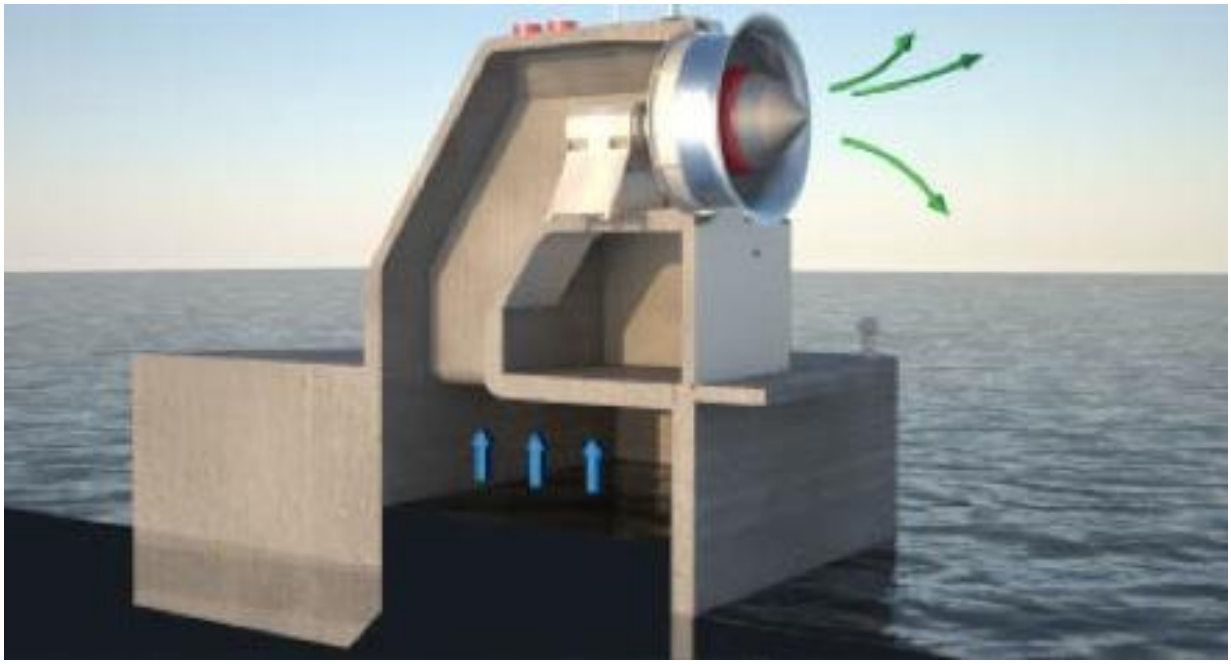

Figure 29. Oceanlinx OWC [www.alternativeconsumer.com]

Figure 30. Ocean Energy Buoy [Heath, 2012]

3.5.3 Oscillating Water Column Wave Power plant

The OWC wave power plant Pico (www.pico-owc.net) was completed in 1999 in the Azores of Portugal. However, malfunctions occurred in the Wells turbine of OWC when the device flooded. The construction was repaired and reopened in 2005. Its output power is 0.4MW. (Falcao , 2005)

Specifications:

Park power: 0.4MW

Year of construction: 1999, 2005

Type of WEC : OWC, Wells

Location: 38°28'19"N 28°51'50"W

Figure 31. Wave power plant Pico at the Azores [Falcão, 2005]

3.6 Floating structure for offshore wind and wave energy sources exploitation

Another challenge that has presented the last years is the design of a device that absorbs not only wave but also wind energy. For instance, a system of three identical OWC devices which are placed at the corners of a triangular floater, in combination with a WT in the center of the platform supported from a solid cylindrical body, can take advantage of wind and wave energy at the same time. Lately, many attempts and researches have been conducted related to the hydrodynamic analysis and the optimization of devices like the ones mentioned above, studying different arrays and characteristics of the configuration. Specifically, Mazarakos et al. (2015) studied the coupled hydro–aero–elastic analysis of a device like the above, consisting of concentric vertical cylinders, moored through tensioned tethers as a TLP platform, under the action of regular surface waves. He calculated for two water depths (at 120m and 200m), the numerical results concerning the motions and the mean second order loads of the floating structure. He also compared the results at the level of RAOs. All the interaction phenomena with neighboring bodies were investigated by Konispoliatis et al. (2016). He parametrically evaluated the wave power efficiency of each device with first and mean second order wave forces, added masses and damping coefficients, together with air volume flow rates. He examined three different arrays. The first one was a three OWC triangle array and the second and third were a four OWC square array, varying in wall thicknesses. In addition, Konispoliatis et al. (2016) studied how OWC draught and thickness affects the total amount of output mean power. The pneumatic admittance at device's turbine was also a parameter that he took into account for the presentation of the oscillating air pressure. Furthermore, Mazarakos et al.(2016) made a parametric hydrodynamic analysis that compared the analytical results of a triangular, quadrate and pentagonal floater with three, four and five identical OWC devices respectively and concluded that firstly, there is no influence of aerodynamics loads on the hydrodynamics of each system, secondly, the interaction phenomena between the devices of the configuration affect the inner air pressure distribution and therefore the mean total absorbed power and thirdly, each examined system is effective for wave frequencies $\omega \leq 1.4$ rad/s. Finally several attempts are taking place currently in order to examine the application of devices like the above in real sea states and conditions. A related attempt in order to combine the RAOs of the configuration with the Spectrum of the Sea had been made from Cruz (2010) and Babarit et al. (2011). Taking under consideration the frequency of occurrence of each sea state (H_S-T_P) is an important factor for the final calculation of the absorbed power in a specific time period.

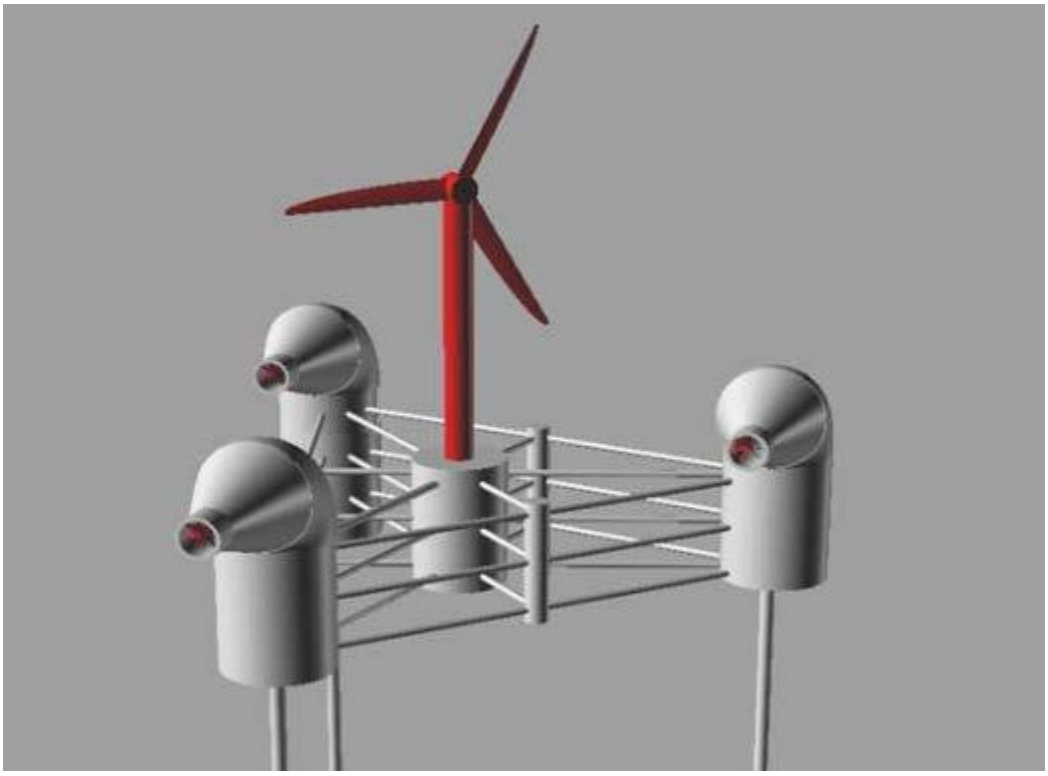

Figure 32. Multi-purpose floating structure with three OWC devices and a WT [Mazarakos et al. , 2015]

3.7 Formulation of the problem

3.7.1 Calculation of the velocity potential function

We assume that there is a group of N vertical axisymmetric oscillating water column devices. This group is excited by a plane periodic wave of amplitude H/2, frequency ω and wave number k propagating in water of finite depth. Each device's chamber q, q=1, 2, 3, has an outer and inner radius that is denoted by α_q, b_q, respectively. In addition, h_q denotes the distance between the bottom of the q device and the sea bed. We assume that the fluid is non-viscous and incompressible and that the water flow is irrotational. As a result, the linear water wave theory can be used. We use the global Cartesian co–ordinate system O–XYZ with the vertical axis OZ directed positive upwards and coinciding with the vertical axis of symmetry of the central body and origin on the sea bed. In addition, there are N local cylindrical co–ordinate systems (r_q, θ_q, z_q) q = 1, 2,. . ., N with origins on the sea bottom and their vertical axes point upwards and coincide with the vertical axis of symmetry of the q device. The fluid flow around the q = 1,2,3,4 body (3 OWC and 1 cylinder for WT) can be described by the potential function (Mazarakos et al., 2015):

$$\Phi^{\,q}\left(r_q,\theta_q,z;t\right)=Re\left\{\Phi^q\left(r_q,\theta_q,z\right)e^{-i\omega t}\right\} \quad (1)$$

According the Falnes and McIver (1985) the spatial function $\Phi^{\,q}$ can

be decomposed, on the basis of linear modeling, as:

$$\Phi^{\,q}=\Phi_0^q+\Phi_7^q+\sum_{p=1}^{N}\sum_{j=1}^{6}\dot{x}_{j0}^{p}\cdot\Phi_j^{qp}+\sum_{p=1}^{N}p_{in0}^{i}\cdot\Phi_P^{qi} \quad (2)$$

Φ_0^q : Velocity potential of the undisturbed incident harmonic wave (Mavrakos et al., 1987)

Φ_7^q : Scattered potential around the *q* device, when it is considered fixed in waves with the duct open to the atmosphere, so that the pressure in the chamber is equal to the atmospheric one.

Φ_j^{qp}: Motion-dependent radiation potential around the q device as a result from the forced oscillation of the *p*–th device, *p*=1,2,3,4, moving with unit velocity amplitude $\dot{x}_{j0}^{p}$ with $\dot{x}_j^p=Re\left\{\dot{x}_{j0}^{p}e^{-i\omega t}\right\}$

Φ_P^{qi} : Pressure-dependent radiation potential around the *q*-th device, due to unit time harmonic oscillating pressure head $P_{in}^{i}=Re\left\{p_{in0}^{i}e^{-i\omega t}\right\}$ in the chamber of the *i*-th device which is considered fixed in calm water.

We express, in the cylindrical co-ordinate frame of the *q*–th body, the velocity potential of the undisturbed incident wave system that is propagating at angle β, with respect to the positive x–axis as follows (Mavrakos et al.,1987) :

$$\Phi_0^q\left(r_q,\theta_q,z\right)=-i\omega\frac{H}{2}\sum_{m=-\infty}^{\infty}i^m\Psi_{0,m}^{q}\left(r_q,z\right)e^{im\theta_q} \quad (3)$$

Where

$$\frac{1}{d}\Psi_{0,m}^{q}(r_q,z) = e^{ikl_{0q}\cos(\theta_{0q}-\beta)}\frac{Z_0(z)}{dZ_0'(d)}J_m(kr_q)e^{-im\beta} \quad (4)$$

The follow sketch defines the OWC device of the array and includes all the symbols that are used here.

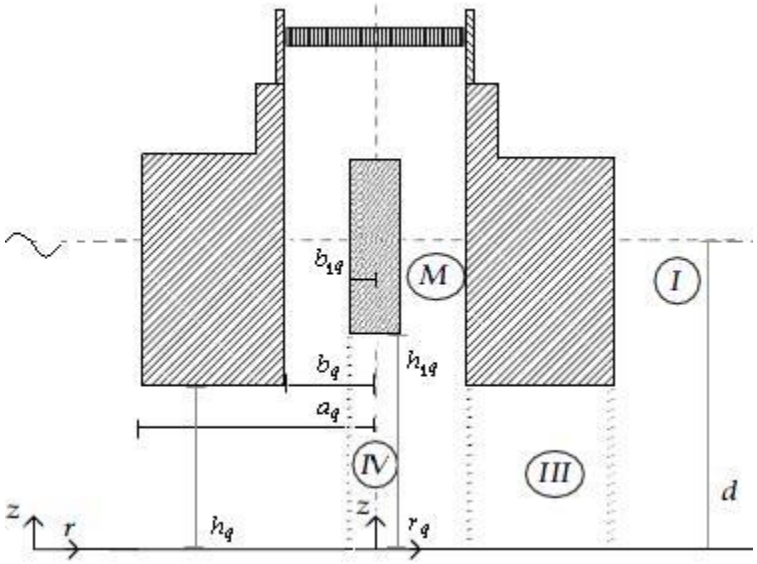

Figure 33. Definition sketch of the q OWC device of the array [Konispoliatis et al., 2016]

In addition, J_m symbolizes the *m*–th order Bessel function of first kind. Finally, $Z_0(z)$ is defined as:

$$Z_0(z) = \left[0.5\left[1+\frac{\sinh(2kd)}{2kd}\right]\right]^{-\frac{1}{2}}\cosh(kz) \quad (5)$$

The frequency ω and the wave number *k* are connected by the dispersion equation.

The diffraction, i.e. $\Phi^q = \Phi_0^q + \Phi_7^q$, q=1,2,3,4 , the motion– and pressure– dependent radiation potential around the isolated q device, when it is considered alone in the field, can be expressed in its own cylindrical co-ordinate system, as follows:

$$\Phi_D^q(r_q, \theta_q, z) = -i\omega \frac{H}{2} \sum_{m=-\infty}^{\infty} i^m \Psi_{D,m}^q(r_q, z)\, e^{im\theta_q} \tag{6}$$

$$\Phi_j^{qq}(r_q, \theta_q, z) = -i\omega \sum_{m=-\infty}^{\infty} \Psi_{j,m}^{qq}(r_q, z)\, e^{im\theta_q} \tag{7}$$

$$\Phi_p^{qq}(r_q, \theta_q, z) = -\frac{1}{i\omega\rho} \sum_{m=-\infty}^{\infty} \Psi_{p,m}^{qq}(r_q, z)\, e^{im\theta_q} \tag{8}$$

Where:

ρ: Water density

Φ_j^l ($l \equiv q$, qp; j=D, 1, …, 6, P; p, q=1,2,3,4, i=1,2,3) : Solutions of Laplace's equation in the entire fluid domain, that satisfy the following boundary conditions (Konispoliatis, 2014; Konispoliatis et al., 2014):

$$\omega^2 \Phi_j^l - g\frac{\partial \Phi_j^l}{\partial z} = \begin{cases} 0 \;\; for \begin{cases} r_q \geq a_q; \acute{\eta} r_q \geq c \\ l \equiv q, j = D; \acute{\eta} \\ l \equiv qp, j = 1,2,\dots,6, P \end{cases} \\ 0 \;\; for \begin{cases} b_{1,q} \leq r_q \leq b_q; \\ l \equiv q, j = D; \acute{\eta} \\ l \equiv qp, j = 1,2,\dots,6, \end{cases} \\ -\delta_{q,i} \frac{i\omega}{\rho} for \begin{cases} b_{1,q} \leq r_q \leq b_q; \\ l \equiv qr, J = P \end{cases} \end{cases} \tag{9}$$

on the outer and inner free sea surface (z=d) and also the zero normal velocity on the sea bed (z=0). Furthermore, the kinematic conditions on the mean device's wet surface have to be fulfilled by the potentials. Moreover, a radiation condition must be imposed in order states that propagate disturbances must be outgoing. The unknown potential functions, $\Psi_{j,m}^{k,l}$, k=*I, III, M, IV* can be established in each fluid region that q-

th device surrounds, using the method of matched axisymmetric eigenfunction expansions.

Finally, the potentials Φ_j^{qp}, Φ_p^{qi}(j=1,…,6) around the device q of the configuration can be expressed either due to oscillation of body p, p=1,2,3,4, in still water (where motion– dependent radiation potential appears), or due to the inner time harmonic oscillating pressure head in the air chamber of the device i=1,2,3, as follows:

$$\Phi_j^{qp}(r_q, \theta_q, z) = -i\omega \sum_{m=-\infty}^{\infty} \Psi_{j,m}^{qp}(r_q, z)\, e^{im\theta_q} \tag{10}$$

$$\Phi_p^{qi}(r_q, \theta_q, z) = \frac{1}{i\omega\rho} \sum_{m=-\infty}^{\infty} \Psi_{p,m}^{qi}(r_q, z)\, e^{im\theta_q} \tag{11}$$

In order to express the related potentials, with the above equations, we use the multiple scattering approach (Twersky, 1952, Okhusu, 1974). This method has also been used to solve the diffraction and the motion- dependent radiation problems around arbitrarily shaped, floating or/and submerged vertical axisymmetric bodies (Mavrakos et al., 1987, Mavrakos 1991). Finally the same method has been used for the diffraction and the pressure– dependent radiation problems for an interacting array of OWC's devices (Konispoliatis et al., 2013).

3.7.2 Volume flow

The volume flow in respect of the time is produced by the oscillating internal water surface in q-th OWC device, q = 1, 2, 3 and is defined as

$$Q^q(\mathrm{r_q}, \theta_q, z, t) = Re[q^q(\mathrm{r_q}, \theta_q, z) e^{-i\omega t}] \tag{12}$$

Where:

$$q^q = \iint_{S_i^q} u_z d\, S_i^q = \iint_{S_i^q} \frac{\partial \Phi^q}{\partial z} r_q dr_q d\theta_q \tag{13}$$

u_z: Vertical velocity of the water surface

S_i^q: Inner water surface in the q-th device, q=1, 2, 3

If we assume that the Wells turbine is placed between the q device's chamber and the outer atmosphere inside a duct and that it is characterized by a pneumatic admittance Λ^q, then we can have the total volume flow as follows (Falnes, 2002, Evans et al., 1996):

$$Q^q(t) = \Lambda^q P_{in}^q(t) \tag{14}$$

In addition for the pneumatic admittance Λ^q we have (Sarmento et al., 1985):

$$\Lambda^q = \frac{KD}{N\rho_{air}^0} - i\omega \frac{V_0^q}{c_{air}^2 \rho_{air}^0} \tag{15}$$

Where:

N: Rotational speed

D: Outer diameter of turbine rotor

V_0^q: the q-th device's air chamber volume

c_{air}: Sound velocity in air and we assume isentropy so that the variations of pressure and air density are proportional to each other with $c_{air}^2 = \frac{dp_{in}^q}{d\rho_{air}}$.

K: Empirical coefficient that depends on the design, the setup and the number of turbines

As long as we assume that the effect of air compressibility is disregarded, then the imaginary part of Λ^q that represents the effect of the air compressibility inside the chamber of each OWC device will be negligible.

If we decompose the total volume flow q^q of the q–th device, as we did for the velocity potential above, into three terms that are related with the diffraction, $q_D{}^q$, the motion– and the pressure– dependent radiation problems $q_R{}^{qp}$, $q_P{}^q$ respectively, we have:

$$q^q = q_D^q + q_R^{qp} + \sum_{i=1}^{3} p_{in0}^i q_P^{qi} \tag{16}$$

Where:

$$q_R^{qp} = \sum_{P=1}^{4} \sum_{J=1}^{6} \dot{x}_{j0}^p q_{3,j}^p - \dot{x}_{30}^p S_i^p \tag{17}$$

With S_i^p is symbolized the inner water surface in the p device, p=1, 2, 3.

3.7.3 Hydrodynamic forces

The forces on each OWC device can be calculated from the pressure distribution that is given by the linearized Bernoulli's equation

$$P(r_q, \theta_q, z; t) = -\rho \frac{\partial \Phi^q}{\partial t} = i\omega\rho\Phi^q e^{-i\omega t} \tag{18}$$

Where:

Φ^q is the q device's velocity potential in each fluid domain I, III, M and IV as it presented at the above figure.

The exciting forces and moments (vertical and horizontal) acting on the configuration can be calculated by the following equations (Konispoliatis et al., 2013):

$$F = \int_{S_p} pndS \tag{19}$$

and

$$M = \int_{S_p} p(r \times n) dS \tag{20}$$

Where r denotes a position vector of an arbitrary point on the wetted surface of the p-th body, S_p. with respect to the *p* body fixed co-ordinate system of body *p*. Moreover, *n* is the normal vector to the wetted surface S_p pointing inside of the body.

The complex form f_{ij}^{qp} of hydrodynamic reaction forces and moments acting on each device *q*, q=1,2,3,4, in the *i*–th direction due to the oscillation of device *p*, *p*=1,2,3,4, in the *j*–th direction, can be written in the form (Newman, 1977):

$$f_{ij}^{qp} = \omega^2 \left(a_{ij}^{qp} + \frac{i}{\omega} b_{ij}^{qp} \right) x_{j0}^{p} = \omega^2 \pi_{ij}^{qp} x_{j0}^{p} \tag{21}$$

Where a_{ij}^{qp} and b_{ij}^{qp} are the well–known added mass and damping coefficients respectively.

Similarly, for the hydrodynamic pressure forces and moments f_{Pi}^{ql} acting on the device *q* in the *i*–th direction due to oscillating pressure head in the *l*=1,2,3 we have:

$$f_{Pi}^{ql} = \left(-e_i^{ql} + i d_i^{ql} \right) \cdot p_{in0}^{\mathrm{l}} \tag{22}$$

Where $e_i^{ql}$and d_i^{ql} denote the pressure damping coefficients.

By superposing the corresponding forces on each device with respect to the reference point of motion, G, of the entire structure we can calculate the total hydrodynamic forces on the entire multi– body configuration (Mavrakos, 1991) and we have:

$$F_{p,total} = \frac{1}{N} \sum_{i=1}^{i=N} \left[B^{(i)} \right] \left[F_p^{(i)} \right] \tag{23}$$

Here, $B^{(i)}$ is the coordinate of the corresponding body *p* (square matrix 6 × 6) with respect to the central coordinate system of structure G:

$$[B^i] = \begin{bmatrix} 1 & 0 & 0 & 0 & 0 & 0 \\ 0 & 1 & 0 & 0 & 0 & 0 \\ 0 & 0 & 1 & 0 & 0 & 0 \\ 0 & -z^i & y^i & 1 & 0 & 0 \\ z^i & 0 & -x^i & 0 & 1 & 0 \\ -y^i & x^i & 0 & 0 & 0 & 1 \end{bmatrix} \quad (24)$$

3.7.4 Aerodynamic loading

Analyzing in the frequency domain formulation, we can examine the contribution of the WT on the 6 floater motion. This is performed with use of the dynamic model of Hamilton, with gravity and aerodynamics being the external forcing. The Blade Element Momentum (BEM) theory can define the aerodynamic loading as a function of the conditions the floater operates and its motions that changes the effective angles of incident at the blades. If we linearize all the terms with respect to static position of the floater (static equilibrium), we can define the additional mass, damping and stiffness matrices which contribute at the WT as aerodynamic, inertial-gyroscopic and gravitational loads (Papadakis et al., 2014)

3.7.5 Mooring System

A very important factor for the design of the OWC and the wave energy absorption is the mooring system that is used for its station keeping. The stability and dynamic positioning are directly related to this system. Therefore, a reliable mooring system is needed, in order to protect the structure from the extreme environmental forces of wind, currents and waves that will present. In the following study, a TLP type mooring system is considered. This system comprises of tethers fixed to the bottom of the interior coaxial cylindrical body of an OWC device. The high tension in the tension legs contains horizontal offsets to a relatively small fraction of the water depth. The heave, roll and pitch motions remain minute, due to the high axial stiffness in the tendons. It is quite common, to employ multiple tension legs (Parker, 2007; Bachynski et al., 2012; Wang et al., 2013) in offshore tension leg platform wind turbines, to capture offshore wind resources in waters of moderate depth. The mooring forces, $f^T_{i,mooring}$, that act on the platform in the i-th direction can be expressed as follows:

$$f_{i,mooring}^{T} = C_{i,j,mooring} \cdot x_{j0}, i, j = 1, \dots, 6 \quad (25)$$

Where:

x_{j0}: Motion component of the entire configuration in *j*-th direction with respect to the global reference point, G, of the platform's motions.

$C_{i,j,mooring}$: Conventional and geometrical mooring line stiffness coefficient of the platform

Regarding the total restoring stiffness matrix $C_{i,j,total}$, of the OWC, includes three parts. The first part is the conventional mooring line stiffness; the second part is the platform hydrostatic restoring stiffness including the influence of tendons and the third part is the tendon geometric stiffness (Senjanovic et al., 2011).

Therefore, the elements of the (6x6) square stiffness matrix $C_{i,j,total}$ can be expressed as follows:

$$C_{1,1} = C_{2,2} = \sum_{n=1}^{M} \frac{T_n}{L} \quad (26)$$

$$C_{3,3} = \rho g A_{WL} + \frac{EA}{L} \quad (27)$$

$$C_{4,4} = \rho g I_{WLX} + U_{z_B} - Q_{z_G} - \sum_{n=1}^{M} T_n z_n + \frac{EI_{xx}}{L} \quad (28)$$

$$C_{5,5} = \rho g I_{WLY} + U_{z_B} - Q_{z_G} - \sum_{n=1}^{M} T_n z_n + \frac{EI_{yy}}{L} \quad (29)$$

$$C_{6,6} = \sum_{n=1}^{M} \frac{T_n}{L} (x_n^2 + y_n^2) \quad (30)$$

Where:

M: Number of tendons

T_n: Tendon pretension forces in kN

A: Total cross-section area in m^2

I_{xx}, I_{yy}: Moments of inertia about x and y axis respectively in $t \cdot m^2$

x_n, y_n, z_n: Horizontal and vertical coordinates of the attaching point of the n tendon with respect to the platform's global reference point of motion, G, in m

L: Length of the tendon in m

A_{WL}: Water plane area of the platform in m^2

I_{WLX}, I_{WLY}: Moments of inertia of A_{WL} about x and y axis, respectively in $t \cdot m^2$

U, *Q*: Buoyancy and weight of the platform, respectively, in t

z_B, z_G: Vertical coordinates of buoyancy and gravity center, respectively , in m

3.7.6 Response Amplitude Operators-RAOs

In order to investigate the dynamic equilibrium of all the forces that are acting on the moored multi-body configuration we use the following well - know system of differential equations of motions. This equation describes the couple hydro-aero-elastic problem in the frequency domain. (Mazarakos et al., 2015)

$$\sum_{j=1}^{6}\left[-\omega^2\left(M_{i,j}+A_{i,j}+M^{WT}+\frac{i}{\omega}B_{i,j}+\frac{i}{\omega}B_{i,j}^{WT}\right)+K_{i,j}+K_{i,j}^{WT}+C_{mooring}\right]x_{j0}=F_i+F_{p,i} \qquad (31)$$

for *i*=1,…,6.

The $M_{i,j}$, $K_{i,j}$ symbolize the elements of the (6x6) mass and stiffness matrices of the entire configuration. In addition, $A_{i,j}$, $B_{i,j}$ are the hydrodynamic masses and potential damping of the entire configuration. F_i are the exciting forces acting on the multi–body system at the *i*–th direction. $F_{p,i}$ are the pressure induced hydrodynamic forces acting on the multi–body system at the *i*–th direction. x_{j0} is the motion displacement of the entire OWC system at the *j*–th direction with respect to a global co – ordinate system G. The M^{WT}, B^{WT}, K^{WT} symbolize the mass, damping and stiffness matrices that contribute to the inertial-gyroscopic, aerodynamic and gravitational loading of the WT respectively. Finally, $C_{mooring}$ is the stiffness matrix of the mooring lines.

3.8 Examined device

In the current thesis we study an array of multiple interacting vertical axisymmetric oscillating water column devices as the one presented above. Our configuration consists of three identical OWC devices which are placed at the corners of a triangular floater in combination with a central solid cylinder that works as a base for a 10MW WT. The WT of 10 MW is the main difference between this specific energy platform and the one we took the experimental measurements. The whole system is exposed to the action of regular surface waves in finite water depth. In addition each device has finite wall thickness and floats independently, as well as the geometric configuration of each one of them consists of a partially immersed toroidal oscillating chamber of finite volume that is formed between an exterior cylindrical shell and a concentric interior truncated cylinder. At these concentric interior truncated cylinders, TLP tethers are mounted on.

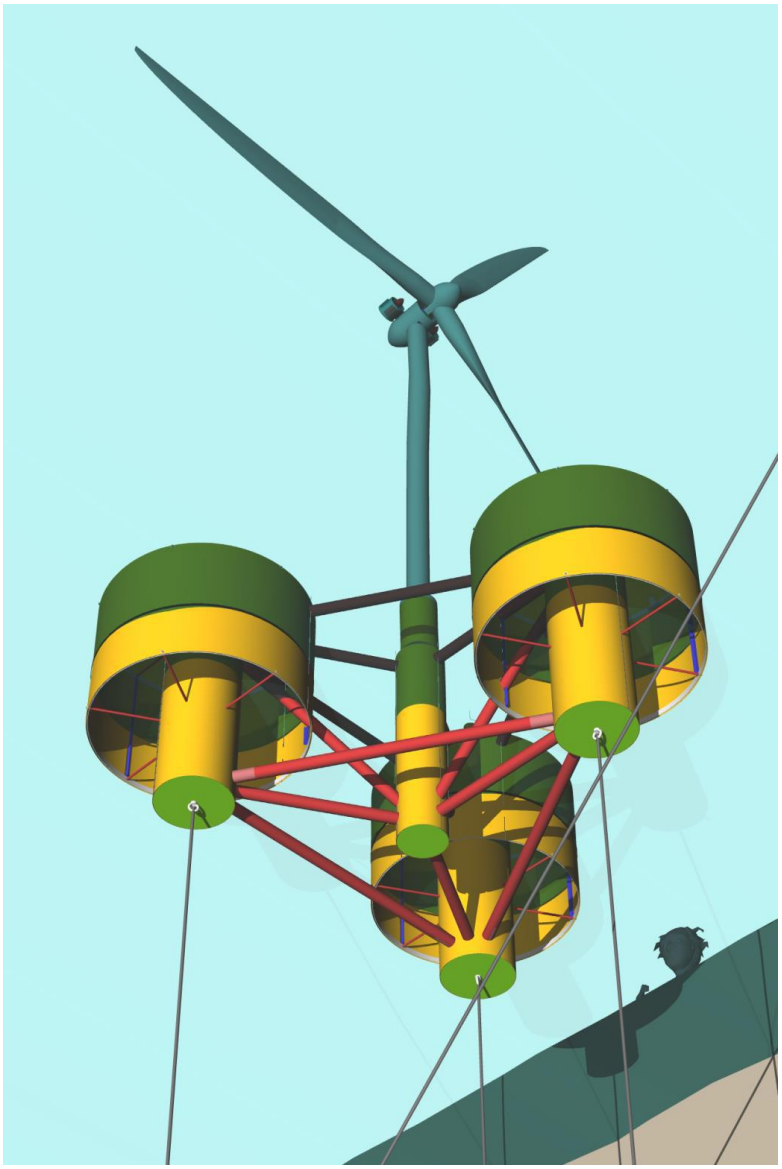

Figure 34. 3D model of the examined configuration [Mazarakos, 2016]

In addition there are four more sets of smaller members:

- Two sets of three pontoons (for a total of six members) connecting the offset columns with each other (forming a triangle, both at the top (AOB1- AOB3) and bottom (KOB1- KOB3))
- Two sets of three pontoons (for a total of six members) connecting the offset columns with the main column (forming a y-connection, both at the top (AKB1- AKB3) and bottom (KKB1- KKB3))

- Three cross braces connecting the bottom of the main column with the top of the offset columns (ΔB1- ΔB3)
- Nine sets of three pontoons (for a total of twenty seven members) connecting the offset columns with the oscillating chambers (forming a y-connection, at the top (AK11,12,13 - AK13,23,33), middle (KK11,12,13 - KK13,23,33) and bottom (BK11,12,13 - BK13,23,33))

Geometric Characteristics

Depth of platform base below SWL (total draught)	20.00 m
Elevation of main column (tower base) above SWL	10.00 m
Elevation of offset columns above SWL	10.00 m
Spacing between columns	50.00 m
Draught of the structure	20.00 m
Diameter of main column	12.00 m
Diameter of inner concentric cylindrical body	14.00 m
Oscillating chamber thickness of each device	1.50 m
Outer radius of the Oscillating chamber on each device	15.50 m
Oscillating chamber's draught	8.00 m
Diameter of pontoons	1.60 m
Diameter of cross braces	0.0175 m

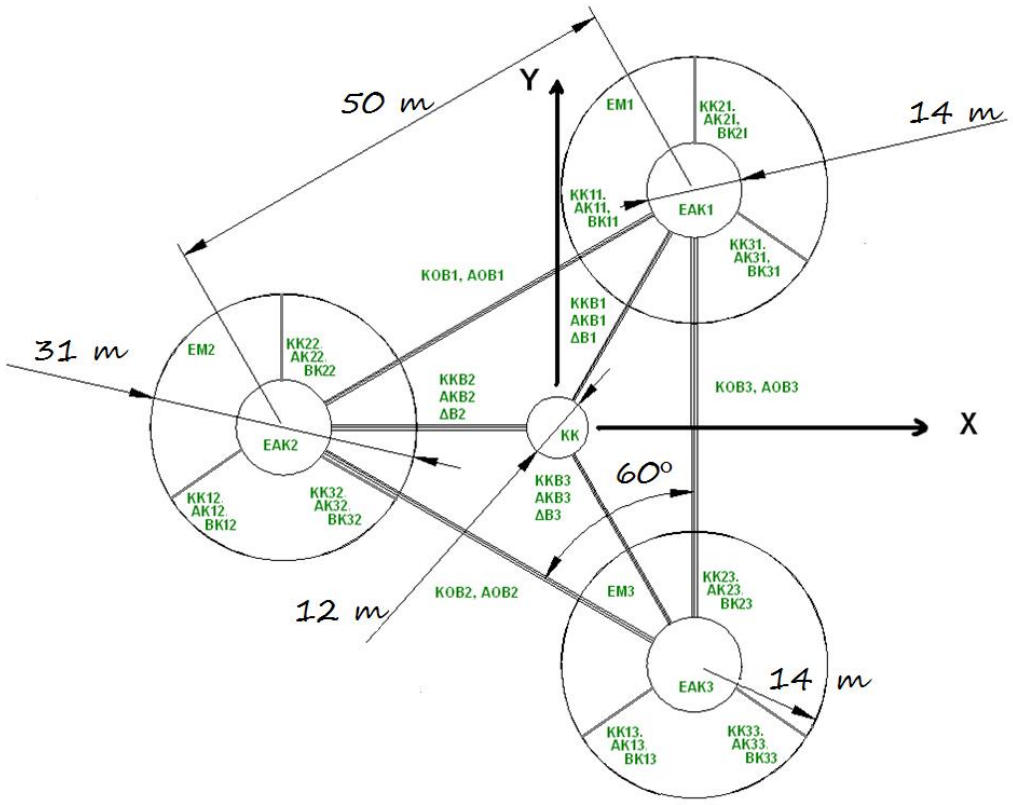

Figure 35. Top view of examined device [Mavrakos, 2018]

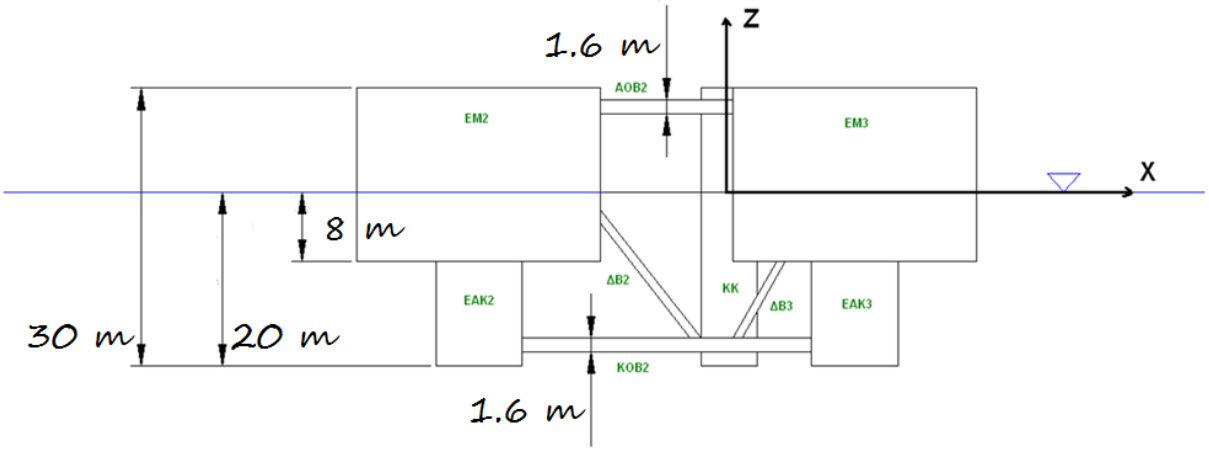

Figure 36. Side view of examined device [Mavrakos, 2018]

Regarding the mass of the structure, the total mass including the water ballast is 9550tn. This mass has been calculated such that the combined weight of the rotor-nacelle assembly, tower, and platform, plus the weight of the mooring system in water, and the applied total pretension balances to the buoyancy of the platform in the static equilibrium position in still water.

Here is the Mass Distribution of the structure:

Mass of the platform (including ballast)	7531.1 tn
Mass of the 10 MW WT	1100.0 tn
Mass of each Wells turbine (including generator)	3.3 tn
Mass of each mooring tendon in water	151.5 tn
Total mass	9550 tn

As we already referred, in order to secure the platform, the floating structure is moored with a TLP type mooring system of three sets of two tendon pipes each (for a total of six members) spread symmetrically about the platform z-axis.

The body-fixed locations, where the sets of the mooring tendon pipes are connected to the platform, are found at the base of the offset columns, at a depth of 20.0m below the SWL. The anchors (fixed to the inertia frame) are located at a water depth of 200m below the SWL. Each of the 6 tendon pipes has an unstretched length of 180m, an outer diameter of 1.117m, an equivalent mass per unit length of 963.63kg/m, an equivalent mass in fluid per unit length of 841.61kg/m. The pretension of each tendon is 9420kN. (Mavrakos, 2018)

Below appears the mooring system properties and stiffness:

Number of mooring tendon pipes	6
Depth to Anchors Below SWL (Water Depth)	200 m
Depth to Fairleads Below SWL	20 m
Mooring Line Length, L_t	180 m
Mooring Line Outer Diameter	1.117 m
Mooring Line Inner Diameter	1.099 m
Equivalent Mooring Line Mass in Water	841.61 kg/m
Pretension of each tendon, F_p	9420 kN
Yeung's modulus of elasticity, E_t	200 Gpa
$C_{11}=C_{22}=F_p/L_t$	52.34 kN/m
$C_{33}=E_tA_t/L_t$	134313 kN/m
A_t	0.121 m^2

Where:

C_{11}, C_{22}: Stiffness of each mooring tendon pipe offered to the floating structure in the horizontal directions along the x- and y-directions.
C_{33}: Stiffness of each mooring tendon pipe along it's longitudinal direction.
A_t: Cross - sectional area of each mooring tendon pipe.
F_p: Pretension of each tendon.

3.8.1 TLP Design Criteria

The TLP Design Criteria are the following (Mavrakos,2018, Bachynski et al., 2012):
1) The surge and sway natural periods T_{n1} should be longer than 25s, therefore:
C_{11} <1707.85 kN/m
2) The heave, roll/bending and pitch/bending natural periods T_{n3} should be shorter than 3.5s, therefore:
C_{33} > 32415.2 kN/m
3) The mean offset should not exceed 5% of the water depth, thus for significant wave height 4 m; wave period 10 s; drag coefficient C_D =1 the mean horizontal force due to waves is F_1 = 1479.9 kN
The mean turbine thrust is 1660 kN (wind speed 11.4m/s). Thus C_{11} = 313.99 kN/m and pretension is 56517.6 kN
4) The tendon area must be sufficient to prevent yield within a safety factor SF=2, for tensions up to twice the initial tension, therefore:
$C_{33} \geq$ 707575.4 kN/m and $A_t \geq 0.637$ m^2
5) A minimum displacement may be required to survive extreme wind and wave conditions, i.e. 14835 m^3 > 2000 m^3
Here C_{11} and C_{33} are the total stiffness of the mooring tendon pipes and A_t is the total cross - sectional area of the mooring tendon pipes.

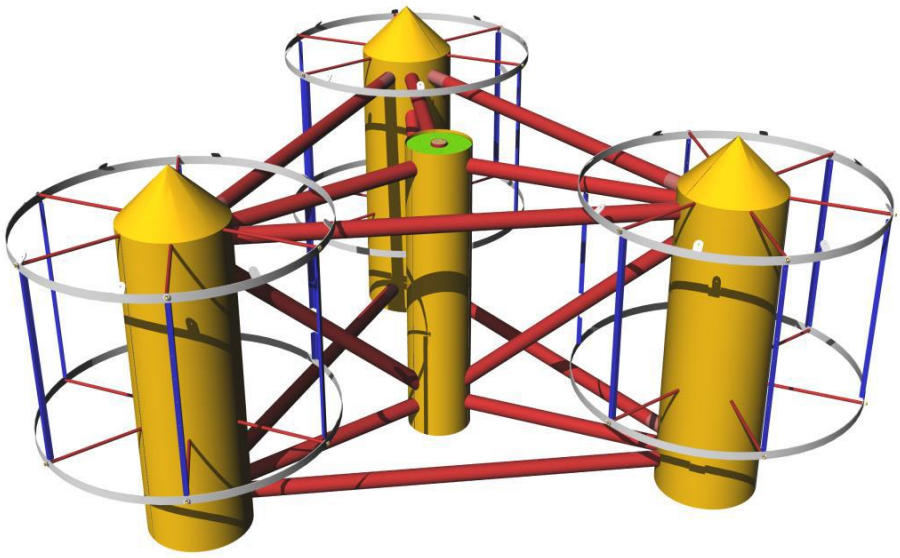

Figure 37. 3D design of the chambers and the main central cylinder [Mazarakos, 2016]

Figure 38. Photo from the construction of the platform [Mazarakos, 2016]

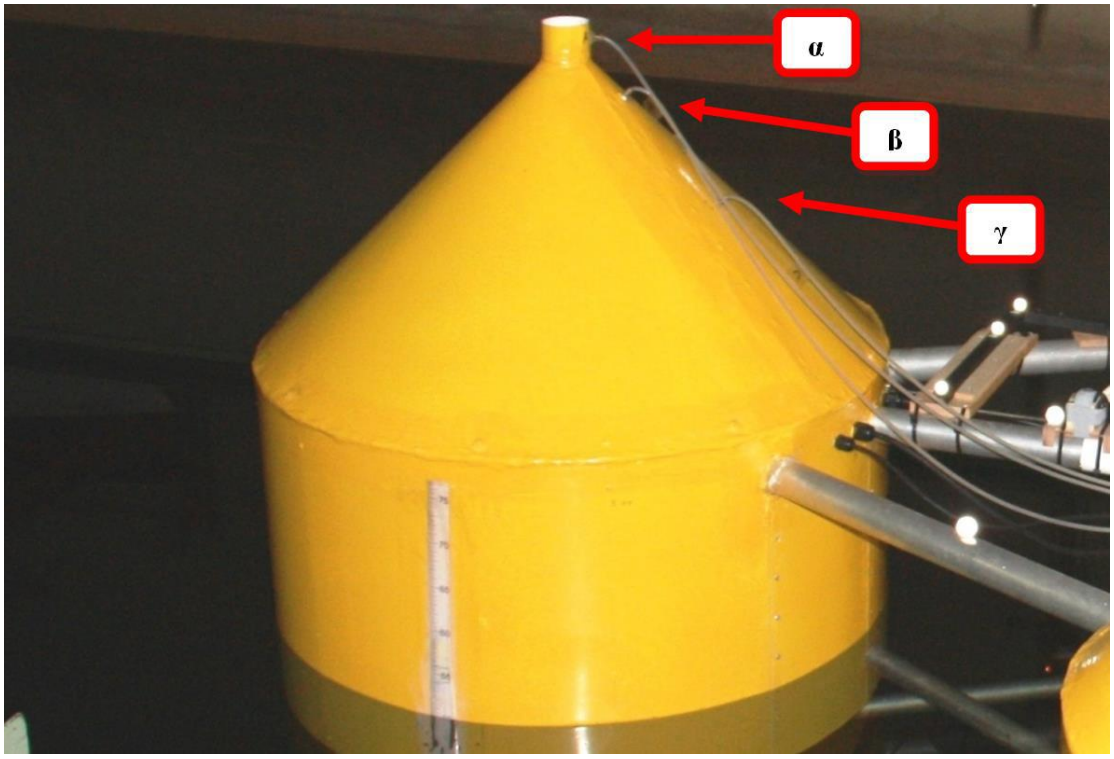

Figure 39. Sensors at the chamber at three different positions [Mazarakos, 2016]

4. Numerical Modelling

4.1 Introduction to HAMVAB

Hydrodynamic Analysis of Multiple Vertical Axisymmetric Bodies (HAMVAB) is a program developed by S. A. Mavrakos, Professor in the School of Naval Architecture and Marine Engineering at the National Technical University of Athens, to solve the linearized diffraction-radiation problems for the interaction between waves and multiple vertical axisymmetric bodies. The shape of the bodies is arbitrary and they can be free-floating or moored. They are also allowed to move as a unite or as independent bodies. HAMVAB provides the first-order exciting wave forces, the mean second – order forces (drift forces) in the horizontal directions and the yaw drift moment, as well as the motions of the configuration.

4.2 Structure and Operation of HAMVAB

HAMVAB uses single body hydrodynamic characteristics and the physical idea of multiple scattering in order to calculate first-order exciting wave forces and motions from the wave. In addition, the program uses finite control volumes around each body and in that way calculates the drift forces in x- and y- directions for the entire multi-body configuration and for each body individually. The hydrodynamic characteristics of the single body are evaluated using matched axisymmetric eigenfunctions expansions. According to this method the flow field around the body is divided into ring shaped regions. In each one of these regions the velocity potential is written in terms of Fourier-Bessel axisymmetric eigenfunctions expansions. By fulfilling the kinematic boundary conditions on the wetted surface of the body and the continuity requirements for the flow velocity and the potential at the common boundaries of adjacent fluid regions, the unknown Fourier coefficients can be calculated. As far as the air pressure head is concerned, it is calculated as a function of the corresponding air turbine characteristics. (Mavrakos, 1996)

4.3 Input File of HAMVAB

As an input file, we prepare a file, having any name, with five characters, containing data like the radiation problem and the diffraction problem. This file defines, if the group of the cylinders is considered as a unit or not, if the individual inertia characteristics of each cylinder of the multi-body configuration are given or not, so that in the first case the inertial characteristics of the entire structure will be evaluated internally by the computer code, as well as if the motions of the entire configuration or of the individual bodies are to be calculated. In addition, data contains information about the water depth, the number of the bodies, the number of the mooring lines, the number of frequencies considered, the radial distance among the structures, the number of interactions considered and more information that the user has to provide at the input file. The geometric characteristics of each individual body are also required.

In fact, it is asked if the bodies have fields above their greater diameter or if they float with their maximum diameter, if they have fields below their greater diameter or if they stand on the sea-bottom with their greater diameter, if the bodies float and pierce the free-surface or if they are submerged under the free-surface, if the bodies stand or not on the sea-bottom, if we have free-floating body etc. The exciting wave forces, the hydrodynamic parameters such as added mass and damping and the motions are computed. In case, there are fields below the greater diameter of the bodies, the user must also report the number of ring elements used for the discretization of the body surface below its greater diameter, the distance of the upper horizontal surface of the discretized body in its middle lower ring element measured from the sea-bottom, the number of terms to be considered in the vertical direction for eigenfunction expansion of velocity potential in the middle lower ring element, the radii of the ring elements measured outbound from the body's vertical axis of symmetry. In case there are fields above the greater diameter of the bodies, the information demonstrated above is requested. In the end, the user must refer the vertical distance of the reference point of body motions located on the body's vertical axis of symmetry and measured from the sea-bottom, the vertical distance of body's center of gravity measured from the reference point of motions (this may be negative in case the center of gravity is located below the reference point of motions), the mass moment of inertia relative to the reference point of motions and the mass of cylinder. Corresponding information and geometric characteristics are asked for the cylinder supporting the Wind Turbine as well.

Appendix lists the input file used in the HAMVAB program for the analysis of floating structure.

4.4 Output File - Results of HAMVAB

In the Output file exist the calculations of the pressure hydrodynamic parameters for each individual device and the complete multi component configuration, the calculations of the wave elevation inside and outside each device as a function of time analysis, the calculations of the inner air pressure head in each device for different values of turbine characteristic, the calculations of drift forces and moments with the direct integration method, the calculation of the total absorbed power from the waves of all the devices as a function of the turbine characteristics, the calculation of the total capture width of all the devices, calculation of the air volume flow , such us diffraction, motion radiation and pressure radiation flow, in each device, the calculation of the first order motions of the complete multi component configuration where the tendors are connected, the calculations of the forces at the tension lines, the calculation of the optimum turbine characteristic as in single floating or moored Oscillation Water Column and as a multiple restrained Oscillation Water Column.

5. Validation of HAMVAB

As mentioned above, by giving the characteristics of the floating structure to be investigated with HAMBAB in the way described above, we receive the theoretical results for values such as the motions of the entire configuration, the inner air pressure head in each device, the stresses and so on.

To validate the numerical results of the HAMVAB program, comparisons with experimental ones will be made for a multi – purpose floating energy platform that supports a 5MW WT. The numerical results were plotted as a function of the wave frequency expressed in rad/sec so that we can compare them with the results we have from the experimental measurements that were conducted in the Laboratory for Ship and Marine Hydrodynamics in the School of Naval Architecture and Marine Engineering at the National Technical University of Athens, in the framework of the POSEIDON program (www.aristeia-poseidon.naval.ntua.gr).

The depth of installation is 120 m, and the sizes used for the dimensionless are as follows:

- Water density $\rho = 1.025$ t / m^3
- Acceleration of gravity $g = 9.81$ m / s^2
- Maximum radius of construction ref = 12.5 m
- Number of bodies nubo = 4
- Wave height H = 2 m
- Angular frequency ω in rad / s
- Wave number k in m^{-1}

The following diagrams depict the comparisons of the generalized motions, pressures and tensions at the top of the mooring lines of the structure, respectively, under the action of harmonic waves. In order to convert chamber pressure into air flow, perforated orifice plates are used at the top of the chamber cone with various bore diameters. Two different cases of bore diameter are presented here. In the first case there is an orifice with bore diameter 20mm and in the second case there is an orifice with bore diameter 50mm.

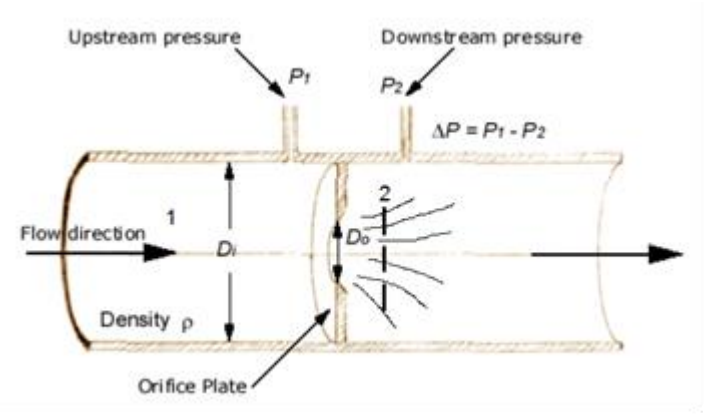

Figure 40. Sketch of pressure flow through the orifice plate [www.aristeia-poseidon.naval.ntua.gr]

5.1 Orifice diameter 20mm

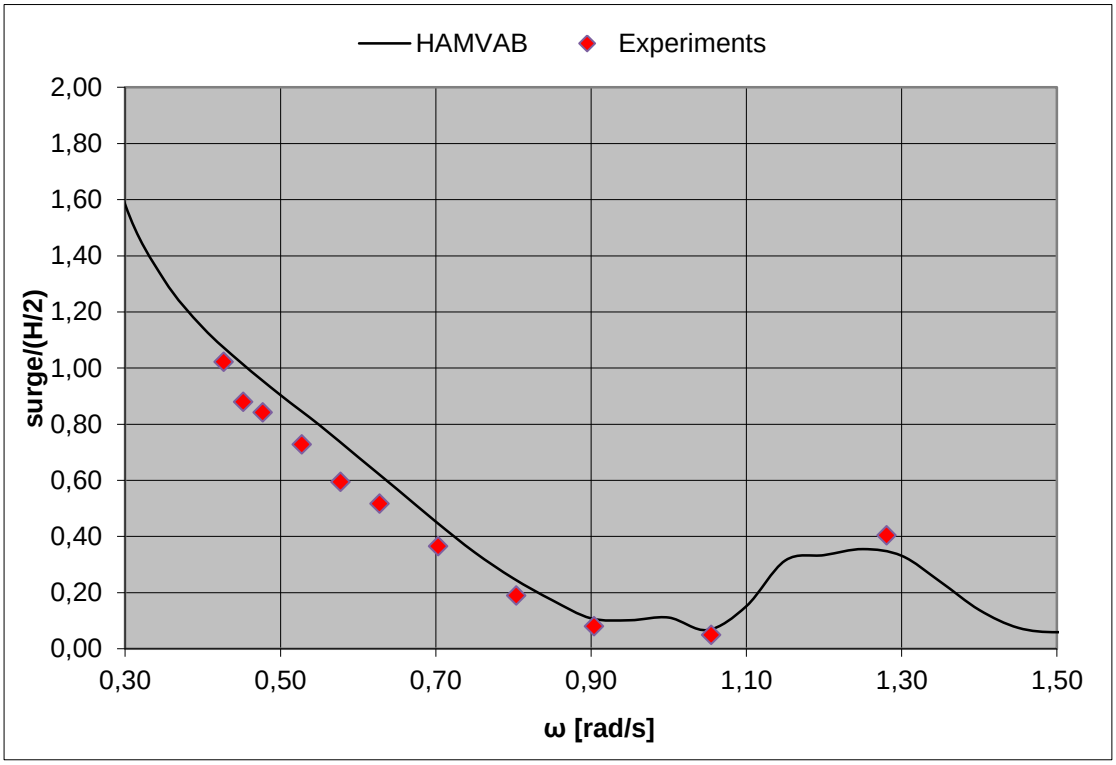

Figure 41. Motions of the entire Configuration in the surge direction [Mazarakos, 2017]

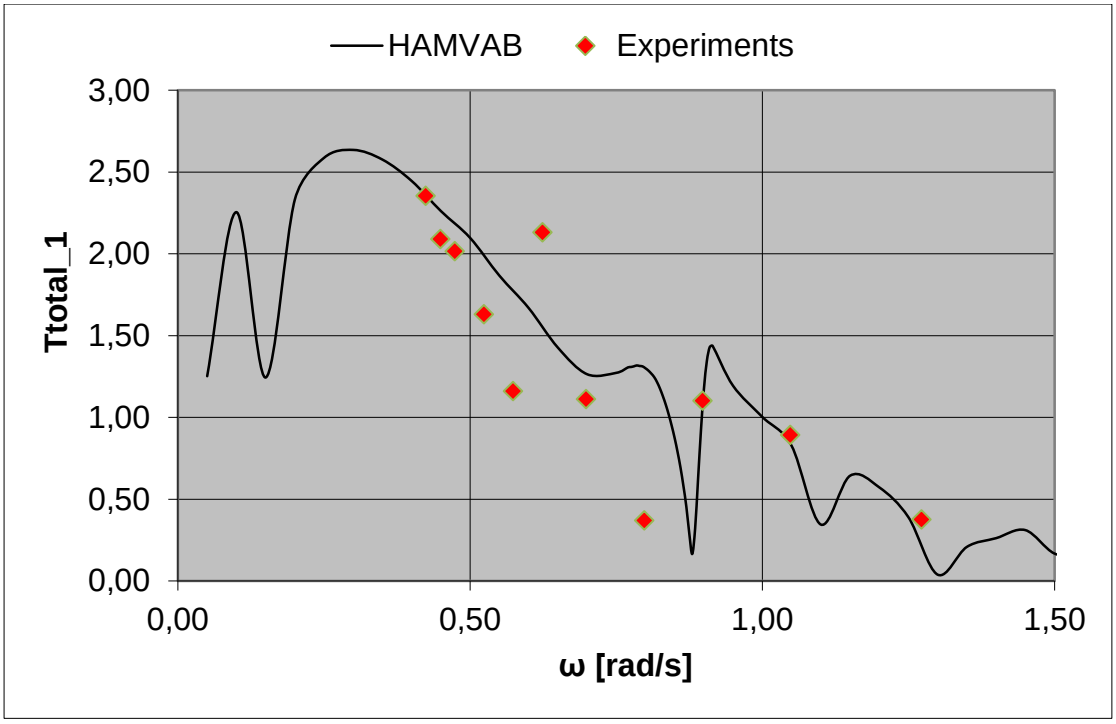

Figure 42. First order line tension for Line No. 1 [Mazarakos, 2017]

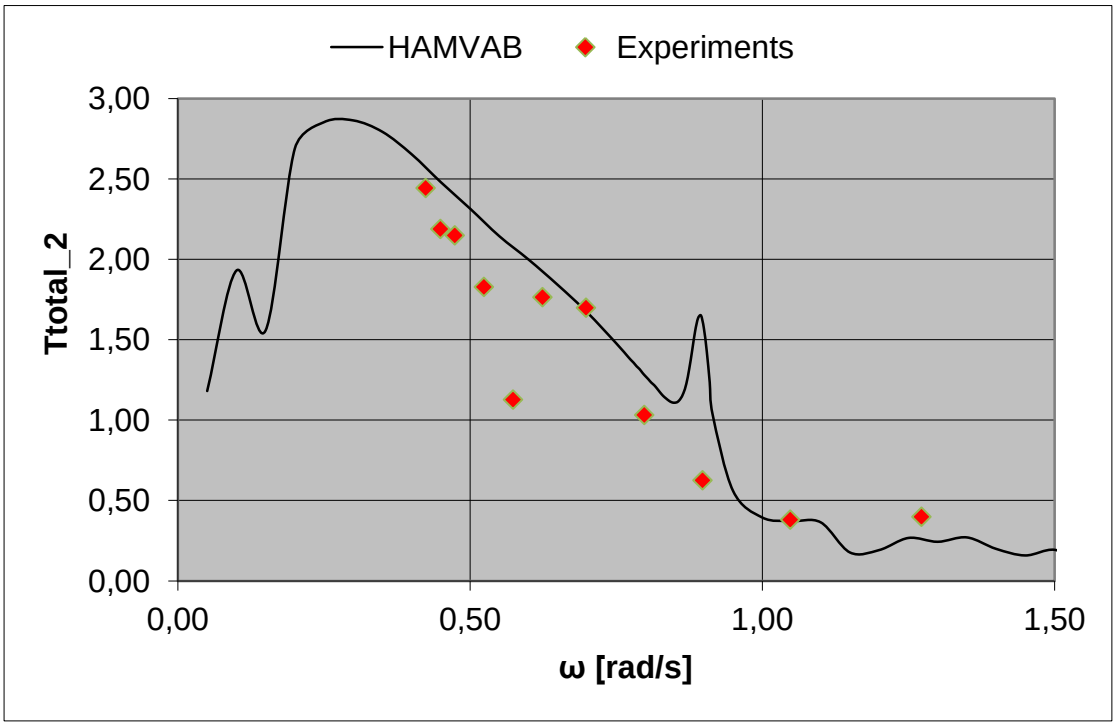

Figure 43. First order line tension for Line No. 2 [Mazarakos, 2017]

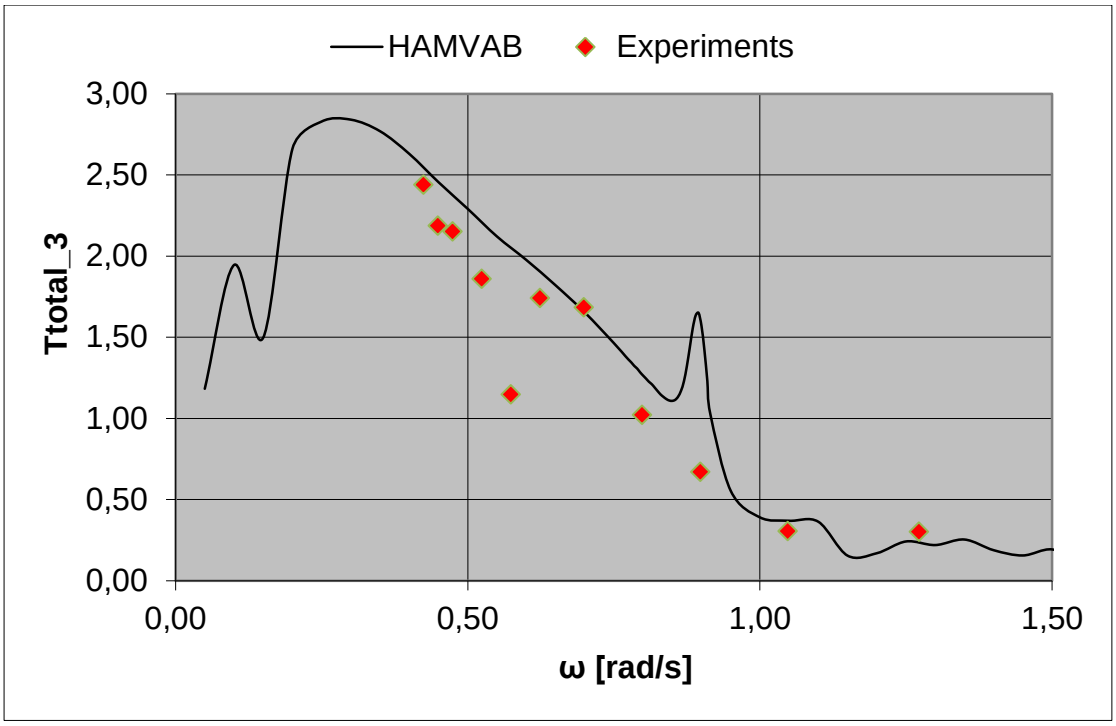

Figure 44. First order line tension for Line No. 3 [Mazarakos, 2017]

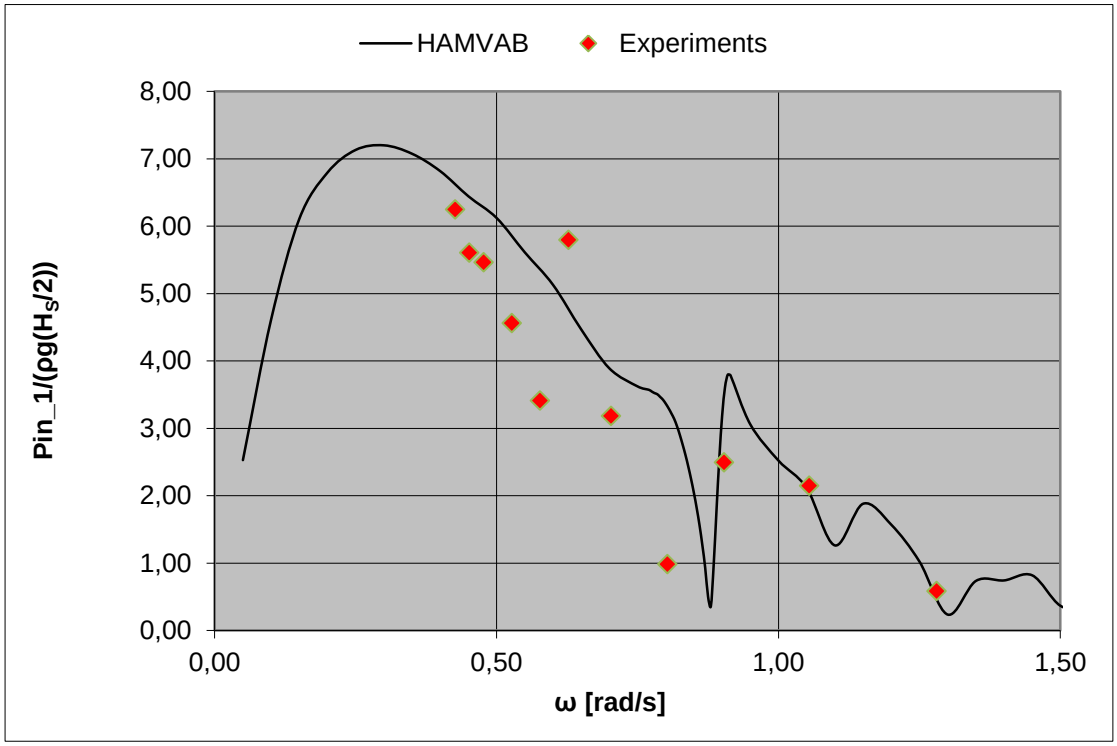

Figure 45. Pressure in chamber No. 1 [Mazarakos, 2017]

5.2 Orifice diameter 50mm

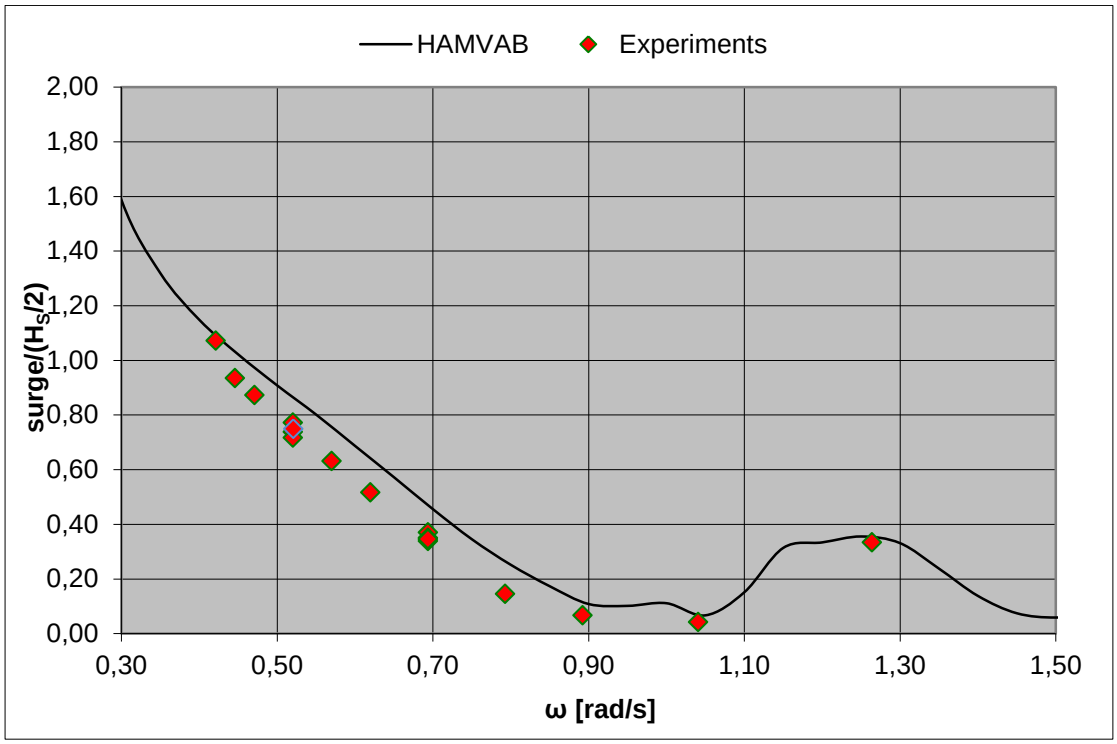

Figure 46. Motions of the entire Configuration in the surge direction [Mazarakos, 2017]

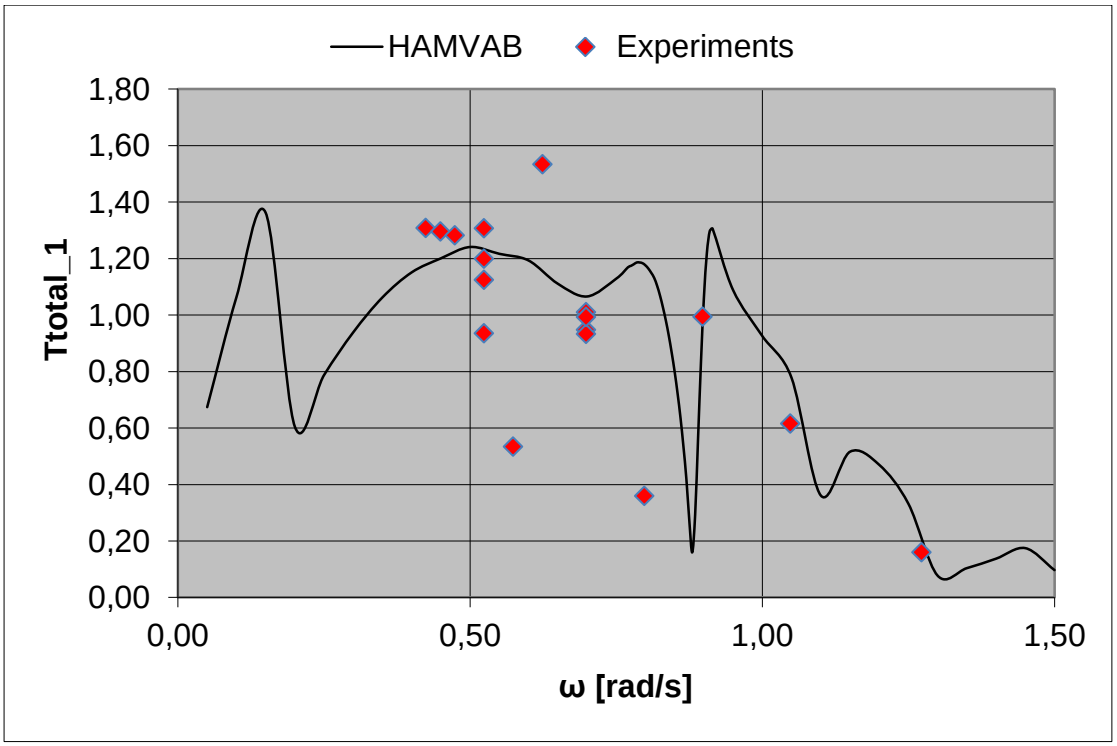

Figure 47. First order line tension for Line No. 1 [Mazarakos, 2017]

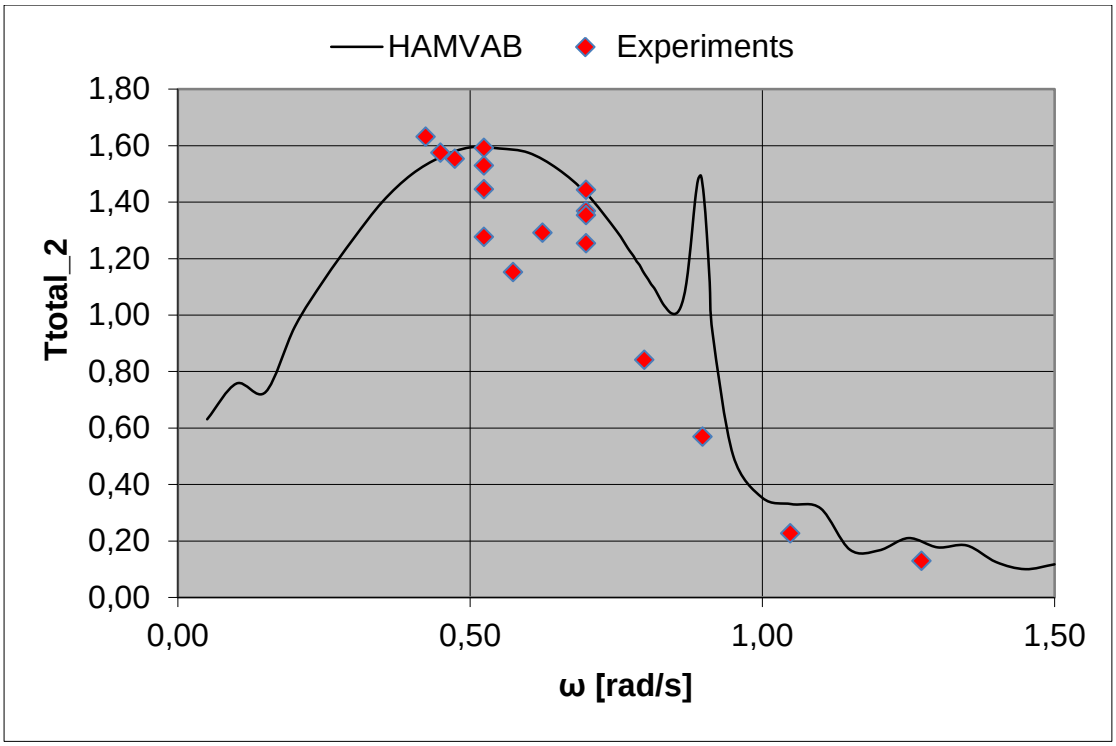

Figure 48. First order line tension for Line No. 2 [Mazarakos, 2017]

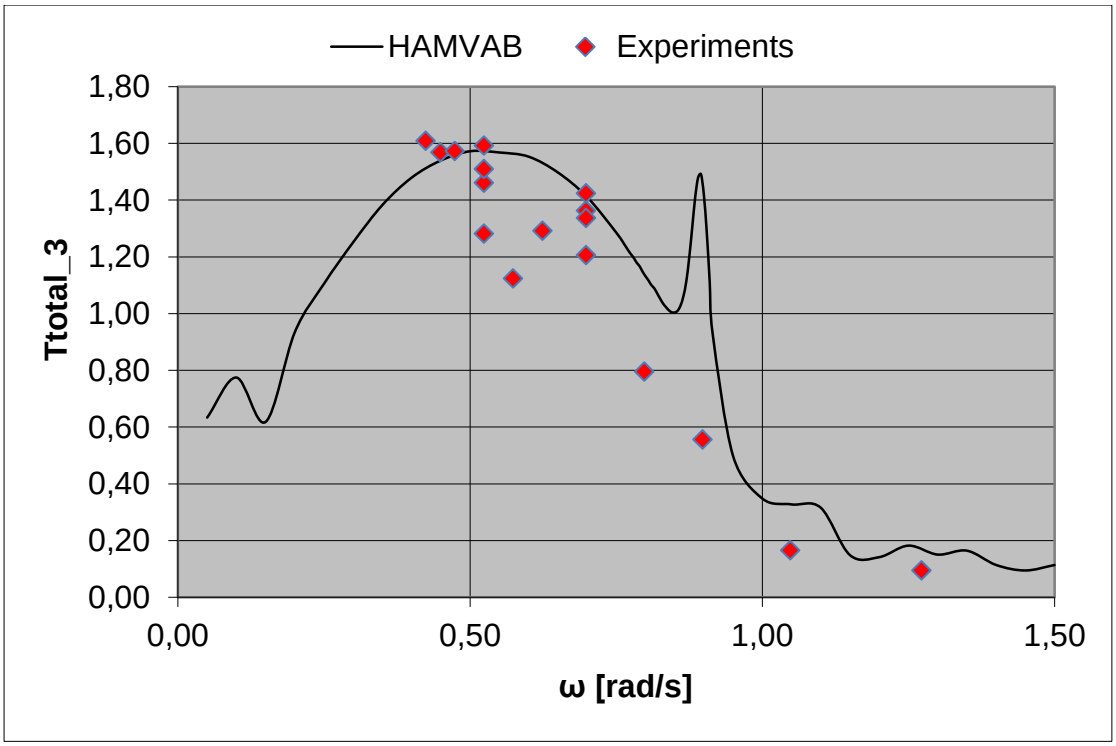

Figure 49. First order line tension for Line No. 3 [Mazarakos, 2017]

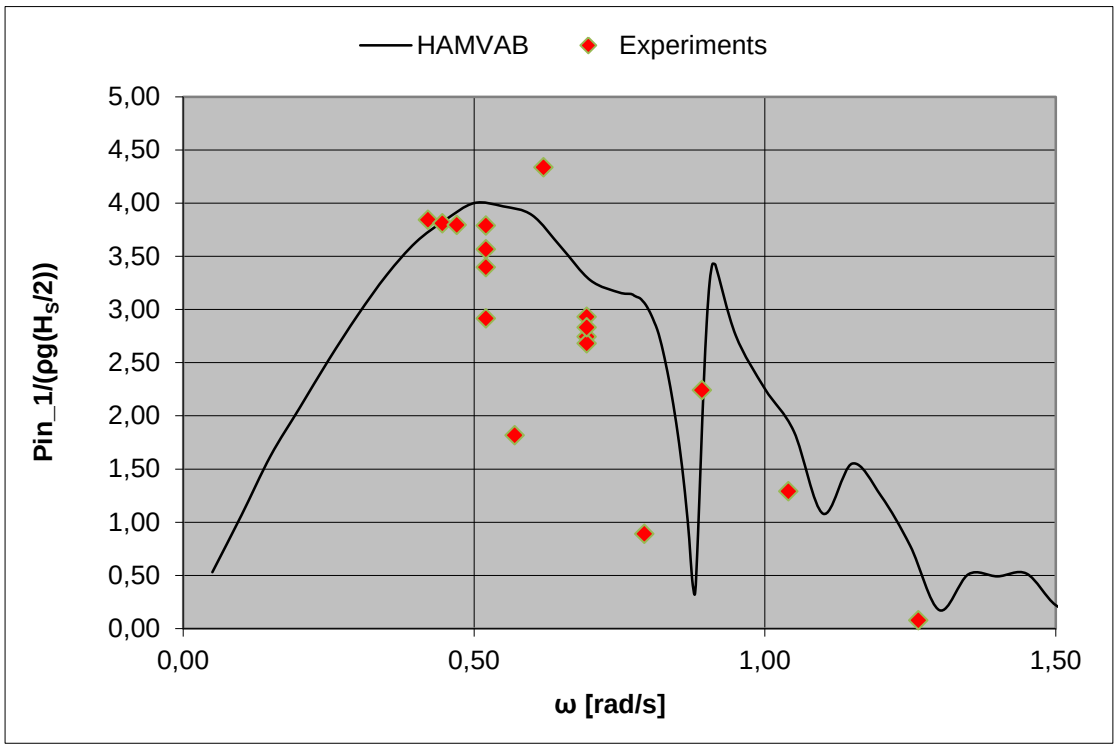

Figure 50. Pressure in chamber No. 1 [Mazarakos, 2017]

5.3 Comparison of different angles of incident wave

In the framework of the POSEIDON program, for the configuration with the WT of 5 MW, one more study took place concerning the comparison of different angles of incident wave

Here are the results, received by HAMVAB, in a diagram form:

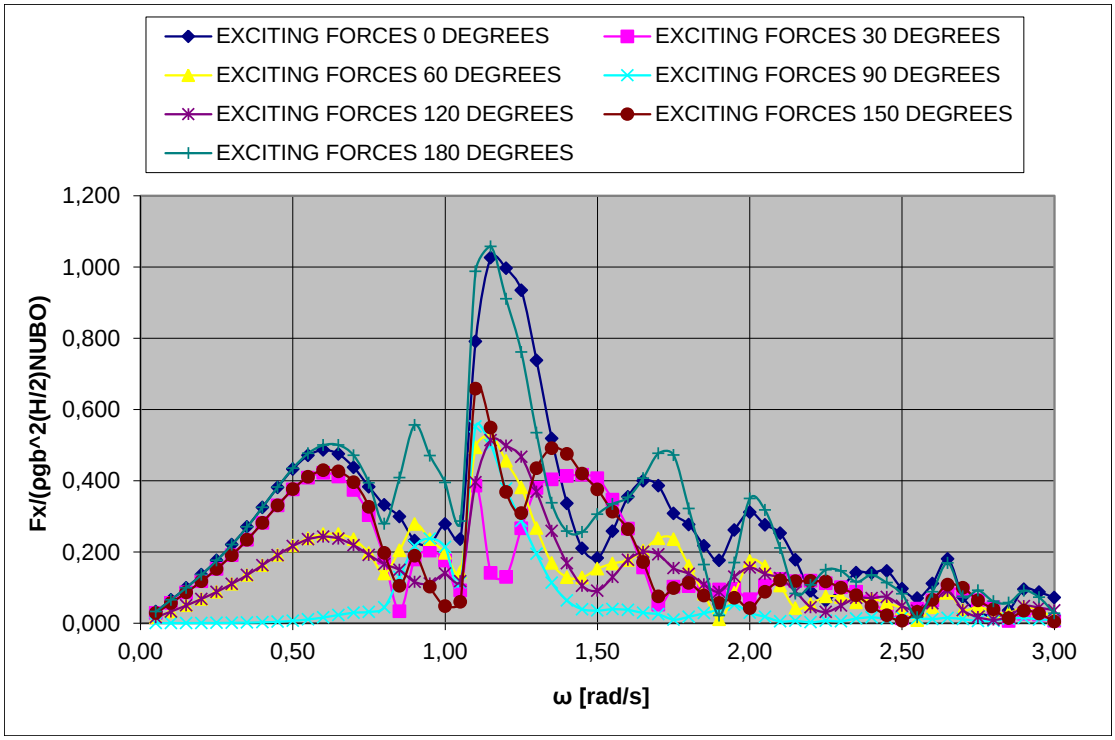

Figure 51. Exciting Force Fx for different angles of incidence

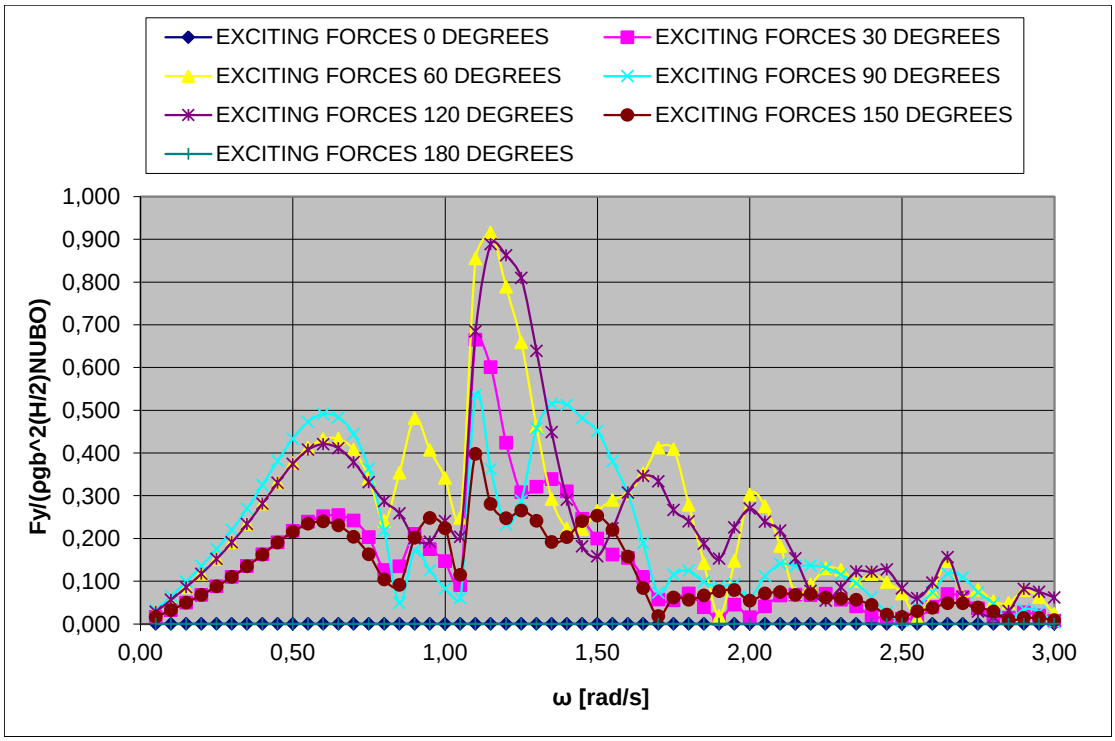

Figure 52. Exciting Force Fy for different angles of incidence

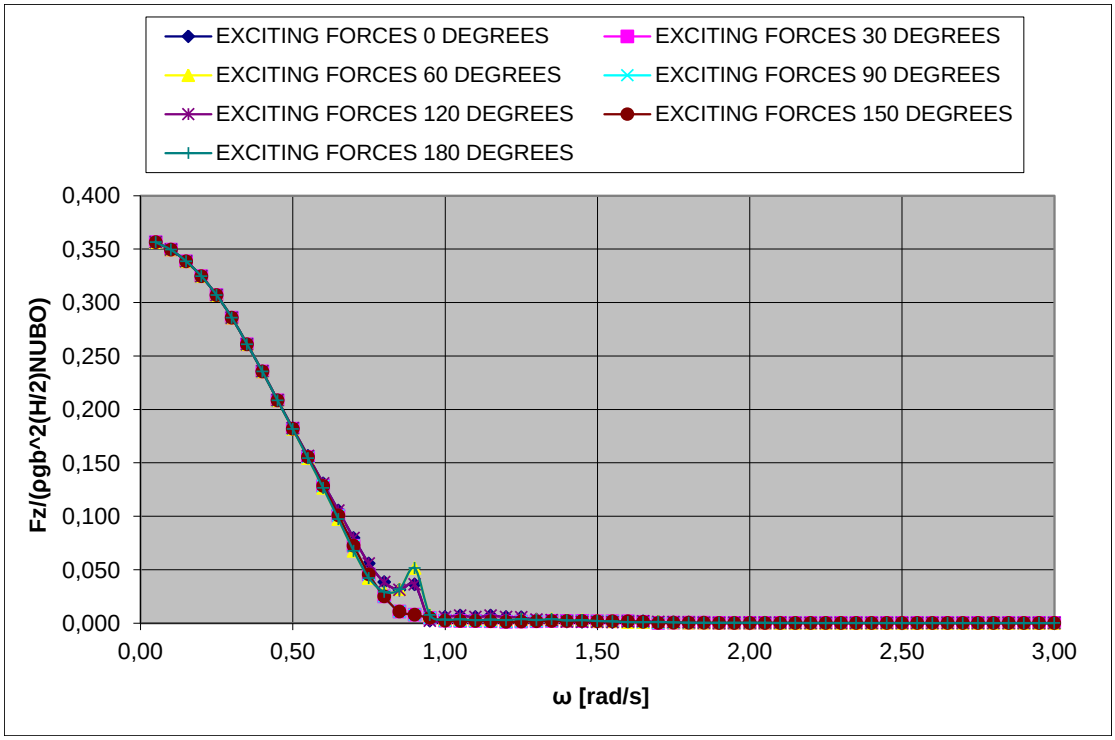

Figure 53. Exciting Force Fz for different angles of incidence

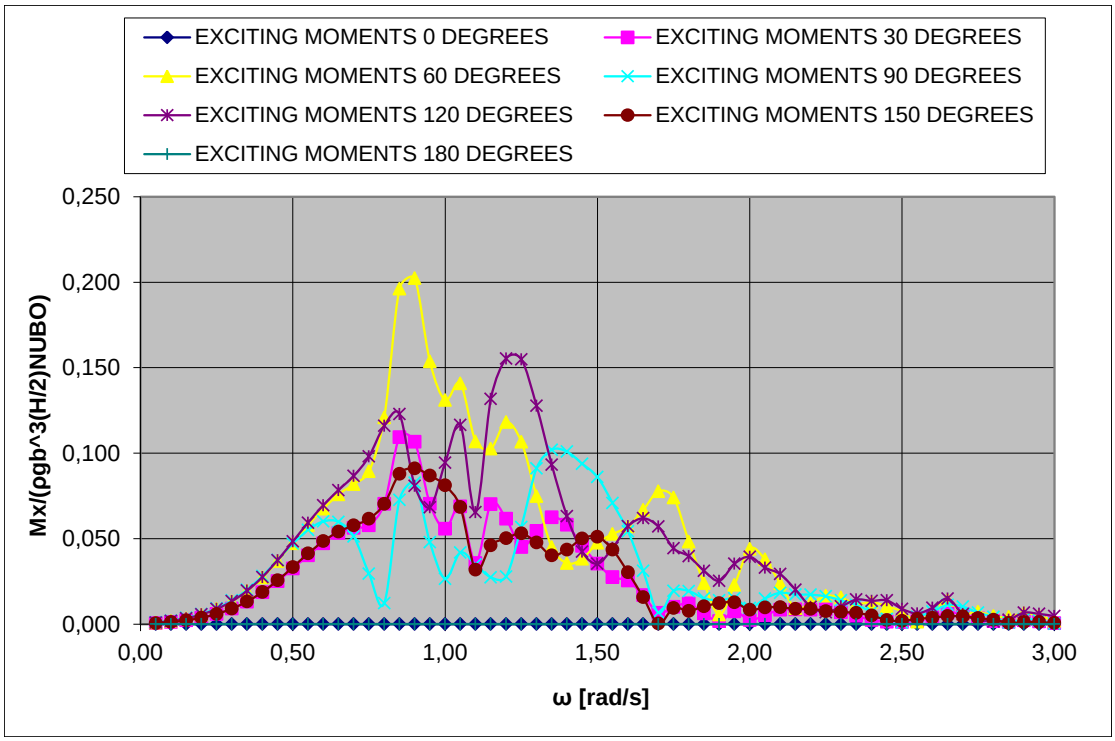

Figure 54. Exciting Moments Mx for different angles of incidence

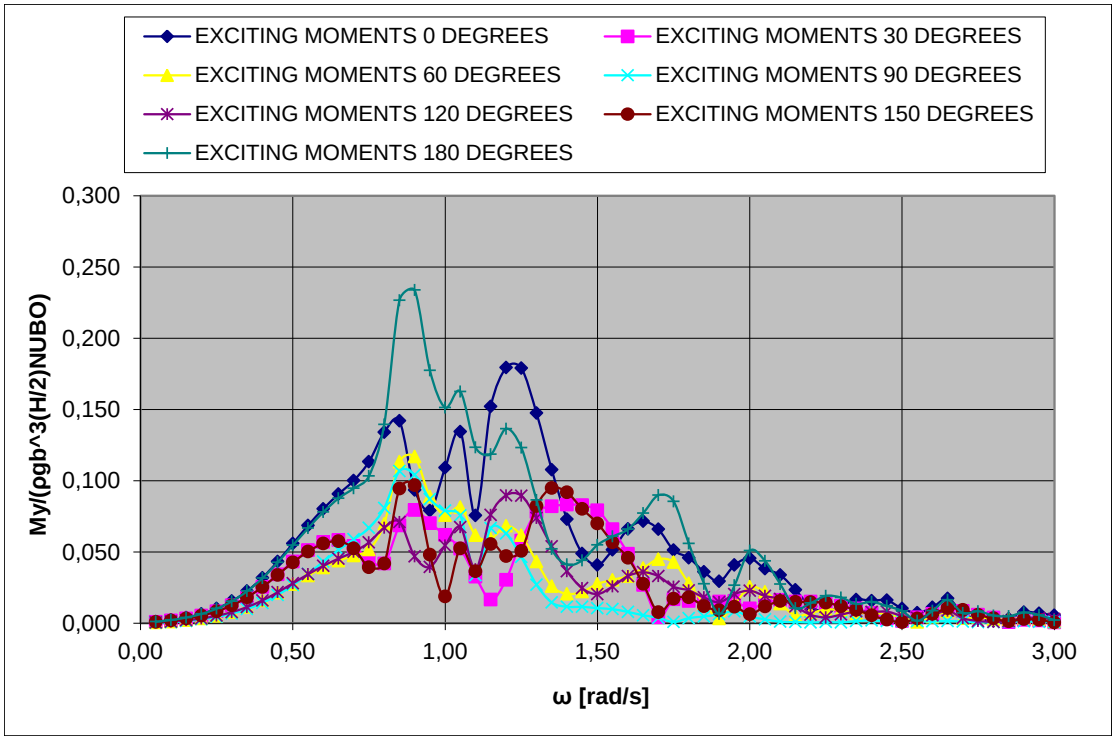

Figure 55. Exciting Moments My for different angles of incidence

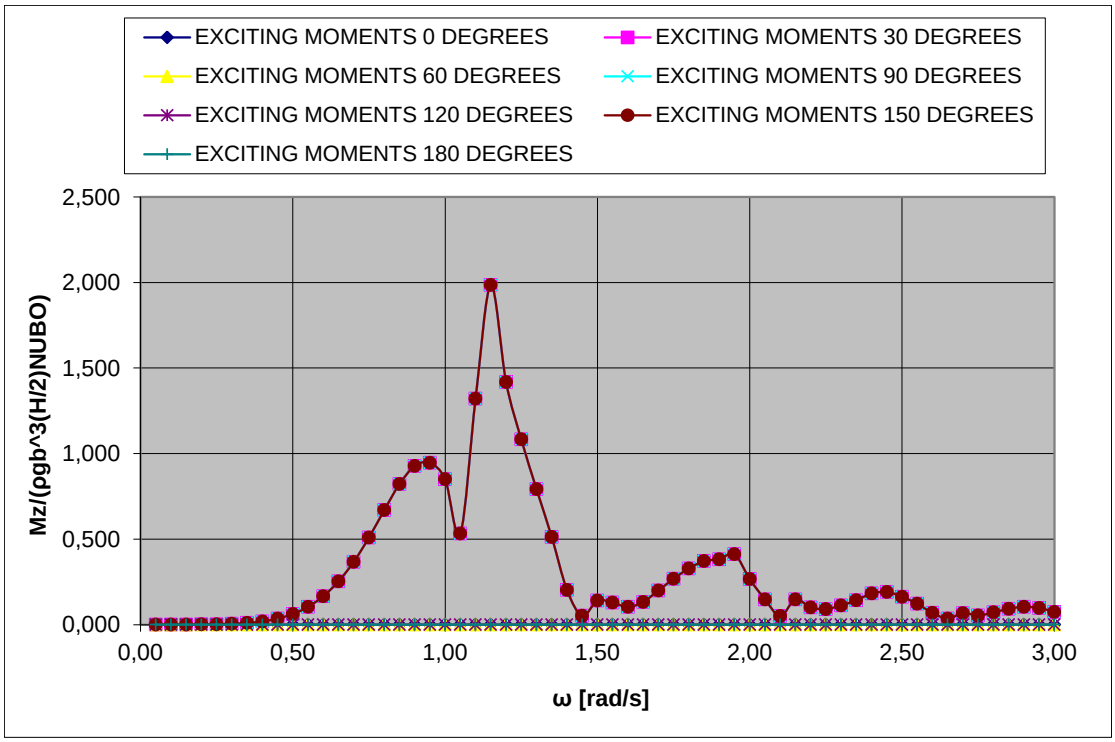

Figure 56. Exciting Moments Mz for different angles of incidence

6. Absorbed Power in Several Real Sea States

In this section, an attempt is made in order to calculate the amount of energy that the under study device with the 10 MW WT can produce in real sea conditions. In fact, three different sea areas were studied according to data provided by the technical report Environmental design conditions of the selected installation locations elaborated within the REFOS project (www.refos-project.eu), accurate measurements were made for the three different regions that took place over 31 years (from 1980 to 2010).

These three sea areas are the following:

1. Location L1 in the Aegean Sea with coordinates 35.34° N, 26.80° E
2. Location L2 in the southern part of Sicily Island with coordinates 37.30° N, 12.69° E
3. Location L3 in the North Sea with coordinates 59.42° N, 3.40° E

All these three locations correspond to water depths around 200m and we can say that as far as the available wind and wave potential that exists in these locations is exploitable, then they may be consider as suitable for offshore floating wind or wave farm development.

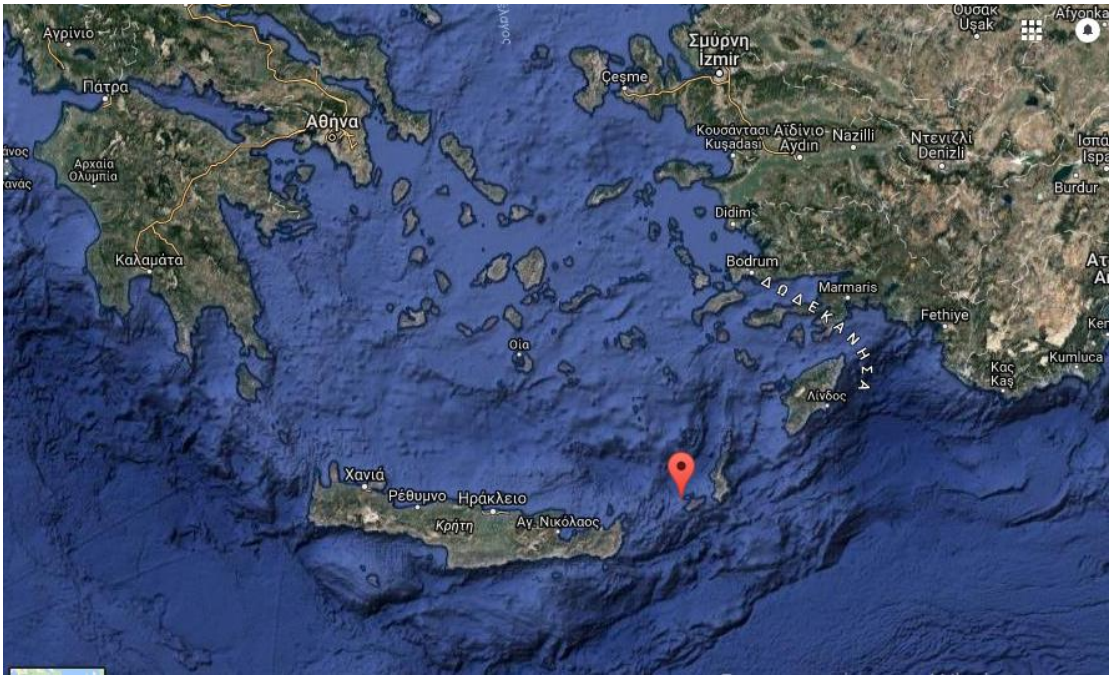

Figure 57. Location L1 in the Aegean Sea with coordinates 35.34° N, 26.80° E [www.google.gr]

Figure 58. Location L2 in the southern part of Sicily Island with coordinates 37.30° N, 12.69° E [www.google.gr]

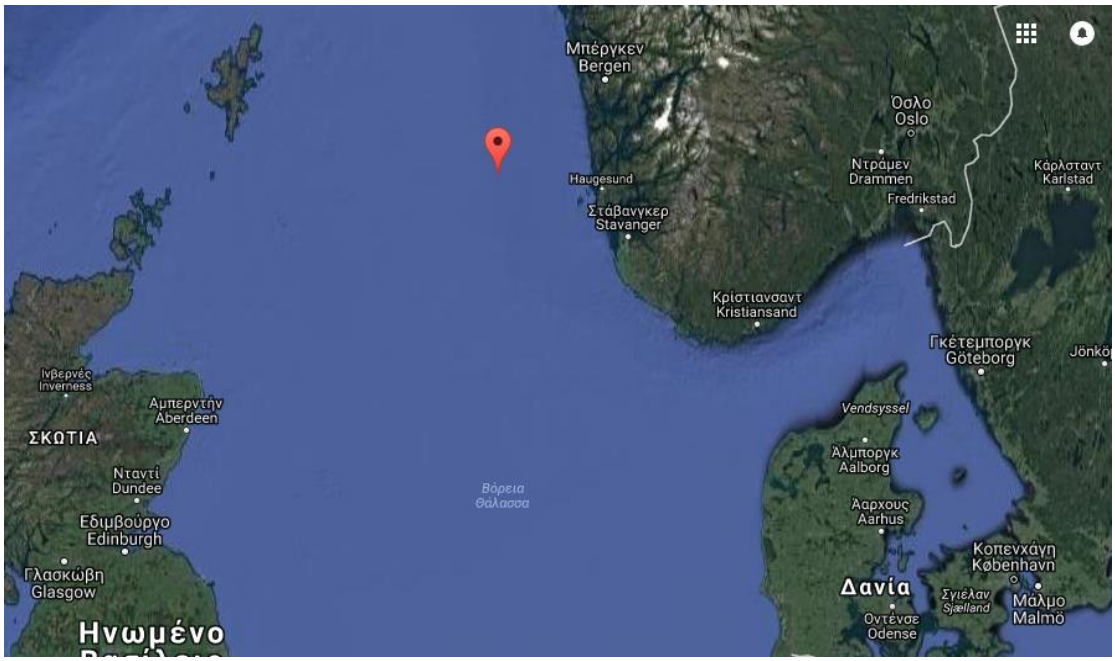

Figure 59. Location L3 in the North Sea with coordinates 59.42° N, 3.40° E [www.google.gr]

In the above report the significant wave height, wind speed and wave spectral peak period are presented. The particular time series that were analyzed at this project are referring to the following values:

- Significant wave height H_s, m
- Mean wave direction θ_H, deg, i.e., the direction from which the waves (sea-states) propagate
- Wind speed U_M, m/s
- Mean wind direction θ_U, deg, i.e., the direction from which the wind blows
- Spectral peak period T_p, sec

Firstly, for our study we will use the significant wave height H_s and the spectral peak period T_p in order to produce a Wave Spectrum in the domain of frequency.

Here, one can find the tables of the frequency of occurrence of H_s - T_p of the three locations (www.refos-project.eu):

Frequency of occurrence of each Tp-Hs pair								
	Hs	**0-1**	**1-2**	**2-3**	**3-4**	**4-5**	**5-6**	**6-7**
Tp								
2-3		221	0	0	0	0	0	0
3-4		6702	7	0	0	0	0	0
4-5		**24291**	1634	0	0	0	0	0
5-6		18937	11619	41	0	0	0	0
6-7		6869	11028	1498	1	0	0	0
7-8		462	2492	2328	223	1	0	0
8-9		100	463	747	517	30	0	0
9-10		24	58	76	121	57	7	0
10-11		0	9	8	5	3	3	0
11-12		0	1	1	0	0	0	0

Table 1. Frequency of occurrence of each H_S-T_P pair of Location 1

Frequency of occurrence of each Tp-Hs pair								
	Hs	**0-1**	**1-2**	**2-3**	**3-4**	**4-5**	**5-6**	**6-7**
Tp								
2-3		1282	0	0	0	0	0	0
3-4		16291	29	0	0	0	0	0
4-5		**21745**	1962	0	0	0	0	0
5-6		13591	6880	58	0	0	0	0
6-7		7622	7404	1481	0	0	0	0
7-8		1571	3363	2389	232	2	0	0
8-9		505	1113	1093	655	57	1	0
9-10		101	163	229	332	218	16	0
10-11		6	24	32	35	52	34	8
11-12		0	0	0	2	0	3	3

Table 2. Frequency of occurrence of each H_S-T_P pair of Location 2

Frequency of occurrence of each Tp-Hs pair											
	Hs	**0-1**	**1-2**	**2-3**	**3-4**	**4-5**	**5-6**	**6-7**	**7-8**	**8-9**	**9-10**
Tp											
3-4		51	2	0	0	0	0	0	0	0	0
4-5		1189	325	0	0	0	0	0	0	0	0
5-6		4103	3882	68	0	0	0	0	0	0	0
6-7		4136	**9074**	1960	31	0	0	0	0	0	0
7-8		2655	6836	5666	947	14	0	0	0	0	0
8-9		2469	5066	5430	3349	542	14	0	0	0	0
9-10		1713	4203	2722	2755	1598	306	12	0	0	0
10-11		956	2913	2154	1190	1091	640	185	10	0	0
11-12		530	1710	1639	721	390	326	194	67	4	0
12-13		236	930	793	459	181	129	84	55	22	7
13-14		59	417	318	229	82	53	43	26	9	2
14-15		5	142	124	69	41	24	9	7	1	1
15-16		1	47	56	7	8	2	0	0	0	0
16-17		1	18	22	8	3	0	0	0	0	0
17-18		0	0	5	11	0	0	0	0	0	0

Table 3. Frequency of occurrence of each H_S-T_P pair of Location 3

As we can notice from the tables 1, 2 and 3, the pair Hs-Tp with the highest occurrence in 31 years, is Tp=4-5 sec and Hs=0-1 m for Location 1 and 2 and Tp=6-7 sec and Hs=1-2 m for Location 3 respectively.

In order to calculate the real Power that can be produced at each location, the JONSWAP Spectrum, provided by DNV (DNV, 2007), will be used. Then we will estimate the exact power that would be produced for the period of 31 years. This Spectrum was calculated in Matlab. The formula for the JONSWAP ocean wave spectrum is the following:

$$S(\omega) = A_\gamma \frac{5}{16} \frac{\omega_p^4 \cdot H_S^2}{\omega^5} e^{-\frac{5\omega_p^4}{4\omega^4}} \gamma^a \qquad (33)$$

$a : e^{-\frac{(\omega-\omega_p)^2}{2\omega_p{}^2\sigma^2}}$

ω : Frequency in radians per second

ω_p : Peak frequency in radians per second

H_s : Significant wave height in m

A_γ: 1- 0,287ln(γ) is a normalizing factor

γ: non-dimensional peak shape parameter, $\begin{cases} 5 \ \ if \ \frac{\mathrm{Tp}}{\sqrt{\mathrm{Hs}}} \leq 3.6 \\ \exp(5.75 - 1.15\frac{\mathrm{Tp}}{\sqrt{\mathrm{Hs}}}) \ \ if \ 3.6 < \frac{\mathrm{Tp}}{\sqrt{\mathrm{Hs}}} < 5 \\ 1 \ if \ \frac{\mathrm{Tp}}{\sqrt{\mathrm{Hs}}} \geq 5 \end{cases}$

$\sigma : \begin{cases} 0{,}07 \ \ if \ \omega < \omega_p \\ 0{,}09 \ \ if \ \omega > \omega_p \end{cases}$

Instead of ω_p , we will use the ratio $2\pi/\omega_p$ that equals to the T_p which is provided by the technical report Environmental design conditions of the selected installation locations (www.refos-project.eu).

Following, one can find the curve of spectrum received from Matlab for the pair H_S-T_P that appeared most in Location 1 during the 31 years.

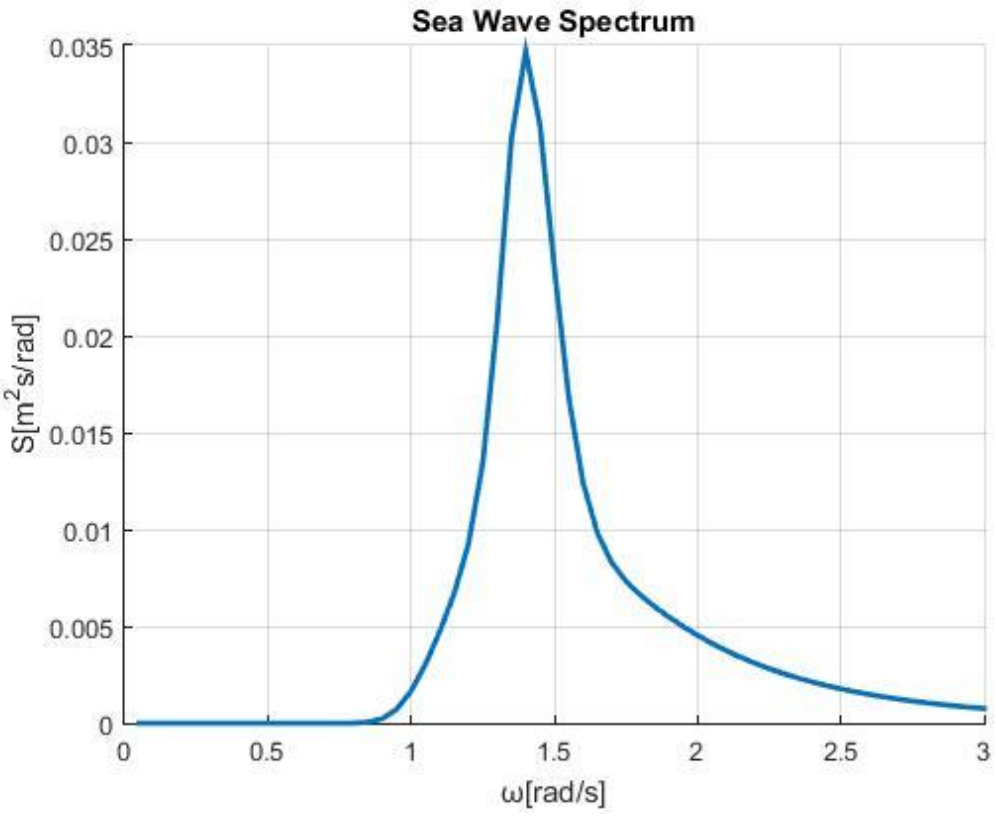

Figure 60. Indicative spectrum for the pair T_P=4-5 sec and H_S=0-1 m

HAMVAB gives us the non-dimensional absorbed energy that equals to:

$$\text{Eabs}' = \frac{\text{Eabs}}{\omega\ REF^2\ \rho\ g\ (\text{Hs}/2)^2} \quad (34)$$

Eabs : Dimensional absorbed energy

ω : Frequency in rad/s

REF : Outer Radius of each individual cylinder of the OWC configuration, equal to 15,5 m

ρ : 1025, Water Density in $^{kg}/_{m^3}$

g : 9.81, Acceleration due to gravity in $^{m}/_{s^2}$

Hs : Significant wave height in m

So, for the Power (divided with $(\text{Hs}/2)^2$) which has dimensions of KW/m^2 we have:

$$\text{Eabs} = (\text{Eabs}')\ \omega\ REF^2\ \rho\ g$$

The above absorbed power [power/(unit wave amplitude squared)] is the RAO of the OWC device. This power is also equal to the following (Cruz, 2010):

$$\text{Eabs} = \frac{1}{2} \cdot B_{ij}^{E} \cdot \omega^2 \cdot \left|\overline{x_j}\right|^2 \quad (35)$$

Where:

B_{ij}^{E} : Radiation damping matrix of the oscillation x_j

$\overline{x_j}$: Normalized complex amplitude of oscillation x_j with the wave amplitude A

Additionally, the result of multiplying the curve of Figure 60 with the values of Eabs received by HAMVAB, we conclude to the following curve:

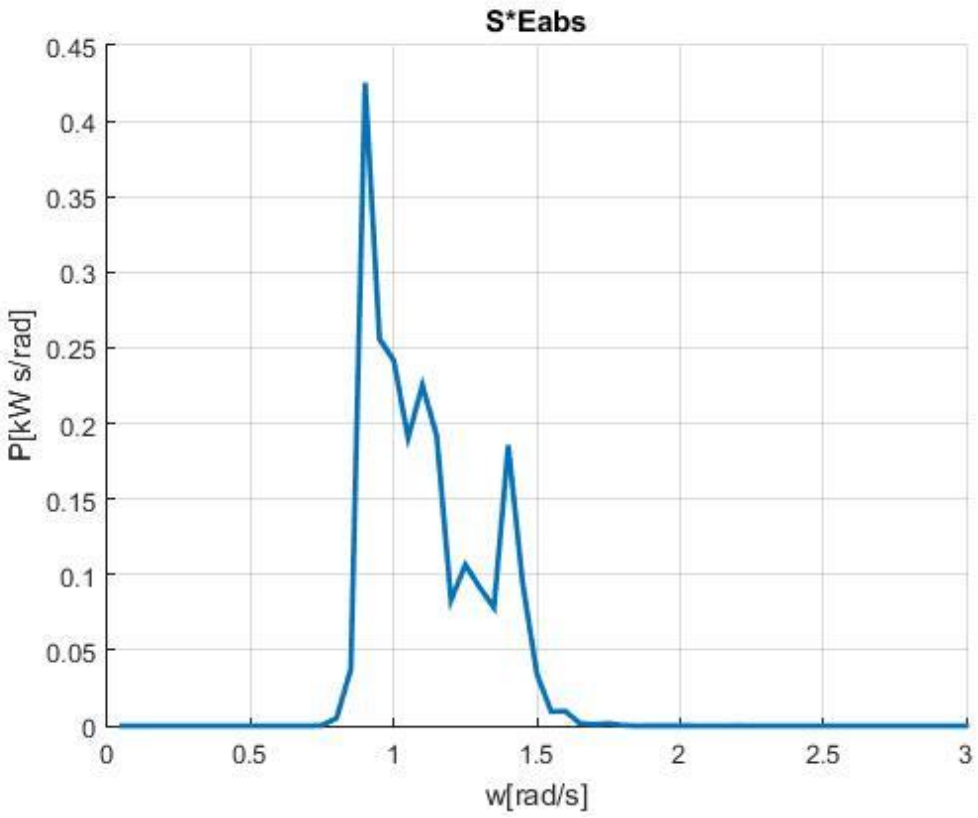

Figure 61. The product of multiplication between the Spectrum and Eabs for the pair Tp=4-5 sec and Hs=0-1 m in Location 1

And thus the real final P can be given by (Vijfhuizen, 2006, Cruz, 2010,):

$$P = \int 2\, Eabs\, S(\omega)\, d\omega \qquad (36)$$

This power corresponds to one specific cell of the Tables 1, 2, 3. Every cell represents a pair of significant wave height Hs and spectral peak period Tp. As a result, we will repeat the procedure for every cell and then we will multiply all the results with the Tables 1, 2, 3, in order to calculate the total absorbed power of every cell for 31 years. Finally, we will multiply with 3, because of the repeated three-hour measurements that we had during the day and we will divide with 31, so as to reach the annual final absorbed power of every cell and then we will compute the sum of all the cells that corresponds to the total final total power of each location for a specific angle of incidence. The integral of the eq. (36) was calculated with trapezoidal integration and the Simpson's rule also, in order to achieve more accurate results.

Finally we will study different angles of incidence, so that to find the optimum one.

Another brief study took place, referring to the power that is absorbed by the WT for a range of different wind speeds and a comparison of it with the corresponding most probable sea states. More specifically, we used data from the following tables:

Wind Speed(m/s)	2-4	4-6	6-8	8-10	10-12	12-14	14-16	16-18.62
Hs(m)	0,548	0,709	0,944	1,576	1,886	2,488	3,116	3,994
Tp(s)	3,777	3,792	4,906	4,906	6,256	6,914	7,573	8,331
Subsample Size	17292	24182	24565	15133	6527	2175	621	89

Table 4. Most probable values of Hs and Tp and subsample's size for various bins of the wind speed at Location 1 [www.refos-project.eu]

Wind Speed(m/s)	2-4	4-6	6-8	8-10	10-12	12-14	14-16	16-18	18-20,13
Hs(m)	0,335	0,756	0,865	1,335	1,982	2,83	3,824	4,897	6,186
Tp(s)	2,821	3,61	4,542	5,404	6,596	6,396	8,556	8,848	10,282
Subsample Size	30024	22419	17505	11100	6040	2479	806	184	27

Table 5. Most probable values of Hs and Tp and subsample's size for various bins of the wind speed at Location 2 [www.refos-project.eu]

Wind Speed(m/s)	2-4	4-6	6-8	8-10	10-12	12-14	14-16	16-18	18-20	20-23,19
Hs(m)	1,429	0,984	1,799	2,162	2,466	2,884	3,486	5,095	6,352	7,254
Tp(s)	5,806	5,682	5,584	5,548	7,129	7,735	8,297	9,695	10,442	11,102
Subsample Size	14199	16965	18597	16083	12134	7256	3691	1304	305	50

Table 6. Most probable values of Hs and Tp and subsample's size for various bins of the wind speed at Location 1 [www.refos-project.eu]

In addition, we used the following figure in order to receive the amount of the absorbed wind power over the wind speed.

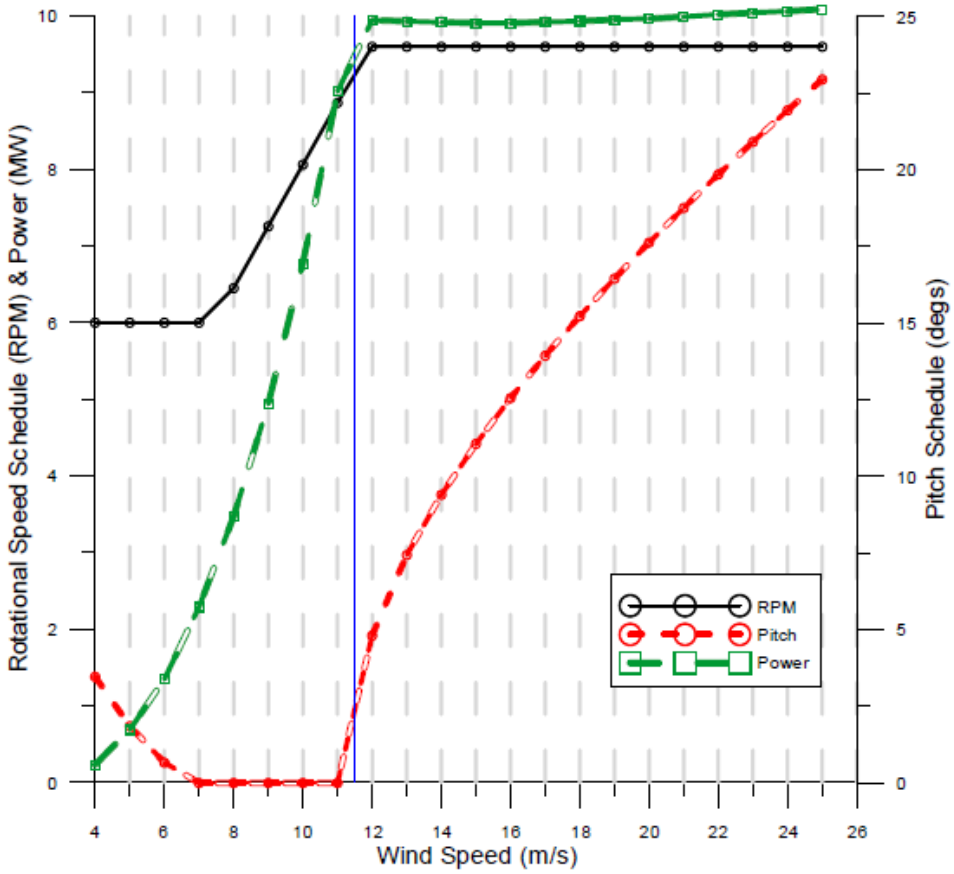

Figure 62. Turbine rotor speed, blade pitch and electrical power over the wind speed, of the 10 MW WT. The blue vertical line distinguishes the variable speed part from the variable pitch part[www.refos-project.eu]

Regarding the absorbed wave power of the sea states at these specific wind speed ranges, we will follow the same procedure that was described above.

7. Results

In this part of the thesis, the results concerning the wave power absorbed by the multi – purpose floating offshore energy platform for the 3 different examined areas are presented, as well as the results of the comparisons among the absorbed power from the WT and the OWC devices over some specific wind speeds at the same locations.

A first check was made on the different wind speeds, which the wind turbine is exposed to. We received seven different output files for seven different wind speeds respectively. As it seems at the below diagram, there are no significant differences in the RAO's of the Absorbed Wave Powers for different wind speeds.

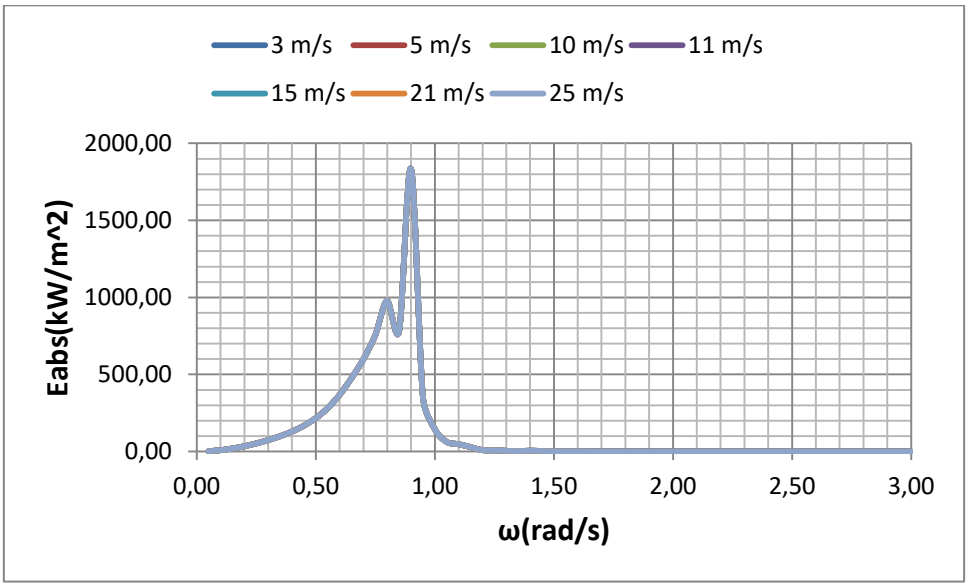

Figure 63. Absorbed wave power received by HAMVAB for several speeds of wind for the Mediterranean Sea

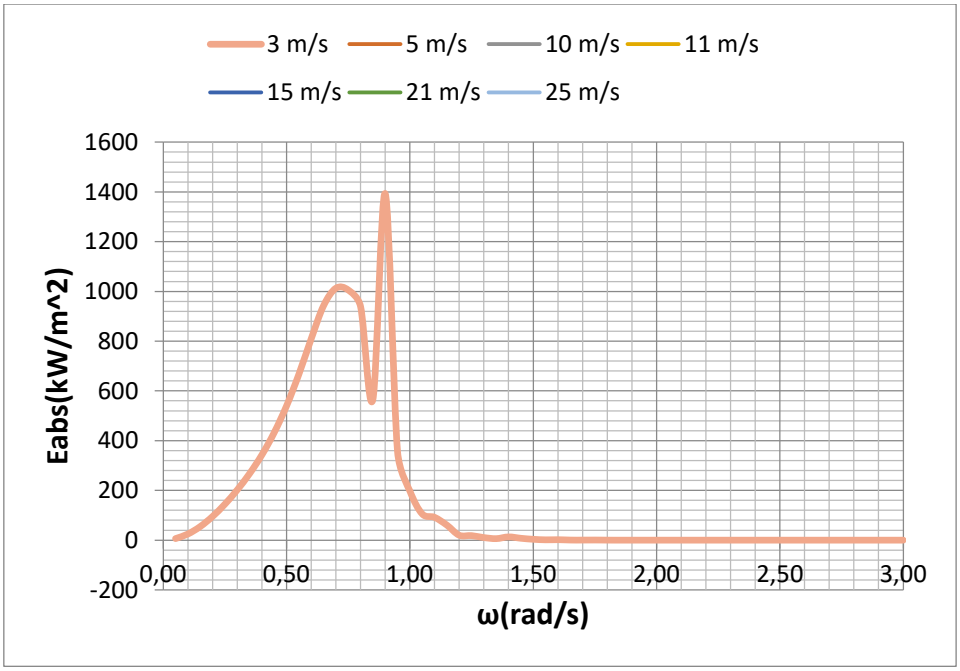

Figure 64. Absorbed wave power received by HAMVAB for several speeds of wind for the North Sea

Therefore, in the input file of HAMVAB we gave as wind speed the value of 11 m/s that is very close to operating speed, 11.4 m/s.

7.1 Location 1

According the eq. (36) for every pair H_S - T_P we calculated the integral of 2*Eabs*S(ω) with the use of Matlab and we found the absorbed powers for location 1 for various angles of incident waves. These absorbed wave powers for every cell are gathered at the following tables:

Absorbed Power from Matlab Code [kW]								
	Hs [m]	0-1	1-2	2-3	3-4	4-5	5-6	6-7
Tp [sec]								
2-3		0,00	0,00	0,00	0,00	0,01	0,01	0,02
3-4		0,01	0,08	0,21	0,42	0,70	1,04	1,45
4-5		0,31	2,01	5,45	10,69	17,67	26,39	36,86
5-6		3,65	28,94	61,03	119,62	197,75	295,40	412,58
6-7		10,37	87,33	303,30	628,66	1039,22	1552,41	2168,25
7-8		15,35	138,14	421,30	1060,15	1949,02	2911,50	**4066,48**
8-9		17,15	154,35	428,75	887,11	1565,32	2417,36	3380,59
9-10		16,82	151,42	420,61	824,40	1355,60	2024,33	2814,31
10-11		15,50	139,51	387,53	759,56	1250,57	1809,06	2480,15
11-12		13,86	124,73	346,48	679,11	1122,61	1656,65	2200,91

Table 7. Matlab results achieved by using Simpson's code for angle of incident wave 0 degrees

Absorbed Power from Matlab Code [kW]								
	Hs [m]	0-1	1-2	2-3	3-4	4-5	5-6	6-7
Tp [sec]								
2-3		0,00	0,00	0,00	0,00	0,01	0,01	0,02
3-4		0,01	0,08	0,21	0,41	0,68	1,02	1,42
4-5		0,29	1,91	5,19	10,18	16,82	25,13	35,10
5-6		3,28	26,16	55,98	109,72	181,37	270,94	378,42
6-7		9,40	80,04	272,99	566,73	936,84	1399,47	1954,63
7-8		14,19	127,67	388,22	973,99	1794,29	2680,35	**3743,63**
8-9		16,11	144,97	402,69	841,69	1508,21	2360,79	3304,49
9-10		15,99	143,95	399,86	783,73	1302,97	1966,95	2760,17
10-11		14,87	133,82	371,73	728,60	1200,02	1739,02	2380,93
11-12		13,39	120,47	334,63	655,87	1084,20	1601,95	2143,61

Table 8. Matlab results achieved by using trapezoidal integration for angle of incident wave 0 degrees

Absorbed Power from Matlab Code [kW]								
	Hs [m]	0-1	1-2	2-3	3-4	4-5	5-6	6-7
Tp [sec]								
2-3		0,00	0,00	0,00	0,01	0,01	0,01	0,02
3-4		0,01	0,07	0,18	0,36	0,59	0,88	1,23
4-5		0,35	2,19	5,91	11,58	19,15	28,61	39,96
5-6		2,66	22,34	53,28	104,43	172,63	257,88	360,18
6-7		7,49	67,43	209,80	433,87	717,21	1071,39	1496,40
7-8		11,81	106,27	320,57	793,70	1458,99	2179,47	**3044,06**
8-9		13,88	124,95	347,08	745,33	1367,62	2162,56	3028,33
9-10		14,13	127,17	353,25	692,37	1161,31	1762,09	2477,85
10-11		13,38	120,41	334,46	655,54	1080,84	1586,42	2201,78
11-12		12,22	109,94	305,39	598,57	989,48	1463,39	1963,00

Table 9. Matlab results achieved by using Simpson's code for angle of incident wave 30 degrees

Absorbed Power from Matlab Code [kW]								
	Hs [m]	**0-1**	**1-2**	**2-3**	**3-4**	**4-5**	**5-6**	**6-7**
Tp [sec]								
2-3		0,00	0,00	0,00	0,00	0,01	0,01	0,02
3-4		0,01	0,06	0,18	0,35	0,58	0,87	1,22
4-5		0,36	2,23	6,02	11,81	19,52	29,16	40,73
5-6		2,71	22,78	54,41	106,64	176,28	263,34	367,80
6-7		7,54	64,89	212,97	443,48	733,11	1095,13	1529,57
7-8		11,81	106,32	320,58	795,64	1468,80	2194,13	**3064,53**
8-9		13,86	124,74	346,49	742,71	1366,00	2171,27	3041,83
9-10		14,10	126,87	352,43	690,76	1162,22	1771,18	2502,13
10-11		13,35	120,13	333,69	654,02	1078,15	1576,55	2174,75
11-12		12,19	109,72	304,77	597,34	987,45	1461,31	1969,33

Table 10. Matlab results achieved by using trapezoidal integration for angle of incident wave 30 degrees

Absorbed Power from Matlab Code [kW]								
	Hs [m]	**0-1**	**1-2**	**2-3**	**3-4**	**4-5**	**5-6**	**6-7**
Tp [sec]								
2-3		0,00	0,00	0,00	0,00	0,01	0,01	0,01
3-4		0,01	0,06	0,16	0,32	0,53	0,79	1,10
4-5		0,29	1,85	5,04	9,87	16,32	24,38	34,05
5-6		4,39	33,97	66,16	129,67	214,35	320,20	447,22
6-7		12,66	103,90	374,41	778,92	1287,61	1923,46	2686,49
7-8		18,15	163,34	503,59	1299,56	2414,70	3607,15	**5038,08**
8-9		19,53	175,80	488,34	994,09	1718,53	2615,21	3653,95
9-10		18,57	167,12	464,23	909,89	1451,65	2109,54	2871,09
10-11		16,71	150,38	417,72	818,73	1345,60	1911,52	2580,79
11-12		14,69	132,18	367,15	719,62	1189,58	1752,14	2308,42

Table 11. Matlab results achieved by using Simpson's code for angle of incident wave 60 degrees

Absorbed Power from Matlab Code [kW]								
	Hs [m]	**0-1**	**1-2**	**2-3**	**3-4**	**4-5**	**5-6**	**6-7**
Tp [sec]								
2-3		0,00	0,00	0,00	0,00	0,01	0,01	0,01
3-4		0,01	0,06	0,16	0,32	0,52	0,78	1,09
4-5		0,27	1,74	4,73	9,26	15,31	22,87	31,94
5-6		3,96	30,69	60,34	118,27	195,50	292,05	407,90
6-7		11,51	97,56	338,11	705,04	1165,48	1741,03	2431,68
7-8		16,76	150,84	464,41	1200,60	2241,36	3348,21	**4676,42**
8-9		18,29	164,60	457,22	939,03	1645,45	2534,47	3544,07
9-10		17,58	158,20	439,43	861,29	1388,32	2038,94	2801,14
10-11		15,95	143,58	398,83	781,71	1285,20	1829,14	2467,18
11-12		14,12	127,07	352,97	691,82	1143,62	1686,54	2237,89

Table 12. Matlab results achieved by using trapezoidal integration for angle of incident wave 60 degrees

Absorbed Power from Matlab Code [kW]								
	Hs [m]	0-1	1-2	2-3	3-4	4-5	5-6	6-7
Tp [sec]								
2-3		0,00	0,00	0,00	0,00	0,01	0,01	0,01
3-4		0,01	0,06	0,18	0,35	0,58	0,86	1,20
4-5		0,35	2,15	5,82	11,41	18,85	28,16	39,34
5-6		2,66	22,33	53,26	104,40	172,58	257,80	360,06
6-7		7,49	67,40	209,85	434,12	717,62	1072,00	1497,26
7-8		11,80	106,18	320,31	793,04	1457,75	2177,63	**3041,48**
8-9		13,87	124,81	346,69	744,40	1365,71	2159,36	3023,84
9-10		14,11	127,00	352,78	691,45	1159,61	1759,32	2473,75
10-11		13,36	120,23	333,97	654,58	1079,24	1583,92	2198,13
11-12		12,20	109,77	304,92	597,64	987,94	1461,11	1959,83

Table 13. Matlab results achieved by using Simpson's code for angle of incident wave 90 degrees

Absorbed Power from Matlab Code [kW]								
	Hs [m]	0-1	1-2	2-3	3-4	4-5	5-6	6-7
Tp [sec]								
2-3		0,00	0,00	0,00	0,00	0,01	0,01	0,01
3-4		0,01	0,06	0,18	0,35	0,57	0,85	1,19
4-5		0,36	2,20	5,93	11,63	19,22	28,71	40,10
5-6		2,71	22,78	54,40	106,62	176,24	263,28	367,72
6-7		7,54	66,87	213,04	443,78	733,60	1095,87	1530,60
7-8		11,80	106,24	320,33	795,02	1467,65	2192,41	**3062,13**
8-9		13,84	124,60	346,11	741,81	1364,14	2168,13	3037,41
9-10		14,08	126,71	351,97	689,87	1160,55	1768,43	2498,04
10-11		13,33	119,95	333,21	653,08	1076,59	1574,12	2171,21
11-12		12,17	109,55	304,30	596,43	985,94	1459,06	1966,18

Table 14. Matlab results achieved by using trapezoidal integration for angle of incident wave 90 degrees

Absorbed Power from Matlab Code [kW]								
	Hs [m]	0-1	1-2	2-3	3-4	4-5	5-6	6-7
Tp [sec]								
2-3		0,00	0,00	0,00	0,00	0,01	0,01	0,01
3-4		0,01	0,07	0,21	0,41	0,67	1,00	1,40
4-5		0,30	1,98	5,37	10,53	17,41	26,01	36,33
5-6		3,64	28,88	60,87	119,31	197,23	294,63	411,51
6-7		10,35	87,19	302,94	627,97	1038,07	1550,70	2165,85
7-8		15,33	137,94	420,67	1058,59	1946,14	2907,20	**4060,47**
8-9		17,12	154,11	428,07	885,64	1562,59	2413,05	3374,55
9-10		16,80	151,17	419,92	823,04	1353,32	2020,88	2809,45
10-11		15,47	139,27	386,87	758,27	1248,44	1805,92	2475,76
11-12		13,84	124,52	345,89	677,94	1120,67	1653,79	2197,06

Table 15. Matlab results achieved by using Simpson's code for angle of incident wave 120 degrees

Absorbed Power from Matlab Code [kW]								
	Hs [m]	**0-1**	**1-2**	**2-3**	**3-4**	**4-5**	**5-6**	**6-7**
Tp [sec]								
2-3		0,00	0,00	0,00	0,00	0,01	0,01	0,01
3-4		0,01	0,07	0,20	0,40	0,66	0,98	1,37
4-5		0,29	1,88	5,11	10,02	16,57	24,75	34,57
5-6		3,27	26,10	55,82	109,40	180,85	270,16	377,33
6-7		9,39	80,04	272,62	566,01	935,64	1397,69	1952,14
7-8		14,16	127,47	387,60	972,43	1791,37	2676,00	**3737,55**
8-9		16,08	144,73	402,02	840,23	1505,52	2356,51	3298,50
9-10		15,97	143,70	399,17	782,38	1300,69	1963,48	2755,27
10-11		14,84	133,59	371,08	727,31	1197,90	1735,91	2376,61
11-12		13,36	120,25	334,04	654,71	1082,28	1599,10	2139,75

Table 16. Matlab results achieved by using trapezoidal integration for angle of incident wave 120 degrees

Absorbed Power from Matlab Code [kW]								
	Hs [m]	**0-1**	**1-2**	**2-3**	**3-4**	**4-5**	**5-6**	**6-7**
Tp [sec]								
2-3		0,00	0,00	0,00	0,00	0,01	0,01	0,01
3-4		0,01	0,06	0,18	0,35	0,58	0,86	1,20
4-5		0,35	2,16	5,82	11,41	18,86	28,18	39,35
5-6		2,66	22,34	53,28	104,43	172,64	257,89	360,19
6-7		7,49	67,43	209,96	434,35	718,01	1072,58	1498,06
7-8		11,80	106,22	320,43	793,34	1458,31	2178,47	**3042,66**
8-9		13,87	124,84	346,79	744,58	1365,99	2159,75	3024,37
9-10		14,11	127,03	352,86	691,61	1159,85	1759,65	2474,17
10-11		13,36	120,25	334,04	654,71	1079,46	1584,21	2198,51
11-12		12,20	109,79	304,97	597,75	988,12	1461,36	1960,15

Table 17. Matlab results achieved by using Simpson's code for angle of incident wave 150 degrees

Absorbed Power from Matlab Code [kW]								
	Hs [m]	**0-1**	**1-2**	**2-3**	**3-4**	**4-5**	**5-6**	**6-7**
Tp [sec]								
2-3		0,00	0,00	0,00	0,00	0,01	0,01	0,01
3-4		0,01	0,06	0,18	0,35	0,57	0,85	1,19
4-5		0,36	2,20	5,94	11,63	19,23	28,73	40,12
5-6		2,71	22,79	54,41	106,65	176,29	263,35	367,82
6-7		7,54	64,89	213,14	444,00	733,96	1096,41	1531,35
7-8		11,81	106,28	320,44	795,29	1468,14	2193,15	**3063,16**
8-9		13,85	124,63	346,20	741,97	1364,40	2168,48	3037,90
9-10		14,08	126,74	352,05	690,02	1160,78	1768,73	2498,43
10-11		13,33	119,98	333,27	653,21	1076,79	1574,38	2171,55
11-12		12,17	109,57	304,35	596,53	986,10	1459,30	1966,48

Table 18. Matlab results achieved by using trapezoidal integration for angle of incident wave 150 degrees

Absorbed Power from Matlab Code [kW]								
	Hs [m]	**0-1**	**1-2**	**2-3**	**3-4**	**4-5**	**5-6**	**6-7**
Tp [sec]								
2-3		0,00	0,00	0,00	0,00	0,01	0,01	0,01
3-4		0,01	0,06	0,17	0,33	0,54	0,81	1,14
4-5		0,29	1,87	5,10	9,99	16,51	24,67	34,46
5-6		4,40	34,04	66,37	130,08	215,03	321,22	448,64
6-7		12,67	103,03	374,92	780,09	1289,54	1926,35	2690,53
7-8		18,16	163,44	503,92	1300,47	2416,45	3609,75	**5041,72**
8-9		19,54	175,84	488,44	994,13	1718,22	2614,36	3652,73
9-10		18,57	167,10	464,17	909,77	1451,09	2108,23	2868,77
10-11		16,70	150,32	417,55	818,39	1345,02	1910,31	2578,69
11-12		14,68	132,09	366,92	719,17	1188,83	1751,00	2306,63

Table 19. Matlab results achieved by using Simpson's code for angle of incident wave 180 degrees

Absorbed Power from Matlab Code [kW]								
	Hs [m]	**0-1**	**1-2**	**2-3**	**3-4**	**4-5**	**5-6**	**6-7**
Tp [sec]								
2-3		0,00	0,00	0,00	0,00	0,01	0,01	0,01
3-4		0,01	0,06	0,17	0,33	0,54	0,80	1,12
4-5		0,27	1,76	4,79	9,38	15,51	23,16	32,35
5-6		3,96	30,76	60,54	118,67	196,16	293,03	409,27
6-7		11,52	97,69	338,62	706,23	1167,45	1743,96	2435,78
7-8		16,77	150,95	464,75	1201,56	2243,22	3350,98	**4680,29**
8-9		18,29	164,64	457,33	939,08	1645,16	2533,60	3542,83
9-10		17,58	158,18	439,38	861,18	1387,77	2037,62	2798,78
10-11		15,95	143,52	398,66	781,38	1284,64	1827,96	2465,16
11-12		14,11	126,99	352,74	691,38	1142,89	1685,41	2236,10

Table 20. Matlab results achieved by using trapezoidal integration for angle of incident wave 180 degrees

After that, we have the final absorbed power of every cell/pair H_S - T_P per year. As it was explained before, this absorbed wave power is named final because is a result of multiplication each of the above tables with the corresponding table with the frequency of occurrence of each H_S - T_P pair for location 1, divided with 31, that are the total years and multiplying with 3, because of the repeated three-hour measurements that we had during the day. This value differs from the Absorbed Power value of the previous tables because here is taking under consideration the frequency of occurrence of each pair and the total number of the years that measurements took place.

Absorbed Power from Matlab Code [kWh/year]								
	Hs [m]	**0-1**	**1-2**	**2-3**	**3-4**	**4-5**	**5-6**	**6-7**
Tp [sec]								
2-3		0,00	0,00	0,00	0,00	0,00	0,00	0,00
3-4		8,48	0,05	0,00	0,00	0,00	0,00	0,00
4-5		720,24	317,21	0,00	0,00	0,00	0,00	0,00
5-6		6680,06	32541,43	242,16	0,00	0,00	0,00	0,00
6-7		6893,12	93197,10	43968,53	60,84	0,00	0,00	0,00
7-8		686,27	33315,17	**94913,94**	22878,62	188,62	0,00	0,00
8-9		165,97	6915,87	30994,43	44384,32	4544,46	0,00	0,00
9-10		39,08	849,91	3093,54	9653,48	7477,67	1371,32	0,00
10-11		0,00	121,51	300,02	367,53	363,07	525,21	0,00
11-12		0,00	12,07	33,53	0,00	0,00	0,00	0,00

Table 21. Final results achieved by using Simpson's code for angle of incident wave 0 degrees

Absorbed Power from Matlab Code [kWh/year]								
	Hs [m]	**0-1**	**1-2**	**2-3**	**3-4**	**4-5**	**5-6**	**6-7**
Tp [sec]								
2-3		0,00	0,00	0,00	0,00	0,00	0,00	0,00
3-4		8,24	0,05	0,00	0,00	0,00	0,00	0,00
4-5		685,76	302,11	0,00	0,00	0,00	0,00	0,00
5-6		6002,99	29410,43	222,11	0,00	0,00	0,00	0,00
6-7		6251,69	85420,75	39574,96	54,84	0,00	0,00	0,00
7-8		634,25	30789,99	**87462,57**	21019,43	173,64	0,00	0,00
8-9		155,88	6495,60	29110,95	42111,72	4378,67	0,00	0,00
9-10		37,15	807,98	2940,93	9177,23	7187,35	1332,45	0,00
10-11		0,00	116,56	287,79	352,55	348,39	504,88	0,00
11-12		0,00	11,66	32,38	0,00	0,00	0,00	0,00

Table 22. Final results achieved by using trapezoidal integration for angle of incident wave 0 degrees

Absorbed Power from Matlab Code [kWh/year]								
	Hs [m]	**0-1**	**1-2**	**2-3**	**3-4**	**4-5**	**5-6**	**6-7**
Tp [sec]								
2-3		0,00	0,00	0,00	0,00	0,00	0,00	0,00
3-4		7,77	0,04	0,00	0,00	0,00	0,00	0,00
4-5		822,43	345,76	0,00	0,00	0,00	0,00	0,00
5-6		4876,00	25118,88	211,41	0,00	0,00	0,00	0,00
6-7		4980,19	71960,12	30414,67	41,99	0,00	0,00	0,00
7-8		527,93	25628,59	**72222,33**	17128,62	141,19	0,00	0,00
8-9		134,35	5598,50	25090,47	37290,70	3970,51	0,00	0,00
9-10		32,82	713,79	2598,09	8107,39	6405,92	1193,67	0,00
10-11		0,00	104,87	258,94	317,20	313,79	460,57	0,00
11-12		0,00	10,64	29,55	0,00	0,00	0,00	0,00

Table 23. Final results achieved by using Simpson's code for angle of incident wave 30 degrees

Absorbed Power from Matlab Code [kWh/year]								
	Hs [m]	**0-1**	**1-2**	**2-3**	**3-4**	**4-5**	**5-6**	**6-7**
Tp [sec]								
2-3		0,00	0,00	0,00	0,00	0,00	0,00	0,00
3-4		7,69	0,04	0,00	0,00	0,00	0,00	0,00
4-5		841,27	352,52	0,00	0,00	0,00	0,00	0,00
5-6		4968,09	25619,54	215,88	0,00	0,00	0,00	0,00
6-7		5014,34	69251,86	30874,37	42,92	0,00	0,00	0,00
7-8		528,19	25641,42	**72222,90**	17170,38	142,14	0,00	0,00
8-9		134,12	5588,95	25047,67	37159,35	3965,80	0,00	0,00
9-10		32,74	712,13	2592,06	8088,59	6410,95	1199,83	0,00
10-11		0,00	104,63	258,34	316,46	313,01	457,71	0,00
11-12		0,00	10,62	29,49	0,00	0,00	0,00	0,00

Table 24. Final results achieved by using trapezoidal integration for angle of incident wave 30 degrees

Absorbed Power from Matlab Code [kWh/year]								
	Hs [m]	**0-1**	**1-2**	**2-3**	**3-4**	**4-5**	**5-6**	**6-7**
Tp [sec]								
2-3		0,00	0,00	0,00	0,00	0,00	0,00	0,00
3-4		6,66	0,04	0,00	0,00	0,00	0,00	0,00
4-5		669,97	293,02	0,00	0,00	0,00	0,00	0,00
5-6		8052,55	38191,29	262,49	0,00	0,00	0,00	0,00
6-7		8412,97	110889,01	54276,84	75,38	0,00	0,00	0,00
7-8		811,42	39390,53	**113454,75**	28045,37	233,68	0,00	0,00
8-9		189,03	7877,06	35302,16	49736,82	4989,27	0,00	0,00
9-10		43,13	938,04	3414,33	10654,52	8007,51	1429,04	0,00
10-11		0,00	130,97	323,39	396,16	390,66	554,96	0,00
11-12		0,00	12,79	35,53	0,00	0,00	0,00	0,00

Table 25. Final results achieved by using Simpson's code for angle of incident wave 60 degrees

Absorbed Power from Matlab Code [kWh/year]								
	Hs [m]	**0-1**	**1-2**	**2-3**	**3-4**	**4-5**	**5-6**	**6-7**
Tp [sec]								
2-3		0,00	0,00	0,00	0,00	0,00	0,00	0,00
3-4		6,51	0,04	0,00	0,00	0,00	0,00	0,00
4-5		632,74	275,11	0,00	0,00	0,00	0,00	0,00
5-6		7249,40	34505,70	239,41	0,00	0,00	0,00	0,00
6-7		7648,62	104113,60	49014,39	68,23	0,00	0,00	0,00
7-8		749,34	36377,18	**104627,03**	25909,78	216,91	0,00	0,00
8-9		176,99	7375,10	33052,57	46981,63	4777,12	0,00	0,00
9-10		40,82	887,94	3231,96	10085,41	7658,17	1381,22	0,00
10-11		0,00	125,05	308,77	378,25	373,12	531,04	0,00
11-12		0,00	12,30	34,16	0,00	0,00	0,00	0,00

Table 26. Final results achieved by using trapezoidal integration for angle of incident wave 60 degrees

Absorbed Power from Matlab Code [kWh/year]								
	Hs [m]	**0-1**	**1-2**	**2-3**	**3-4**	**4-5**	**5-6**	**6-7**
Tp [sec]								
2-3		0,00	0,00	0,00	0,00	0,00	0,00	0,00
3-4		7,52	0,04	0,00	0,00	0,00	0,00	0,00
4-5		817,99	340,68	0,00	0,00	0,00	0,00	0,00
5-6		4875,02	25112,96	211,34	0,00	0,00	0,00	0,00
6-7		4978,23	71931,72	30421,78	42,01	0,00	0,00	0,00
7-8		527,50	25607,61	**72163,05**	17114,30	141,07	0,00	0,00
8-9		134,20	5592,21	25062,28	37243,87	3964,98	0,00	0,00
9-10		32,77	712,84	2594,63	8096,60	6396,54	1191,80	0,00
10-11		0,00	104,72	258,56	316,73	313,33	459,85	0,00
11-12		0,00	10,62	29,51	0,00	0,00	0,00	0,00

Table 27. Final results achieved by using Simpson's code for angle of incident wave 90 degrees

Absorbed Power from Matlab Code [kWh/year]								
	Hs [m]	**0-1**	**1-2**	**2-3**	**3-4**	**4-5**	**5-6**	**6-7**
Tp [sec]								
2-3		0,00	0,00	0,00	0,00	0,00	0,00	0,00
3-4		7,45	0,04	0,00	0,00	0,00	0,00	0,00
4-5		836,95	347,39	0,00	0,00	0,00	0,00	0,00
5-6		4967,59	25616,11	215,83	0,00	0,00	0,00	0,00
6-7		5012,75	71363,30	30884,48	42,95	0,00	0,00	0,00
7-8		527,79	25622,01	**72168,08**	17157,10	142,03	0,00	0,00
8-9		133,98	5582,94	25020,74	37114,31	3960,42	0,00	0,00
9-10		32,70	711,21	2588,71	8078,13	6401,76	1197,97	0,00
10-11		0,00	104,48	257,97	316,01	312,56	457,00	0,00
11-12		0,00	10,60	29,45	0,00	0,00	0,00	0,00

Table 28. Final results achieved by using trapezoidal integration for angle of incident wave 90 degrees

Absorbed Power from Matlab Code [kWh/year]								
	Hs [m]	**0-1**	**1-2**	**2-3**	**3-4**	**4-5**	**5-6**	**6-7**
Tp [sec]								
2-3		0,00	0,00	0,00	0,00	0,00	0,00	0,00
3-4		8,15	0,05	0,00	0,00	0,00	0,00	0,00
4-5		714,63	312,80	0,00	0,00	0,00	0,00	0,00
5-6		6668,66	32478,21	241,53	0,00	0,00	0,00	0,00
6-7		6883,36	93056,11	43916,09	60,77	0,00	0,00	0,00
7-8		685,24	33265,33	**94773,29**	22844,99	188,34	0,00	0,00
8-9		165,70	6904,91	30945,33	44310,66	4536,56	0,00	0,00
9-10		39,01	848,51	3088,43	9637,53	7465,09	1368,98	0,00
10-11		0,00	121,30	299,51	366,90	362,45	524,30	0,00
11-12		0,00	12,05	33,47	0,00	0,00	0,00	0,00

Table 29. Final results achieved by using Simpson's code for angle of incident wave 120 degrees

Absorbed Power from Matlab Code [kWh/year]								
	Hs [m]	0-1	1-2	2-3	3-4	4-5	5-6	6-7
Tp [sec]								
2-3		0,00	0,00	0,00	0,00	0,00	0,00	0,00
3-4		7,92	0,05	0,00	0,00	0,00	0,00	0,00
4-5		680,16	297,69	0,00	0,00	0,00	0,00	0,00
5-6		5991,32	29345,91	221,47	0,00	0,00	0,00	0,00
6-7		6241,81	85420,75	39521,02	54,77	0,00	0,00	0,00
7-8		633,22	30740,06	**87321,65**	20985,58	173,36	0,00	0,00
8-9		155,62	6484,68	29062,00	42038,72	4370,85	0,00	0,00
9-10		37,08	806,58	2935,84	9161,36	7174,78	1330,10	0,00
10-11		0,00	116,35	287,29	351,93	347,78	503,97	0,00
11-12		0,00	11,64	32,33	0,00	0,00	0,00	0,00

Table 30. Final results achieved by using trapezoidal integration for angle of incident wave 120 degrees

Absorbed Power from Matlab Code [kWh/year]								
	Hs [m]	0-1	1-2	2-3	3-4	4-5	5-6	6-7
Tp [sec]								
2-3		0,00	0,00	0,00	0,00	0,00	0,00	0,00
3-4		7,52	0,04	0,00	0,00	0,00	0,00	0,00
4-5		818,17	340,81	0,00	0,00	0,00	0,00	0,00
5-6		4877,42	25124,17	211,41	0,00	0,00	0,00	0,00
6-7		4980,46	71963,92	30437,50	42,03	0,00	0,00	0,00
7-8		527,68	25616,67	**72189,39**	17120,87	141,13	0,00	0,00
8-9		134,24	5593,81	25069,43	37252,99	3965,78	0,00	0,00
9-10		32,78	713,01	2595,24	8098,53	6397,89	1192,02	0,00
10-11		0,00	104,74	258,61	316,80	313,39	459,93	0,00
11-12		0,00	10,62	29,51	0,00	0,00	0,00	0,00

Table 31. Final results achieved by using Simpson's code for angle of incident wave 150 degrees

Absorbed Power from Matlab Code [kWh/year]								
	Hs [m]	0-1	1-2	2-3	3-4	4-5	5-6	6-7
Tp [sec]								
2-3		0,00	0,00	0,00	0,00	0,00	0,00	0,00
3-4		7,46	0,04	0,00	0,00	0,00	0,00	0,00
4-5		837,10	347,53	0,00	0,00	0,00	0,00	0,00
5-6		4969,76	25626,14	215,89	0,00	0,00	0,00	0,00
6-7		5014,73	69257,55	30898,88	42,97	0,00	0,00	0,00
7-8		527,96	25630,09	**72191,46**	17162,88	142,08	0,00	0,00
8-9		134,01	5584,38	25027,17	37122,56	3961,15	0,00	0,00
9-10		32,71	711,37	2589,27	8079,87	6402,99	1198,17	0,00
10-11		0,00	104,50	258,01	316,07	312,62	457,08	0,00
11-12		0,00	10,60	29,45	0,00	0,00	0,00	0,00

Table 32. Final results achieved by using trapezoidal integration for angle of incident wave 150 degrees

Absorbed Power from Matlab Code [kWh/year]								
	Hs [m]	**0-1**	**1-2**	**2-3**	**3-4**	**4-5**	**5-6**	**6-7**
Tp [sec]								
2-3		0,00	0,00	0,00	0,00	0,00	0,00	0,00
3-4		6,84	0,04	0,00	0,00	0,00	0,00	0,00
4-5		675,21	296,46	0,00	0,00	0,00	0,00	0,00
5-6		8068,62	38278,43	263,33	0,00	0,00	0,00	0,00
6-7		8422,60	109960,95	54351,29	75,49	0,00	0,00	0,00
7-8		811,93	39415,61	**113529,25**	28065,08	233,85	0,00	0,00
8-9		189,08	7878,77	35309,83	49738,75	4988,39	0,00	0,00
9-10		43,12	937,92	3413,88	10653,11	8004,41	1428,16	0,00
10-11		0,00	130,92	323,26	395,99	390,49	554,61	0,00
11-12		0,00	12,78	35,51	0,00	0,00	0,00	0,00

Table 33. Final results achieved by using Simpson's code for angle of incident wave 180 degrees

Absorbed Power from Matlab Code [kWh/year]								
	Hs [m]	**0-1**	**1-2**	**2-3**	**3-4**	**4-5**	**5-6**	**6-7**
Tp [sec]								
2-3		0,00	0,00	0,00	0,00	0,00	0,00	0,00
3-4		6,69	0,04	0,00	0,00	0,00	0,00	0,00
4-5		637,89	278,55	0,00	0,00	0,00	0,00	0,00
5-6		7265,23	34591,01	240,22	0,00	0,00	0,00	0,00
6-7		7658,24	104252,53	49089,20	68,35	0,00	0,00	0,00
7-8		749,87	36402,54	**104702,92**	25930,38	217,09	0,00	0,00
8-9		177,03	7376,89	33060,58	46984,05	4776,26	0,00	0,00
9-10		40,82	887,82	3231,54	10084,11	7655,10	1380,32	0,00
10-11		0,00	125,00	308,64	378,09	372,96	530,70	0,00
11-12		0,00	12,29	34,14	0,00	0,00	0,00	0,00

Table 34. Final results achieved by using trapezoidal integration for angle of incident wave 180 degrees

Furthermore, the sum of all the cells that corresponds to the total final power per year depending on the angle of incidence of Location 1, if we apply Simpson's code is:

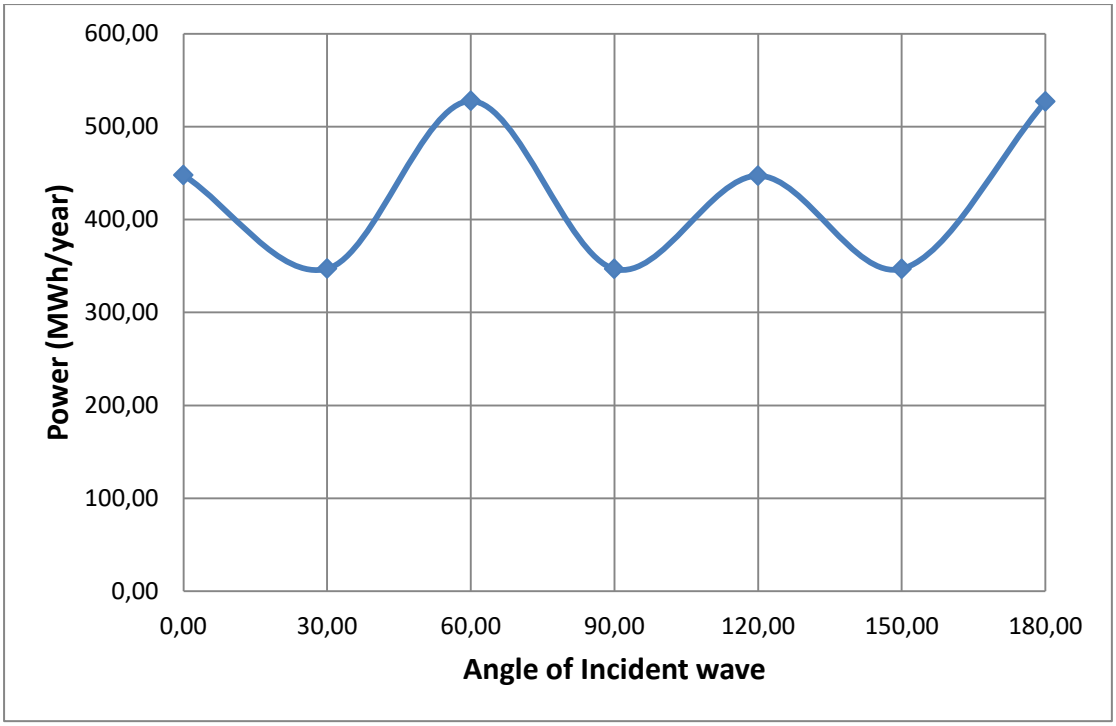

Figure 65. Total amount of Power per year for Location 1 depending on the angle of incidence achieved by using Simpson's code

Respectively, the sum of all the cells that corresponds to the total final power per year depending on the angle of incidence of Location 1, if we apply trapezoid integration is:

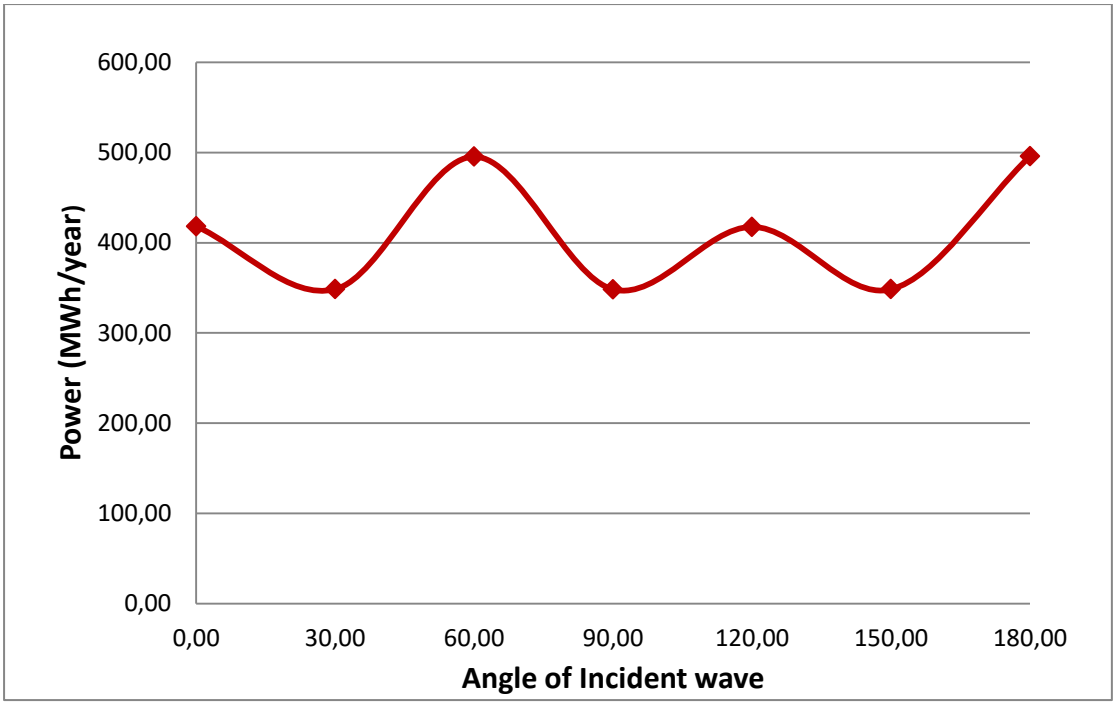

Figure 66. Total amount of Power per year for Location 1 depending on the angle of incidence achieved by using trapezoidal integration

Finally, if we compare the two integration methods, we have the following diagram:

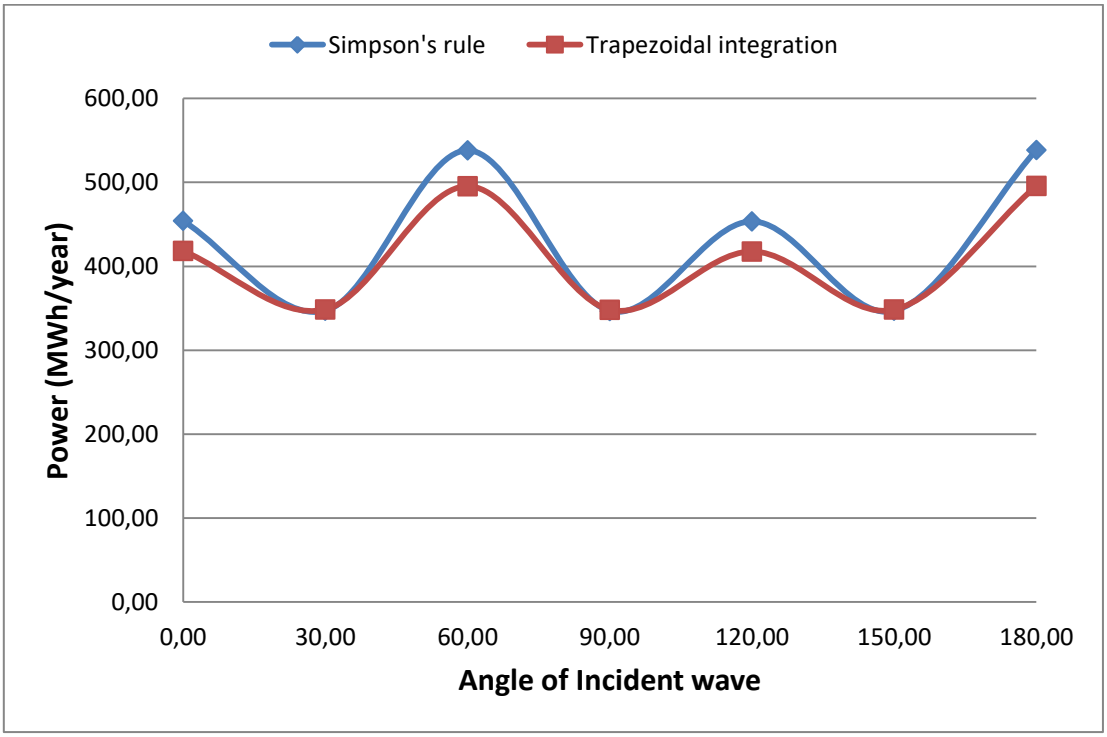

Figure 67. Comparison of two Integration methods

7.2 Location 2

For the Location 2 the calculated absorbed powers received by HAMVAB for every pair Hs - Tp and for various angles of incidence are the following tables:

Absorbed Power from Matlab Code [kW]								
	Hs [m]	**0-1**	**1-2**	**2-3**	**3-4**	**4-5**	**5-6**	**6-7**
Tp [sec]								
2-3		0,00	0,00	0,00	0,00	0,01	0,01	0,02
3-4		0,01	0,08	0,21	0,42	0,70	1,04	1,45
4-5		0,31	2,01	5,45	10,69	17,67	26,39	36,86
5-6		3,65	28,94	61,03	119,62	197,75	295,40	412,58
6-7		10,37	93,33	303,30	628,66	1039,22	1552,41	2168,25
7-8		15,35	138,14	421,30	1060,15	1949,02	2911,50	**4066,48**
8-9		17,15	154,35	428,75	887,11	1565,32	2417,36	3380,59
9-10		16,82	151,42	420,61	824,40	1355,60	2024,33	2814,31
10-11		15,50	139,51	387,53	759,56	1250,57	1809,06	2480,15
11-12		13,86	124,73	346,48	679,11	1122,61	1656,65	2200,91

Table 35. Matlab results achieved by using Simpson's code for angle of incident wave 0 degrees

Absorbed Power from Matlab Code [kW]								
	Hs [m]	**0-1**	**1-2**	**2-3**	**3-4**	**4-5**	**5-6**	**6-7**
Tp [sec]								
2-3		0,00	0,00	0,00	0,00	0,01	0,01	0,02
3-4		0,01	0,08	0,21	0,41	0,68	1,02	1,42
4-5		0,29	1,91	5,19	10,18	16,82	25,13	35,10
5-6		3,28	26,16	55,98	109,72	181,37	270,94	378,42
6-7		9,40	84,64	272,99	566,73	936,84	1399,47	1954,63
7-8		14,19	127,67	388,22	973,99	1794,29	2680,35	**3743,63**
8-9		16,11	144,97	402,69	841,69	1508,21	2360,79	3304,49
9-10		15,99	143,95	399,86	783,73	1302,97	1966,95	2760,17
10-11		14,87	133,82	371,73	728,60	1200,02	1739,02	2380,93
11-12		13,39	120,47	334,63	655,87	1084,20	1601,95	2143,61

Table 36. Matlab results achieved by using trapezoidal integration for angle of incident wave 0 degrees

Absorbed Power from Matlab Code [kW]								
	Hs [m]	**0-1**	**1-2**	**2-3**	**3-4**	**4-5**	**5-6**	**6-7**
Tp [sec]								
2-3		0,00	0,00	0,00	0,01	0,01	0,01	0,02
3-4		0,01	0,07	0,18	0,36	0,59	0,88	1,23
4-5		0,35	2,19	5,91	11,58	19,15	28,61	39,96
5-6		2,66	22,34	53,28	104,43	172,63	257,88	360,18
6-7		7,49	67,43	209,80	433,87	717,21	1071,39	1496,40
7-8		11,81	106,27	320,57	793,70	1458,99	2179,47	**3044,06**
8-9		13,88	124,95	347,08	745,33	1367,62	2162,56	3028,33
9-10		14,13	127,17	353,25	692,37	1161,31	1762,09	2477,85
10-11		13,38	120,41	334,46	655,54	1080,84	1586,42	2201,78
11-12		12,22	109,94	305,39	598,57	989,48	1463,39	1963,00

Table 37. Matlab results achieved by using Simpson's code for angle of incident wave 30 degrees

Absorbed Power from Matlab Code [kW]								
	Hs [m]	**0-1**	**1-2**	**2-3**	**3-4**	**4-5**	**5-6**	**6-7**
Tp [sec]								
2-3		0,00	0,00	0,00	0,00	0,01	0,01	0,02
3-4		0,01	0,06	0,18	0,35	0,58	0,87	1,22
4-5		0,36	2,23	6,02	11,81	19,52	29,16	40,73
5-6		2,71	22,78	54,41	106,64	176,28	263,34	367,80
6-7		7,54	67,89	212,97	443,48	733,11	1095,13	1529,57
7-8		11,81	106,32	320,58	795,64	1468,80	2194,13	**3064,53**
8-9		13,86	124,74	346,49	742,71	1366,00	2171,27	3041,83
9-10		14,10	126,87	352,43	690,76	1162,22	1771,18	2502,13
10-11		13,35	120,13	333,69	654,02	1078,15	1576,55	2174,75
11-12		12,19	109,72	304,77	597,34	987,45	1461,31	1969,33

Table 38. Matlab results achieved by using trapezoidal integration for angle of incident wave 30 degrees

Absorbed Power from Matlab Code [kW]								
	Hs [m]	**0-1**	**1-2**	**2-3**	**3-4**	**4-5**	**5-6**	**6-7**
Tp [sec]								
2-3		0,00	0,00	0,00	0,00	0,01	0,01	0,01
3-4		0,01	0,06	0,16	0,32	0,53	0,79	1,10
4-5		0,29	1,85	5,04	9,87	16,32	24,38	34,05
5-6		4,39	33,97	66,16	129,67	214,35	320,20	447,22
6-7		12,66	113,90	374,41	778,92	1287,61	1923,46	2686,49
7-8		18,15	163,34	503,59	1299,56	2414,70	3607,15	**5038,08**
8-9		19,53	175,80	488,34	994,09	1718,53	2615,21	3653,95
9-10		18,57	167,12	464,23	909,89	1451,65	2109,54	2871,09
10-11		16,71	150,38	417,72	818,73	1345,60	1911,52	2580,79
11-12		14,69	132,18	367,15	719,62	1189,58	1752,14	2308,42

Table 39. Matlab results achieved by using Simpson's code for angle of incident wave 60 degrees

Absorbed Power from Matlab Code [kW]								
	Hs [m]	0-1	1-2	2-3	3-4	4-5	5-6	6-7
Tp [sec]								
2-3		0,00	0,00	0,00	0,00	0,01	0,01	0,01
3-4		0,01	0,06	0,16	0,32	0,52	0,78	1,09
4-5		0,27	1,74	4,73	9,26	15,31	22,87	31,94
5-6		3,96	30,69	60,34	118,27	195,50	292,05	407,90
6-7		11,51	103,56	338,11	705,04	1165,48	1741,03	2431,68
7-8		16,76	150,84	464,41	1200,60	2241,36	3348,21	**4676,42**
8-9		18,29	164,60	457,22	939,03	1645,45	2534,47	3544,07
9-10		17,58	158,20	439,43	861,29	1388,32	2038,94	2801,14
10-11		15,95	143,58	398,83	781,71	1285,20	1829,14	2467,18
11-12		14,12	127,07	352,97	691,82	1143,62	1686,54	2237,89

Table 40. Matlab results achieved by using trapezoidal integration for angle of incident wave 60 degrees

Absorbed Power from Matlab Code [kW]								
	Hs [m]	0-1	1-2	2-3	3-4	4-5	5-6	6-7
Tp [sec]								
2-3		0,00	0,00	0,00	0,00	0,01	0,01	0,01
3-4		0,01	0,06	0,18	0,35	0,58	0,86	1,20
4-5		0,35	2,15	5,82	11,41	18,85	28,16	39,34
5-6		2,66	22,33	53,26	104,40	172,58	257,80	360,06
6-7		7,49	67,40	209,85	434,12	717,62	1072,00	1497,26
7-8		11,80	106,18	320,31	793,04	1457,75	2177,63	**3041,48**
8-9		13,87	124,81	346,69	744,40	1365,71	2159,36	3023,84
9-10		14,11	127,00	352,78	691,45	1159,61	1759,32	2473,75
10-11		13,36	120,23	333,97	654,58	1079,24	1583,92	2198,13
11-12		12,20	109,77	304,92	597,64	987,94	1461,11	1959,83

Table 41. Matlab results achieved by using Simpson's code for angle of incident wave 90 degrees

Absorbed Power from Matlab Code [kW]								
	Hs [m]	0-1	1-2	2-3	3-4	4-5	5-6	6-7
Tp [sec]								
2-3		0,00	0,00	0,00	0,00	0,01	0,01	0,01
3-4		0,01	0,06	0,18	0,35	0,57	0,85	1,19
4-5		0,36	2,20	5,93	11,63	19,22	28,71	40,10
5-6		2,71	22,78	54,40	106,62	176,24	263,28	367,72
6-7		7,54	67,87	213,04	443,78	733,60	1095,87	1530,60
7-8		11,80	106,24	320,33	795,02	1467,65	2192,41	**3062,13**
8-9		13,84	124,60	346,11	741,81	1364,14	2168,13	3037,41
9-10		14,08	126,71	351,97	689,87	1160,55	1768,43	2498,04
10-11		13,33	119,95	333,21	653,08	1076,59	1574,12	2171,21
11-12		12,17	109,55	304,30	596,43	985,94	1459,06	1966,18

Table 42. Matlab results achieved by using trapezoidal integration for angle of incident wave 90 degrees

Absorbed Power from Matlab Code [kW]								
	Hs [m]	**0-1**	**1-2**	**2-3**	**3-4**	**4-5**	**5-6**	**6-7**
Tp [sec]								
2-3		0,00	0,00	0,00	0,00	0,01	0,01	0,01
3-4		0,01	0,07	0,21	0,41	0,67	1,00	1,40
4-5		0,30	1,98	5,37	10,53	17,41	26,01	36,33
5-6		3,64	28,88	60,87	119,31	197,23	294,63	411,51
6-7		10,35	93,19	302,94	627,97	1038,07	1550,70	2165,85
7-8		15,33	137,94	420,67	1058,59	1946,14	2907,20	**4060,47**
8-9		17,12	154,11	428,07	885,64	1562,59	2413,05	3374,55
9-10		16,80	151,17	419,92	823,04	1353,32	2020,88	2809,45
10-11		15,47	139,27	386,87	758,27	1248,44	1805,92	2475,76
11-12		13,84	124,52	345,89	677,94	1120,67	1653,79	2197,06

Table 43. Matlab results achieved by using Simpson's code for angle of incident wave 120 degrees

Absorbed Power from Matlab Code [kW]								
	Hs [m]	**0-1**	**1-2**	**2-3**	**3-4**	**4-5**	**5-6**	**6-7**
Tp [sec]								
2-3		0,00	0,00	0,00	0,00	0,01	0,01	0,01
3-4		0,01	0,07	0,20	0,40	0,66	0,98	1,37
4-5		0,29	1,88	5,11	10,02	16,57	24,75	34,57
5-6		3,27	26,10	55,82	109,40	180,85	270,16	377,33
6-7		9,39	84,51	272,62	566,01	935,64	1397,69	1952,14
7-8		14,16	127,47	387,60	972,43	1791,37	2676,00	**3737,55**
8-9		16,08	144,73	402,02	840,23	1505,52	2356,51	3298,50
9-10		15,97	143,70	399,17	782,38	1300,69	1963,48	2755,27
10-11		14,84	133,59	371,08	727,31	1197,90	1735,91	2376,61
11-12		13,36	120,25	334,04	654,71	1082,28	1599,10	2139,75

Table 44. Matlab results achieved by using trapezoidal integration for angle of incident wave 120 degrees

Absorbed Power from Matlab Code [kW]								
	Hs [m]	**0-1**	**1-2**	**2-3**	**3-4**	**4-5**	**5-6**	**6-7**
Tp [sec]								
2-3		0,00	0,00	0,00	0,00	0,01	0,01	0,01
3-4		0,01	0,06	0,18	0,35	0,58	0,86	1,20
4-5		0,35	2,16	5,82	11,41	18,86	28,18	39,35
5-6		2,66	22,34	53,28	104,43	172,64	257,89	360,19
6-7		7,49	67,43	209,96	434,35	718,01	1072,58	1498,06
7-8		11,80	106,22	320,43	793,34	1458,31	2178,47	**3042,66**
8-9		13,87	124,84	346,79	744,58	1365,99	2159,75	3024,37
9-10		14,11	127,03	352,86	691,61	1159,85	1759,65	2474,17
10-11		13,36	120,25	334,04	654,71	1079,46	1584,21	2198,51
11-12		12,20	109,79	304,97	597,75	988,12	1461,36	1960,15

Table 45. Matlab results achieved by using Simpson's code for angle of incident wave 150 degrees

Absorbed Power from Matlab Code [kW]								
	Hs [m]	0-1	1-2	2-3	3-4	4-5	5-6	6-7
Tp [sec]								
2-3		0,00	0,00	0,00	0,00	0,01	0,01	0,01
3-4		0,01	0,06	0,18	0,35	0,57	0,85	1,19
4-5		0,36	2,20	5,94	11,63	19,23	28,73	40,12
5-6		2,71	22,79	54,41	106,65	176,29	263,35	367,82
6-7		7,54	67,89	213,14	444,00	733,96	1096,41	1531,35
7-8		11,81	106,28	320,44	795,29	1468,14	2193,15	**3063,16**
8-9		13,85	124,63	346,20	741,97	1364,40	2168,48	3037,90
9-10		14,08	126,74	352,05	690,02	1160,78	1768,73	2498,43
10-11		13,33	119,98	333,27	653,21	1076,79	1574,38	2171,55
11-12		12,17	109,57	304,35	596,53	986,10	1459,30	1966,48

Table 46. Matlab results achieved by using trapezoidal integration for angle of incident wave 150 degrees

Absorbed Power from Matlab Code [kW]								
	Hs [m]	0-1	1-2	2-3	3-4	4-5	5-6	6-7
Tp [sec]								
2-3		0,00	0,00	0,00	0,00	0,01	0,01	0,01
3-4		0,01	0,06	0,17	0,33	0,54	0,81	1,14
4-5		0,29	1,87	5,10	9,99	16,51	24,67	34,46
5-6		4,40	34,04	66,37	130,08	215,03	321,22	448,64
6-7		12,67	114,03	374,92	780,09	1289,54	1926,35	2690,53
7-8		18,16	163,44	503,92	1300,47	2416,45	3609,75	**5041,72**
8-9		19,54	175,84	488,44	994,13	1718,22	2614,36	3652,73
9-10		18,57	167,10	464,17	909,77	1451,09	2108,23	2868,77
10-11		16,70	150,32	417,55	818,39	1345,02	1910,31	2578,69
11-12		14,68	132,09	366,92	719,17	1188,83	1751,00	2306,63

Table 47. Matlab results achieved by using Simpson's code for angle of incident wave 180 degrees

Absorbed Power from Matlab Code [kW]								
	Hs [m]	0-1	1-2	2-3	3-4	4-5	5-6	6-7
Tp [sec]								
2-3		0,00	0,00	0,00	0,00	0,01	0,01	0,01
3-4		0,01	0,06	0,17	0,33	0,54	0,80	1,12
4-5		0,27	1,76	4,79	9,38	15,51	23,16	32,35
5-6		3,96	30,76	60,54	118,67	196,16	293,03	409,27
6-7		11,52	103,69	338,62	706,23	1167,45	1743,96	2435,78
7-8		16,77	150,95	464,75	1201,56	2243,22	3350,98	**4680,29**
8-9		18,29	164,64	457,33	939,08	1645,16	2533,60	3542,83
9-10		17,58	158,18	439,38	861,18	1387,77	2037,62	2798,78
10-11		15,95	143,52	398,66	781,38	1284,64	1827,96	2465,16
11-12		14,11	126,99	352,74	691,38	1142,89	1685,41	2236,10

Table 48. Matlab results achieved by using trapezoidal integration for angle of incident wave 180 degrees

After that, we have the final absorbed power of every cell/pair H_S - T_P for location 2 per year.

Absorbed Power from Matlab Code [kWh/year]								
	Hs [m]	**0-1**	**1-2**	**2-3**	**3-4**	**4-5**	**5-6**	**6-7**
Tp [sec]								
2-3		0,01	0,00	0,00	0,00	0,00	0,00	0,00
3-4		20,61	0,22	0,00	0,00	0,00	0,00	0,00
4-5		644,75	380,88	0,00	0,00	0,00	0,00	0,00
5-6		4794,25	19268,87	342,57	0,00	0,00	0,00	0,00
6-7		7648,76	66869,95	43469,55	0,00	0,00	0,00	0,00
7-8		2333,61	44959,44	**97400,95**	23801,97	377,23	0,00	0,00
8-9		838,14	16624,97	45350,62	56231,59	8634,48	233,94	0,00
9-10		164,45	2388,54	9321,33	26487,22	28598,81	3134,45	0,00
10-11		9,00	324,02	1200,09	2572,70	6293,19	5952,40	1920,11
11-12		0,00	0,00	0,00	131,44	0,00	480,96	638,97

Table 49. Final results achieved by using Simpson's code for angle of incident wave 0 degrees

Absorbed Power from Matlab Code [kWh/year]								
	Hs [m]	**0-1**	**1-2**	**2-3**	**3-4**	**4-5**	**5-6**	**6-7**
Tp [sec]								
2-3		0,01	0,00	0,00	0,00	0,00	0,00	0,00
3-4		20,04	0,21	0,00	0,00	0,00	0,00	0,00
4-5		613,89	362,75	0,00	0,00	0,00	0,00	0,00
5-6		4308,32	17414,90	314,21	0,00	0,00	0,00	0,00
6-7		6937,02	60647,53	39125,85	0,00	0,00	0,00	0,00
7-8		2156,73	41551,65	**89754,33**	21867,75	347,28	0,00	0,00
8-9		787,20	15614,69	42594,73	53352,38	8319,47	228,46	0,00
9-10		156,33	2270,70	8861,47	25180,51	27488,45	3045,60	0,00
10-11		8,63	310,82	1151,17	2467,82	6038,81	5721,94	1843,30
11-12		0,00	0,00	0,00	126,94	0,00	465,08	622,34

Table 50. Final results achieved by using trapezoidal integration for angle of incident wave 0 degrees

Absorbed Power from Matlab Code [kWh/year]								
	Hs [m]	**0-1**	**1-2**	**2-3**	**3-4**	**4-5**	**5-6**	**6-7**
Tp [sec]								
2-3		0,01	0,00	0,00	0,00	0,00	0,00	0,00
3-4		18,89	0,18	0,00	0,00	0,00	0,00	0,00
4-5		736,23	415,17	0,00	0,00	0,00	0,00	0,00
5-6		3499,48	14873,73	299,06	0,00	0,00	0,00	0,00
6-7		5526,14	48312,72	30069,51	0,00	0,00	0,00	0,00
7-8		1795,19	34586,26	**74114,76**	17819,90	282,38	0,00	0,00
8-9		678,48	13458,17	36712,03	47244,50	7543,97	209,28	0,00
9-10		138,11	2006,00	7828,44	22245,08	24499,82	2728,40	0,00
10-11		7,77	279,65	1035,75	2220,39	5439,08	5219,84	1704,60
11-12		0,00	0,00	0,00	115,85	0,00	424,86	569,90

Table 51. Final results achieved by using Simpson's code for angle of incident wave 30 degrees

Absorbed Power from Matlab Code [kWh/year]								
	Hs [m]	**0-1**	**1-2**	**2-3**	**3-4**	**4-5**	**5-6**	**6-7**
Tp [sec]								
2-3		0,01	0,00	0,00	0,00	0,00	0,00	0,00
3-4		18,70	0,18	0,00	0,00	0,00	0,00	0,00
4-5		753,09	423,28	0,00	0,00	0,00	0,00	0,00
5-6		3565,57	15170,19	305,39	0,00	0,00	0,00	0,00
6-7		5564,03	48644,00	30524,00	0,00	0,00	0,00	0,00
7-8		1796,09	34603,56	**74115,34**	17863,36	284,28	0,00	0,00
8-9		677,33	13435,21	36649,40	47078,09	7535,03	210,12	0,00
9-10		137,79	2001,34	7810,28	22193,48	24519,08	2742,47	0,00
10-11		7,75	279,00	1033,35	2215,24	5425,54	5187,37	1683,68
11-12		0,00	0,00	0,00	115,62	0,00	424,25	571,74

Table 52. Final results achieved by using trapezoidal integration for angle of incident wave 30 degrees

Absorbed Power from Matlab Code [kWh/year]								
	Hs [m]	**0-1**	**1-2**	**2-3**	**3-4**	**4-5**	**5-6**	**6-7**
Tp [sec]								
2-3		0,01	0,00	0,00	0,00	0,00	0,00	0,00
3-4		16,20	0,16	0,00	0,00	0,00	0,00	0,00
4-5		599,75	351,84	0,00	0,00	0,00	0,00	0,00
5-6		5779,28	22614,35	371,33	0,00	0,00	0,00	0,00
6-7		9335,23	81614,04	53660,88	0,00	0,00	0,00	0,00
7-8		2759,16	53158,24	**116427,57**	29177,25	467,36	0,00	0,00
8-9		954,62	18935,57	51653,63	63012,79	9479,61	253,08	0,00
9-10		181,50	2636,23	10287,93	29233,89	30625,23	3266,39	0,00
10-11		9,70	349,27	1293,58	2773,10	6771,41	6289,51	1998,03
11-12		0,00	0,00	0,00	139,28	0,00	508,69	670,19

Table 53. Final results achieved by using Simpson's code for angle of incident wave 60 degrees

Absorbed Power from Matlab Code [kWh/year]								
	Hs [m]	**0-1**	**1-2**	**2-3**	**3-4**	**4-5**	**5-6**	**6-7**
Tp [sec]								
2-3		0,01	0,00	0,00	0,00	0,00	0,00	0,00
3-4		15,82	0,16	0,00	0,00	0,00	0,00	0,00
4-5		566,42	330,34	0,00	0,00	0,00	0,00	0,00
5-6		5202,86	20431,98	338,68	0,00	0,00	0,00	0,00
6-7		8487,09	74199,09	48458,15	0,00	0,00	0,00	0,00
7-8		2548,09	49091,68	**107368,55**	26955,47	433,81	0,00	0,00
8-9		893,79	17728,92	48362,05	59522,18	9076,54	245,27	0,00
9-10		171,80	2495,41	9738,40	27672,37	29289,16	3157,07	0,00
10-11		9,26	333,47	1235,09	2647,72	6467,47	6018,46	1910,08
11-12		0,00	0,00	0,00	133,90	0,00	489,64	649,71

Table 54. Final results achieved by using trapezoidal integration for angle of incident wave 60 degrees

Absorbed Power from Matlab Code [kWh/year]								
	Hs [m]	**0-1**	**1-2**	**2-3**	**3-4**	**4-5**	**5-6**	**6-7**
Tp [sec]								
2-3		0,01	0,00	0,00	0,00	0,00	0,00	0,00
3-4		18,27	0,18	0,00	0,00	0,00	0,00	0,00
4-5		732,26	409,06	0,00	0,00	0,00	0,00	0,00
5-6		3498,78	14870,23	298,97	0,00	0,00	0,00	0,00
6-7		5523,96	48293,66	30076,54	0,00	0,00	0,00	0,00
7-8		1793,72	34557,94	**74053,92**	17805,01	282,15	0,00	0,00
8-9		677,72	13443,04	36670,78	47185,17	7533,46	208,97	0,00
9-10		137,92	2003,33	7818,02	22215,47	24463,98	2724,11	0,00
10-11		7,76	279,24	1034,23	2217,13	5431,04	5211,61	1701,78
11-12		0,00	0,00	0,00	115,67	0,00	424,19	568,98

Table 55. Final results achieved by using Simpson's code for angle of incident wave 90 degrees

Absorbed Power from Matlab Code [kWh/year]								
	Hs [m]	**0-1**	**1-2**	**2-3**	**3-4**	**4-5**	**5-6**	**6-7**
Tp [sec]								
2-3		0,01	0,00	0,00	0,00	0,00	0,00	0,00
3-4		18,11	0,18	0,00	0,00	0,00	0,00	0,00
4-5		749,22	417,12	0,00	0,00	0,00	0,00	0,00
5-6		3565,22	15168,16	305,32	0,00	0,00	0,00	0,00
6-7		5562,26	48628,55	30533,99	0,00	0,00	0,00	0,00
7-8		1794,73	34577,37	**74059,08**	17849,54	284,06	0,00	0,00
8-9		676,60	13420,77	36610,00	47021,03	7524,79	209,82	0,00
9-10		137,61	1998,75	7800,18	22164,78	24483,93	2738,21	0,00
10-11		7,74	278,60	1031,86	2212,06	5417,69	5179,35	1680,94
11-12		0,00	0,00	0,00	115,44	0,00	423,60	570,83

Table 56. Final results achieved by using trapezoidal integration for angle of incident wave 90 degrees

Absorbed Power from Matlab Code [kWh/year]								
	Hs [m]	**0-1**	**1-2**	**2-3**	**3-4**	**4-5**	**5-6**	**6-7**
Tp [sec]								
2-3		0,01	0,00	0,00	0,00	0,00	0,00	0,00
3-4		19,81	0,21	0,00	0,00	0,00	0,00	0,00
4-5		639,73	375,59	0,00	0,00	0,00	0,00	0,00
5-6		4786,07	19231,44	341,68	0,00	0,00	0,00	0,00
6-7		7637,93	66775,29	43417,71	0,00	0,00	0,00	0,00
7-8		2330,12	44892,17	**97256,61**	23766,99	376,67	0,00	0,00
8-9		836,81	16598,63	45278,77	56138,27	8619,47	233,52	0,00
9-10		164,17	2384,59	9305,93	26443,47	28550,68	3129,10	0,00
10-11		8,99	323,47	1198,05	2568,33	6282,48	5942,06	1916,72
11-12		0,00	0,00	0,00	131,21	0,00	480,13	637,86

Table 57. Final results achieved by using Simpson's code for angle of incident wave 120 degrees

Absorbed Power from Matlab Code [kWh/year]								
	Hs [m]	**0-1**	**1-2**	**2-3**	**3-4**	**4-5**	**5-6**	**6-7**
Tp [sec]								
2-3		0,01	0,00	0,00	0,00	0,00	0,00	0,00
3-4		19,24	0,20	0,00	0,00	0,00	0,00	0,00
4-5		608,87	357,45	0,00	0,00	0,00	0,00	0,00
5-6		4299,94	17376,70	313,30	0,00	0,00	0,00	0,00
6-7		6926,05	60551,61	39072,52	0,00	0,00	0,00	0,00
7-8		2153,23	41484,28	**89609,71**	21832,53	346,72	0,00	0,00
8-9		785,88	15588,43	42523,11	53259,89	8304,62	228,05	0,00
9-10		156,06	2266,78	8846,15	25136,96	27440,37	3040,22	0,00
10-11		8,62	310,27	1149,14	2463,48	6028,15	5711,69	1839,96
11-12		0,00	0,00	0,00	126,72	0,00	464,26	621,22

Table 58. Final results achieved by using trapezoidal integration for angle of incident wave 120 degrees

Absorbed Power from Matlab Code [kWh/year]								
	Hs [m]	**0-1**	**1-2**	**2-3**	**3-4**	**4-5**	**5-6**	**6-7**
Tp [sec]								
2-3		0,01	0,00	0,00	0,00	0,00	0,00	0,00
3-4		18,28	0,18	0,00	0,00	0,00	0,00	0,00
4-5		732,42	409,22	0,00	0,00	0,00	0,00	0,00
5-6		3500,50	14876,86	299,07	0,00	0,00	0,00	0,00
6-7		5526,43	48315,27	30092,08	0,00	0,00	0,00	0,00
7-8		1794,35	34570,16	**74080,95**	17811,85	282,25	0,00	0,00
8-9		677,91	13446,88	36681,24	47196,72	7534,99	209,01	0,00
9-10		137,96	2003,80	7819,88	22220,76	24469,11	2724,62	0,00
10-11		7,76	279,30	1034,44	2217,58	5432,13	5212,58	1702,07
11-12		0,00	0,00	0,00	115,69	0,00	424,27	569,08

Table 59. Final results achieved by using Simpson's code for angle of incident wave 150 degrees

Absorbed Power from Matlab Code [kWh/year]								
	Hs [m]	**0-1**	**1-2**	**2-3**	**3-4**	**4-5**	**5-6**	**6-7**
Tp [sec]								
2-3		0,01	0,00	0,00	0,00	0,00	0,00	0,00
3-4		18,12	0,18	0,00	0,00	0,00	0,00	0,00
4-5		749,36	417,29	0,00	0,00	0,00	0,00	0,00
5-6		3566,77	15174,10	305,41	0,00	0,00	0,00	0,00
6-7		5564,46	48647,82	30548,23	0,00	0,00	0,00	0,00
7-8		1795,30	34588,28	**74083,07**	17855,55	284,16	0,00	0,00
8-9		676,77	13424,21	36619,40	47031,49	7526,19	209,85	0,00
9-10		137,64	1999,19	7801,87	22169,57	24488,61	2738,68	0,00
10-11		7,74	278,66	1032,06	2212,47	5418,69	5180,23	1681,20
11-12		0,00	0,00	0,00	115,46	0,00	423,67	570,91

Table 60. Final results achieved by using trapezoidal integration for angle of incident wave 150 degrees

Absorbed Power from Matlab Code [kWh/year]								
	Hs [m]	**0-1**	**1-2**	**2-3**	**3-4**	**4-5**	**5-6**	**6-7**
Tp [sec]								
2-3		0,01	0,00	0,00	0,00	0,00	0,00	0,00
3-4		16,62	0,17	0,00	0,00	0,00	0,00	0,00
4-5		604,44	355,97	0,00	0,00	0,00	0,00	0,00
5-6		5790,81	22665,94	372,51	0,00	0,00	0,00	0,00
6-7		9345,91	81707,47	53734,49	0,00	0,00	0,00	0,00
7-8		2760,92	53192,09	**116504,03**	29197,75	467,70	0,00	0,00
8-9		954,83	18939,68	51664,85	63015,24	9477,94	253,00	0,00
9-10		181,47	2635,88	10286,57	29230,03	30613,36	3264,36	0,00
10-11		9,70	349,12	1293,04	2771,96	6768,50	6285,53	1996,41
11-12		0,00	0,00	0,00	139,19	0,00	508,35	669,67

Table 61. Final results achieved by using Simpson's code for angle of incident wave 180 degrees

Absorbed Power from Matlab Code [kWh/year]								
	Hs [m]	**0-1**	**1-2**	**2-3**	**3-4**	**4-5**	**5-6**	**6-7**
Tp [sec]								
2-3		0,01	0,00	0,00	0,00	0,00	0,00	0,00
3-4		16,26	0,17	0,00	0,00	0,00	0,00	0,00
4-5		571,03	334,47	0,00	0,00	0,00	0,00	0,00
5-6		5214,22	20482,50	339,83	0,00	0,00	0,00	0,00
6-7		8497,75	74292,36	48532,12	0,00	0,00	0,00	0,00
7-8		2549,87	49125,91	**107446,43**	26976,90	434,17	0,00	0,00
8-9		894,01	17733,21	48373,77	59525,25	9074,90	245,19	0,00
9-10		171,78	2495,09	9737,15	27668,80	29277,41	3155,03	0,00
10-11		9,26	333,33	1234,57	2646,61	6464,62	6014,58	1908,51
11-12		0,00	0,00	0,00	133,82	0,00	489,31	649,19

Table 62. Final results achieved by using trapezoidal integration for angle of incident wave 180 degrees

Furthermore, the sum of all the cells that corresponds to the total final power per year depending on the angle of incidence of Location 2, if we apply Simpson's code is:

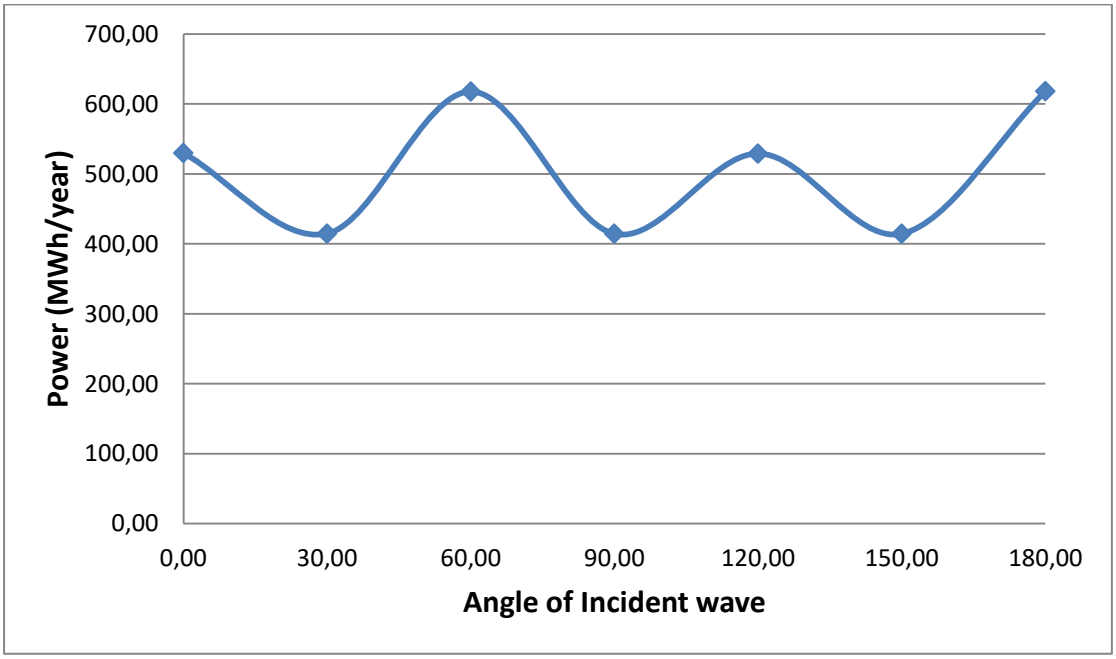

Figure 68. Total amount of Power per year for Location 2 depending on the angle of incidence achieved by using Simpson's code

Respectively, the sum of all the cells that corresponds to the total final power per year depending on the angle of incidence of Location 2, if we apply trapezoid integration is:

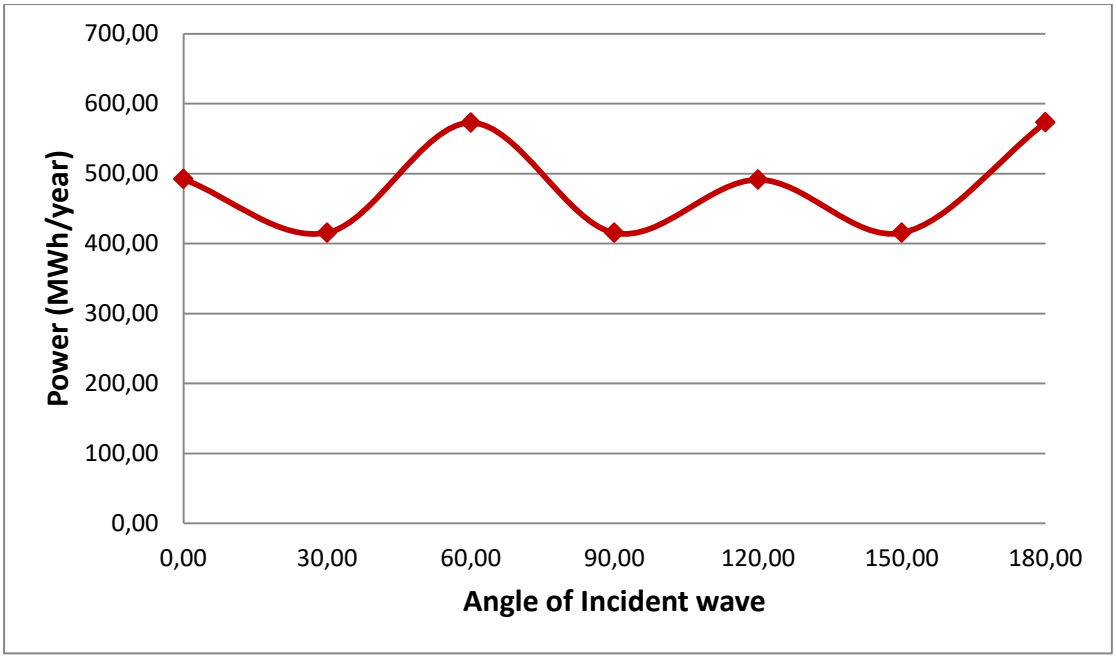

Figure 69. Total amount of Power per year for Location 2 depending on the angle of incidence achieved by using trapezoidal integration

Finally, if we compare the two integration methods, we have the following diagram:

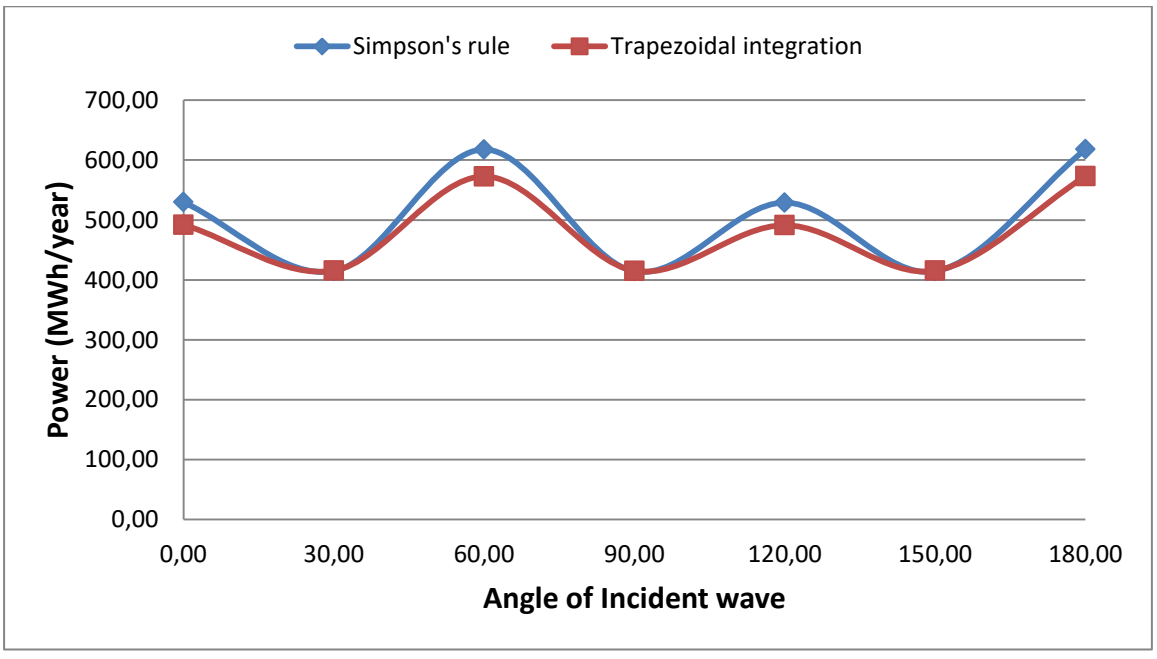

Figure 70. Comparison of two Integration methods

7.3 Location 3

For the Location 3 the calculated absorbed powers received by HAMVAB for every pair Hs - Tp and for various angles of incidence are the following tables:

Absorbed Power from Matlab Code [kW]											
	Hs [m]	**0-1**	**1-2**	**2-3**	**3-4**	**4-5**	**5-6**	**6-7**	**7-8**	**8-9**	**9-10**
Tp [sec]											
3-4		0,03	0,19	0,54	1,06	1,75	2,62	3,66	4,87	6,25	7,81
4-5		0,46	3,46	9,51	18,64	30,81	46,03	64,29	85,60	109,94	137,33
5-6		3,49	29,03	68,96	135,17	223,44	333,78	466,19	620,67	797,22	995,83
6-7		9,66	86,96	276,65	571,26	944,33	1410,66	1970,27	2623,14	3369,27	4208,67
7-8		15,70	141,27	419,06	987,12	1764,22	2635,44	3680,91	4900,61	6294,57	7862,76
8-9		19,78	177,99	494,42	1041,48	1878,61	2946,26	4124,11	5490,68	7052,48	8809,50
9-10		21,74	195,65	543,47	1065,19	1857,85	2913,40	4197,85	5636,11	7239,27	**9042,82**
10-11		22,10	198,86	552,39	1082,68	1793,22	2754,82	3967,15	5419,74	7087,11	8853,31
11-12		21,45	193,08	536,33	1051,21	1737,72	2589,06	3584,70	4741,49	6044,25	7472,88
12-13		20,29	182,65	507,37	994,45	1643,89	2455,69	3415,36	4503,61	5772,16	7218,77
13-14		18,91	170,16	472,68	926,45	1531,48	2287,76	3195,30	4228,78	5303,15	6500,19
14-15		17,46	157,12	436,45	855,43	1414,08	2112,40	2950,37	3928,01	5030,08	6092,71
15-16		16,06	144,54	401,50	786,94	1300,87	1943,27	2714,16	3613,52	4641,37	5797,69
16-17		14,77	132,95	369,31	723,84	1196,56	1787,45	2496,52	3323,76	4269,19	5332,80
17-18		13,60	122,44	340,11	666,62	1101,97	1646,15	2299,16	3061,02	3931,70	4911,23

Table 63. Matlab results achieved by using Simpson's code for angle of incident wave 0 degrees

Absorbed Power from Matlab Code [kW]											
	Hs [m]	**0-1**	**1-2**	**2-3**	**3-4**	**4-5**	**5-6**	**6-7**	**7-8**	**8-9**	**9-10**
Tp [sec]											
3-4		0,03	0,19	0,53	1,04	1,72	2,57	3,58	4,77	6,13	7,66
4-5		0,45	3,35	9,19	18,02	29,79	44,50	62,15	82,74	106,28	132,75
5-6		3,20	26,89	65,16	127,72	211,13	315,38	440,50	586,46	753,27	940,94
6-7		8,91	80,20	253,77	525,39	868,50	1297,39	1812,06	2412,50	3098,73	3870,73
7-8		14,79	133,10	392,86	915,40	1631,18	2436,70	3403,32	4531,05	5819,88	7269,81
8-9		18,96	170,67	474,08	1006,38	1838,49	2917,19	4086,70	5440,87	6988,49	8729,57
9-10		21,09	189,82	527,27	1033,44	1821,98	2888,77	4202,59	5665,02	7276,40	**9089,21**
10-11		21,60	194,43	540,07	1058,55	1753,46	2689,42	3853,04	5228,32	6787,21	8478,38
11-12		21,09	189,78	527,16	1033,23	1707,99	2548,19	3557,06	4752,18	6123,28	7652,95
12-13		20,01	180,10	500,29	980,56	1620,92	2421,38	3365,31	4418,76	5629,94	6992,99
13-14		18,69	168,20	467,22	915,74	1513,78	2261,33	3158,38	4182,23	5259,74	6467,11
14-15		17,30	155,71	432,53	847,75	1401,39	2093,43	2923,89	3892,75	4987,00	6072,62
15-16		15,95	143,54	398,71	781,47	1291,82	1929,76	2695,29	3588,40	4609,10	5757,39
16-17		14,68	132,10	366,95	719,23	1188,93	1776,05	2480,60	3302,58	4241,98	5298,80
17-18		13,51	121,59	337,75	661,98	1094,30	1634,70	2283,17	3039,73	3904,36	4877,07

Table 64. Matlab results achieved by using trapezoidal integration for angle of incident wave 0 degrees

Absorbed Power from Matlab Code [kW]											
	Hs [m]	**0-1**	**1-2**	**2-3**	**3-4**	**4-5**	**5-6**	**6-7**	**7-8**	**8-9**	**9-10**
Tp [sec]											
3-4		0,03	0,16	0,44	0,87	1,44	2,15	3,00	4,00	5,13	6,41
4-5		0,59	4,02	10,94	21,44	35,45	52,95	73,96	98,46	126,47	157,98
5-6		3,06	27,32	73,91	144,87	239,47	357,73	499,64	665,21	854,42	1067,29
6-7		7,82	70,40	218,86	455,04	752,21	1123,67	1569,42	2089,47	2683,81	3352,44
7-8		13,17	118,53	346,28	789,91	1398,53	2089,16	2917,92	3884,80	4989,81	6232,95
8-9		17,24	155,15	430,98	926,89	1708,32	2713,58	3801,13	5060,68	6500,17	8119,58
9-10		19,49	175,43	487,30	955,10	1683,07	2658,84	3849,47	5176,95	6649,50	8306,13
10-11		20,22	182,02	505,60	990,97	1642,88	2547,21	3694,48	5075,19	6665,17	**8326,37**
11-12		19,94	179,48	498,55	977,15	1615,29	2410,45	3359,59	4467,73	5720,41	7098,23
12-13		19,09	171,82	477,29	935,48	1546,40	2310,06	3217,63	4266,67	5495,43	6902,06
13-14		17,95	161,58	448,82	879,69	1454,19	2172,31	3034,05	4018,75	5058,69	6221,33
14-15		16,70	150,30	417,51	818,32	1352,73	2020,74	2822,36	3757,58	4813,03	5845,06
15-16		15,46	139,10	386,40	757,34	1251,93	1870,17	2612,06	3477,59	4466,77	5579,60
16-17		14,29	128,59	357,18	700,08	1157,27	1728,77	2414,56	3214,65	4129,04	5157,72
17-18		13,21	118,91	330,31	647,40	1070,20	1598,69	2232,89	2972,78	3818,37	4769,65

Table 65. Matlab results achieved by using Simpson's code for angle of incident wave 30 degrees

Absorbed Power from Matlab Code [kW]											
	Hs [m]	**0-1**	**1-2**	**2-3**	**3-4**	**4-5**	**5-6**	**6-7**	**7-8**	**8-9**	**9-10**
Tp [sec]											
3-4		0,03	0,16	0,44	0,86	1,43	2,13	2,97	3,96	5,08	6,35
4-5		0,61	4,09	11,12	21,80	36,04	53,84	75,20	100,12	128,60	160,64
5-6		3,12	27,88	75,49	147,96	244,59	365,38	510,32	679,43	872,68	1090,10
6-7		7,87	70,81	222,17	464,87	768,45	1147,93	1603,31	2134,59	2741,76	3424,82
7-8		13,17	118,50	345,51	785,16	1390,05	2076,49	2900,22	3861,24	4959,55	6195,14
8-9		17,21	154,88	430,22	924,53	1710,13	2732,94	3830,08	5099,22	6549,67	8181,42
9-10		19,46	175,10	486,38	953,30	1688,27	2684,99	3913,60	5278,86	6780,41	**8469,65**
10-11		20,19	181,72	504,79	989,39	1639,77	2527,97	3636,13	4949,23	6440,51	8045,38
11-12		19,92	179,27	497,96	976,00	1613,39	2409,83	3380,58	4534,97	5863,27	7348,61
12-13		19,07	171,59	476,64	934,22	1544,32	2306,95	3209,75	4231,43	5410,15	6740,34
13-14		17,93	161,37	448,25	878,57	1452,33	2169,53	3030,17	4015,18	5065,00	6244,63
14-15		16,69	150,24	417,34	817,99	1352,19	2019,94	2821,24	3756,09	4812,94	5873,82
15-16		15,46	139,15	386,53	757,59	1252,34	1870,78	2612,91	3478,73	4468,24	5581,43
16-17		14,29	128,57	357,13	699,97	1157,09	1728,49	2414,17	3214,14	4128,38	5156,90
17-18		13,19	118,72	329,77	646,36	1068,46	1596,10	2229,27	2967,96	3812,18	4761,92

Table 66. Matlab results achieved by using trapezoidal integration for angle of incident wave 30 degrees

Absorbed Power from Matlab Code [kW]											
	Hs [m]	**0-1**	**1-2**	**2-3**	**3-4**	**4-5**	**5-6**	**6-7**	**7-8**	**8-9**	**9-10**
Tp [sec]											
3-4		0,03	0,15	0,41	0,81	1,34	2,00	2,79	3,72	4,77	5,96
4-5		0,37	2,91	8,01	15,70	25,95	38,77	54,15	72,10	92,60	115,68
5-6		3,91	30,99	64,45	126,33	208,83	311,95	435,70	580,07	745,07	930,69
6-7		11,26	101,31	328,13	682,24	1127,79	1684,72	2353,04	3132,75	4023,84	5026,32
7-8		17,57	158,11	476,22	1164,59	2116,23	3161,28	4415,34	5878,42	7550,50	**9431,59**
8-9		21,14	190,25	528,47	1098,89	1951,28	3027,07	4234,43	5637,55	7241,12	9045,13
9-10		22,48	202,36	562,12	1101,76	1869,23	2865,76	4062,43	5421,66	6963,82	8698,75
10-11		22,40	201,62	560,05	1097,69	1815,30	2747,99	3913,69	5302,26	6889,56	8606,30
11-12		21,51	193,57	537,69	1053,86	1742,10	2592,38	3571,03	4704,40	5977,75	7371,61
12-13		20,22	182,02	505,60	990,98	1638,15	2447,11	3402,07	4479,79	5735,07	7165,76
13-14		18,78	169,06	469,61	920,44	1521,54	2272,92	3174,57	4201,12	5267,28	6455,05
14-15		17,32	155,89	433,03	848,75	1403,03	2095,88	2927,31	3897,30	4990,86	6046,45
15-16		15,93	143,35	398,20	780,47	1290,17	1927,28	2691,83	3583,79	4603,18	5750,00
16-17		14,65	131,87	366,30	717,95	1186,82	1772,91	2476,21	3296,73	4234,46	5289,41
17-18		13,50	121,49	337,47	661,43	1093,39	1633,33	2281,27	3037,19	3901,10	4873,00

Table 67. Matlab results achieved by using Simpson's code for angle of incident wave 60 degrees

Absorbed Power from Matlab Code [kW]											
	Hs [m]	**0-1**	**1-2**	**2-3**	**3-4**	**4-5**	**5-6**	**6-7**	**7-8**	**8-9**	**9-10**
Tp [sec]											
3-4		0,03	0,15	0,41	0,80	1,32	1,98	2,76	3,68	4,72	5,90
4-5		0,36	2,77	7,61	14,92	24,66	36,84	51,45	68,50	87,99	109,91
5-6		3,59	28,57	60,34	118,27	195,51	292,05	407,91	543,07	697,54	871,33
6-7		10,37	93,32	301,37	629,42	1040,47	1554,29	2170,86	2890,20	3712,30	4637,17
7-8		16,48	148,35	445,04	1081,07	1964,19	2934,16	4098,12	5456,08	7008,03	8753,98
8-9		20,16	181,48	504,10	1056,13	1898,58	2979,06	4170,54	5552,49	7131,87	**8908,67**
9-10		21,71	195,36	542,67	1063,64	1824,67	2829,69	4052,04	5430,61	6975,31	8713,11
10-11		21,81	196,29	545,25	1068,69	1767,61	2672,86	3789,04	5100,86	6581,86	8221,67
11-12		21,07	189,59	526,63	1032,20	1706,29	2542,72	3532,62	4701,97	6040,79	7532,23
12-13		19,88	178,95	497,09	974,31	1610,59	2405,94	3342,71	4383,88	5580,18	6925,87
13-14		18,52	166,70	463,07	907,61	1500,34	2241,25	3130,34	4145,10	5213,11	6410,03
14-15		17,13	154,18	428,28	839,43	1387,64	2072,89	2895,19	3854,55	4938,23	6015,42
15-16		15,79	142,11	394,76	773,73	1279,02	1910,63	2668,57	3552,83	4563,42	5700,32
16-17		14,54	130,84	363,44	712,34	1177,54	1759,03	2456,83	3270,93	4201,33	5248,03
17-18		13,39	120,49	334,69	656,00	1084,40	1619,91	2262,52	3012,22	3869,04	4832,95

Table 68. Matlab results achieved by using trapezoidal integration for angle of incident wave 60 degrees

Absorbed Power from Matlab Code [kW]											
	Hs [m]	**0-1**	**1-2**	**2-3**	**3-4**	**4-5**	**5-6**	**6-7**	**7-8**	**8-9**	**9-10**
Tp [sec]											
3-4		0,03	0,16	0,43	0,85	1,40	2,10	2,93	3,90	5,01	6,26
4-5		0,59	3,94	10,69	20,95	34,64	51,74	72,27	96,22	123,59	154,38
5-6		3,05	27,25	73,70	144,45	238,78	356,70	498,20	663,29	851,95	1064,20
6-7		7,81	70,28	218,61	454,65	751,57	1122,71	1568,09	2087,69	2681,52	3349,58
7-8		13,15	118,31	345,65	788,54	1396,18	2085,65	2913,01	3878,27	4981,42	6222,46
8-9		17,20	154,83	430,10	924,95	1704,65	2707,65	3792,83	5049,63	6485,97	8101,85
9-10		19,45	175,05	486,24	953,02	1679,26	2652,62	3840,27	5164,47	6633,47	8286,10
10-11		20,18	181,61	504,48	988,77	1639,22	2541,37	3685,82	5063,11	6649,11	**8306,30**
11-12		19,90	179,08	497,44	974,99	1611,72	2405,09	3352,05	4457,63	5707,39	7082,00
12-13		19,05	171,45	476,25	933,45	1543,05	2305,05	3210,65	4257,44	5483,58	6887,22
13-14		17,92	161,24	447,88	877,85	1451,13	2167,74	3027,67	4010,32	5048,17	6208,49
14-15		16,67	150,00	416,67	816,67	1350,00	2016,67	2816,67	3750,00	4803,33	5833,45
15-16		15,43	138,84	385,66	755,89	1249,52	1866,57	2607,03	3470,90	4458,18	5568,87
16-17		14,26	128,35	356,53	698,80	1155,16	1725,61	2410,15	3208,78	4121,50	5148,31
17-18		13,19	118,71	329,74	646,29	1068,35	1595,94	2229,04	2967,65	3811,78	4761,43

Table 69. Matlab results achieved by using Simpson's code for angle of incident wave 90 degrees

Absorbed Power from Matlab Code [kW]											
	Hs [m]	**0-1**	**1-2**	**2-3**	**3-4**	**4-5**	**5-6**	**6-7**	**7-8**	**8-9**	**9-10**
Tp [sec]											
3-4		0,03	0,15	0,43	0,84	1,39	2,08	2,91	3,87	4,97	6,21
4-5		0,60	4,00	10,87	21,31	35,23	52,63	73,50	97,86	125,69	157,01
5-6		3,11	27,81	75,30	147,58	243,96	364,43	509,00	677,66	870,41	1087,26
6-7		7,86	70,70	221,94	464,53	767,89	1147,09	1602,14	2133,02	2739,75	3422,32
7-8		13,14	118,28	344,91	783,86	1387,82	2073,16	2895,57	3855,05	4951,60	6185,22
8-9		17,17	154,57	429,36	922,63	1706,51	2727,05	3821,83	5088,23	6535,55	8163,78
9-10		19,41	174,72	485,34	951,26	1684,49	2678,76	3904,29	5266,19	6764,13	**8449,31**
10-11		20,15	181,33	503,68	987,22	1636,16	2522,22	3627,68	4937,54	6425,10	8026,13
11-12		19,87	178,87	496,87	973,86	1609,85	2404,53	3373,05	4524,78	5849,99	7331,87
12-13		19,02	171,22	475,62	932,21	1541,00	2301,98	3202,84	4222,32	5398,52	6725,87
13-14		17,89	161,03	447,31	876,74	1449,30	2165,00	3023,84	4006,81	5054,54	6231,85
14-15		16,66	149,94	416,51	816,35	1349,48	2015,89	2815,58	3748,55	4803,30	5862,23
15-16		15,43	138,88	385,79	756,14	1249,95	1867,20	2607,91	3472,07	4459,69	5570,75
16-17		14,26	128,33	356,48	698,70	1154,99	1725,35	2409,79	3208,30	4120,88	5147,53
17-18		13,17	118,51	329,21	645,24	1066,63	1593,36	2225,43	2962,85	3805,62	4753,73

Table 70. Matlab results achieved by using trapezoidal integration for angle of incident wave 90 degrees

Absorbed Power from Matlab Code [kW]											
	Hs [m]	**0-1**	**1-2**	**2-3**	**3-4**	**4-5**	**5-6**	**6-7**	**7-8**	**8-9**	**9-10**
Tp [sec]											
3-4		0,03	0,19	0,52	1,02	1,69	2,53	3,53	4,70	6,03	7,54
4-5		0,45	3,39	9,32	18,26	30,19	45,10	62,98	83,86	107,71	134,54
5-6		3,48	28,93	68,65	134,56	222,43	332,27	464,08	617,86	793,61	991,33
6-7		9,64	86,79	276,19	570,37	942,86	1408,48	1967,21	2619,07	3364,05	4202,15
7-8		15,67	141,02	418,33	985,44	1761,24	2630,99	3674,68	4892,33	6283,92	7849,47
8-9		19,74	177,68	493,54	1039,62	1875,23	2940,96	4116,69	5480,79	7039,78	8793,63
9-10		21,70	195,30	542,50	1063,29	1854,56	2908,27	4190,50	5626,26	7226,61	**9027,02**
10-11		22,06	198,50	551,39	1080,73	1789,99	2749,81	3959,87	5409,71	7073,91	8836,82
11-12		21,41	192,73	535,37	1049,33	1734,60	2584,40	3578,19	4732,80	6033,08	7459,00
12-13		20,26	182,33	506,47	992,69	1640,97	2451,33	3409,29	4495,57	5761,80	7205,77
13-14		18,87	169,87	471,86	924,84	1528,82	2283,79	3189,75	4221,44	5293,95	6488,92
14-15		17,43	156,86	435,71	853,99	1411,70	2108,83	2945,39	3921,38	5021,60	6082,53
15-16		16,03	144,31	400,85	785,67	1298,75	1940,11	2709,74	3607,65	4633,82	5788,27
16-17		14,75	132,74	368,73	722,71	1194,69	1784,66	2492,63	3318,59	4262,54	5324,49
17-18		13,58	122,26	339,61	665,63	1100,33	1643,70	2295,75	3056,47	3925,87	4903,94

Table 71. Matlab results achieved by using Simpson's code for angle of incident wave 120 degrees

Absorbed Power from Matlab Code [kW]											
	Hs [m]	**0-1**	**1-2**	**2-3**	**3-4**	**4-5**	**5-6**	**6-7**	**7-8**	**8-9**	**9-10**
Tp [sec]											
3-4		0,03	0,18	0,51	1,00	1,66	2,47	3,45	4,60	5,91	7,38
4-5		0,44	3,28	9,00	17,64	29,16	43,56	60,84	81,00	104,04	129,96
5-6		3,19	26,79	64,85	127,10	210,11	313,87	438,38	583,64	749,65	936,41
6-7		8,89	80,03	253,31	524,48	867,00	1295,14	1808,92	2408,33	3093,36	3864,03
7-8		14,76	132,85	392,13	913,73	1628,21	2432,26	3397,12	4522,80	5809,28	7256,58
8-9		18,93	170,36	473,22	1004,54	1835,15	2911,93	4079,33	5431,05	6975,89	8713,83
9-10		21,05	189,47	526,30	1031,55	1818,69	2883,60	4195,12	5654,97	7263,49	**9073,08**
10-11		21,56	194,07	539,09	1056,61	1750,26	2684,47	3845,90	5218,58	6774,51	8462,52
11-12		21,05	189,43	526,20	1031,35	1704,89	2543,55	3550,51	4743,36	6111,84	7638,57
12-13		19,98	179,78	499,39	978,80	1618,02	2417,04	3359,27	4410,80	5619,77	6980,31
13-14		18,66	167,90	466,40	914,14	1511,13	2257,37	3152,85	4174,92	5250,57	6455,86
14-15		17,27	155,45	431,79	846,32	1399,01	2089,88	2918,93	3886,14	4978,55	6062,42
15-16		15,92	143,30	398,06	780,20	1289,71	1926,61	2690,89	3582,54	4601,58	5747,99
16-17		14,66	131,90	366,38	718,10	1187,07	1773,28	2476,72	3297,41	4235,34	5290,52
17-18		13,49	121,41	337,24	661,00	1092,67	1632,26	2279,77	3035,19	3898,54	4869,80

Table 72. Matlab results achieved by using trapezoidal integration for angle of incident wave 120 degrees

Absorbed Power from Matlab Code [kW]											
	Hs [m]	**0-1**	**1-2**	**2-3**	**3-4**	**4-5**	**5-6**	**6-7**	**7-8**	**8-9**	**9-10**
Tp [sec]											
3-4		0,03	0,16	0,43	0,85	1,41	2,10	2,94	3,91	5,02	6,27
4-5		0,59	3,94	10,70	20,98	34,68	51,81	72,36	96,34	123,74	154,57
5-6		3,06	27,28	73,78	144,61	239,05	357,10	498,76	664,03	852,91	1065,40
6-7		7,82	70,35	218,87	455,21	752,50	1124,10	1570,02	2090,27	2684,83	3353,72
7-8		13,16	118,42	345,95	789,20	1397,30	2087,33	2915,36	3881,39	4985,43	6227,47
8-9		17,22	154,96	430,43	925,64	1705,88	2709,57	3795,51	5053,19	6490,54	8107,56
9-10		19,46	175,17	486,58	953,70	1680,47	2654,54	3843,07	5168,25	6638,33	8292,17
10-11		20,19	181,73	504,80	989,41	1640,27	2542,96	3688,10	5066,18	6653,10	**8311,29**
11-12		19,91	179,18	497,73	975,55	1612,65	2406,47	3353,90	4460,00	5710,34	7085,56
12-13		19,06	171,54	476,50	933,93	1543,85	2306,24	3212,29	4259,48	5486,07	6890,19
13-14		17,92	161,31	448,09	878,25	1451,80	2168,74	3029,07	4012,15	5050,35	6211,05
14-15		16,67	150,06	416,84	817,00	1350,56	2017,50	2817,83	3751,54	4805,30	5835,73
15-16		15,43	138,89	385,80	756,16	1249,98	1867,26	2607,99	3472,18	4459,82	5570,92
16-17		14,27	128,39	356,65	699,03	1155,54	1726,18	2410,95	3209,84	4122,86	5150,01
17-18		13,19	118,74	329,84	646,48	1068,67	1596,41	2229,69	2968,53	3812,91	4762,84

Table 73. Matlab results achieved by using Simpson's code for angle of incident wave 150 degrees

Absorbed Power from Matlab Code [kW]											
	Hs [m]	**0-1**	**1-2**	**2-3**	**3-4**	**4-5**	**5-6**	**6-7**	**7-8**	**8-9**	**9-10**
Tp [sec]											
3-4		0,03	0,16	0,43	0,84	1,40	2,08	2,91	3,88	4,98	6,22
4-5		0,60	4,01	10,89	21,34	35,27	52,69	73,59	97,98	125,85	157,20
5-6		3,12	27,84	75,36	147,71	244,18	364,76	509,45	678,27	871,20	1088,24
6-7		7,86	70,76	222,19	465,08	768,81	1148,47	1604,06	2135,58	2743,04	3426,43
7-8		13,15	118,38	345,19	784,47	1388,86	2074,71	2897,74	3857,93	4955,30	6189,84
8-9		17,19	154,69	429,69	923,31	1707,72	2728,96	3824,50	5091,79	6540,12	8169,49
9-10		19,43	174,84	485,68	951,93	1685,67	2680,66	3907,09	5269,98	6769,00	**8455,40**
10-11		20,16	181,44	504,00	987,84	1637,19	2523,79	3629,90	4940,53	6428,95	8030,94
11-12		19,89	178,97	497,15	974,42	1610,77	2405,88	3374,87	4527,13	5852,93	7335,46
12-13		19,03	171,31	475,86	932,68	1541,78	2303,16	3204,45	4224,33	5400,96	6728,78
13-14		17,90	161,11	447,52	877,13	1449,96	2165,99	3025,22	4008,61	5056,69	6234,37
14-15		16,67	150,00	416,68	816,68	1350,03	2016,71	2816,73	3750,08	4805,25	5864,48
15-16		15,44	138,93	385,93	756,42	1250,40	1867,88	2608,86	3473,34	4461,31	5572,77
16-17		14,26	128,37	356,59	698,92	1155,36	1725,91	2410,57	3209,34	4122,22	5149,21
17-18		13,17	118,55	329,30	645,43	1066,94	1593,82	2226,08	2963,72	3806,73	4755,12

Table 74. Matlab results achieved by using trapezoidal integration for angle of incident wave 150 degrees

Absorbed Power from Matlab Code [kW]											
	Hs [m]	**0-1**	**1-2**	**2-3**	**3-4**	**4-5**	**5-6**	**6-7**	**7-8**	**8-9**	**9-10**
Tp [sec]											
3-4		0,03	0,15	0,42	0,83	1,38	2,06	2,87	3,82	4,91	6,13
4-5		0,38	2,96	8,15	15,97	26,40	39,43	55,08	73,33	94,18	117,65
5-6		3,92	31,09	64,78	126,97	209,89	313,53	437,91	583,01	748,85	935,41
6-7		11,27	101,43	328,59	683,28	1129,50	1687,28	2356,61	3137,50	4029,95	5033,95
7-8		17,57	158,17	476,41	1165,12	2117,24	3162,80	4417,46	5881,23	7554,11	**9436,11**
8-9		21,13	190,21	528,35	1098,48	1950,22	3025,10	4231,64	5633,83	7236,35	9039,18
9-10		22,47	202,23	561,75	1101,03	1867,55	2862,63	4057,43	5414,71	6954,89	8687,60
10-11		22,38	201,42	559,51	1096,63	1813,51	2744,75	3908,48	5294,56	6878,91	8593,00
11-12		21,48	193,34	537,06	1052,64	1740,07	2589,30	3566,39	4697,87	5969,01	7360,39
12-13		20,20	181,78	504,95	989,71	1636,05	2443,97	3397,65	4473,66	5726,90	7155,20
13-14		18,76	168,83	468,98	919,20	1519,49	2269,86	3170,30	4195,45	5259,99	6445,93
14-15		17,30	155,68	432,44	847,59	1401,11	2093,02	2923,31	3891,98	4984,04	6038,15
15-16		15,91	143,16	397,66	779,41	1288,41	1924,67	2688,17	3578,93	4596,93	5742,19
16-17		14,63	131,69	365,82	717,00	1185,24	1770,55	2472,91	3292,34	4228,83	5282,37
17-18		13,48	121,33	337,03	660,58	1091,98	1631,23	2278,32	3033,27	3896,07	4866,71

Table 75. Matlab results achieved by using Simpson's code for angle of incident wave 180 degrees

Absorbed Power from Matlab Code [kW]											
	Hs [m]	**0-1**	**1-2**	**2-3**	**3-4**	**4-5**	**5-6**	**6-7**	**7-8**	**8-9**	**9-10**
Tp [sec]											
3-4		0,03	0,15	0,42	0,82	1,36	2,03	2,84	3,78	4,86	6,07
4-5		0,36	2,82	7,75	15,19	25,11	37,50	52,38	69,74	89,58	111,89
5-6		3,60	28,67	60,66	118,89	196,53	293,58	410,04	545,91	701,19	875,89
6-7		10,38	93,44	301,82	630,47	1042,20	1556,87	2174,47	2895,01	3718,48	4644,88
7-8		16,49	148,41	445,23	1081,62	1965,27	2935,77	4100,37	5459,07	7011,88	8758,78
8-9		20,16	181,43	503,98	1055,73	1897,53	2977,08	4167,74	5548,76	7127,08	**8902,68**
9-10		21,69	195,23	542,30	1062,92	1822,98	2826,51	4046,90	5423,43	6966,09	8701,59
10-11		21,79	196,10	544,71	1067,63	1765,83	2669,66	3783,95	5093,44	6571,71	8208,98
11-12		21,04	189,36	526,01	1030,97	1704,26	2539,64	3527,94	4695,29	6031,75	7520,47
12-13		19,86	178,72	496,45	973,04	1608,49	2402,80	3338,30	4377,82	5572,16	6915,59
13-14		18,50	166,48	462,44	906,38	1498,30	2238,20	3126,08	4139,43	5205,83	6400,92
14-15		17,11	153,97	427,69	838,28	1385,72	2070,03	2891,20	3849,23	4931,42	6007,08
15-16		15,77	141,92	394,22	772,67	1277,27	1908,02	2664,92	3547,97	4557,17	5692,52
16-17		14,52	130,66	362,95	711,38	1175,96	1756,68	2453,54	3266,55	4195,70	5240,99
17-18		13,37	120,33	334,26	655,14	1082,99	1617,80	2259,57	3008,31	3864,00	4826,66

Table 76. Matlab results achieved by using trapezoidal integration for angle of incident wave 180 degrees

After that, we have the final absorbed power of every cell/pair H_S - T_P for location 3 per year.

Final Absorbed Power per year [kWh/year]											
	Hs [m]	**0-1**	**1-2**	**2-3**	**3-4**	**4-5**	**5-6**	**6-7**	**7-8**	**8-9**	**9-10**
Tp [sec]											
3-4		0,16	0,04	0,00	0,00	0,00	0,00	0,00	0,00	0,00	0,00
4-5		52,80	108,92	0,00	0,00	0,00	0,00	0,00	0,00	0,00	0,00
5-6		1384,87	10905,39	453,83	0,00	0,00	0,00	0,00	0,00	0,00	0,00
6-7		3867,25	76359,40	52474,03	1713,78	0,00	0,00	0,00	0,00	0,00	0,00
7-8		4033,10	93458,57	229781,43	90464,36	2390,24	0,00	0,00	0,00	0,00	0,00
8-9		4725,34	87260,97	259807,79	**337539,49**	98535,88	3991,71	0,00	0,00	0,00	0,00
9-10		3603,70	79578,04	143159,27	283993,91	287307,62	86274,17	4874,92	0,00	0,00	0,00
10-11		2044,18	56058,94	115145,66	124682,33	189328,95	170621,40	71024,82	5244,91	0,00	0,00
11-12		1100,35	31951,67	85069,50	73347,66	65585,00	81680,65	67299,85	30743,19	2339,71	0,00
12-13		463,51	16438,90	38936,81	44172,90	28794,58	30656,48	27763,54	23970,83	12289,11	4890,13
13-14		107,95	6866,94	14546,27	20531,28	12153,00	11733,99	13296,57	10640,17	4618,87	1258,10
14-15		8,45	2159,14	5237,34	5712,08	5610,72	4906,21	2569,68	2660,91	486,78	589,62
15-16		1,55	657,43	2175,88	533,09	1007,12	376,12	0,00	0,00	0,00	0,00
16-17		1,43	231,59	786,27	560,39	347,39	0,00	0,00	0,00	0,00	0,00
17-18		0,00	0,00	164,57	709,63	0,00	0,00	0,00	0,00	0,00	0,00

Table 77. Final results achieved by using Simpson's code for angle of incident wave 0 degrees

Final Absorbed Power per year [kWh/year]											
	Hs [m]	**0-1**	**1-2**	**2-3**	**3-4**	**4-5**	**5-6**	**6-7**	**7-8**	**8-9**	**9-10**
Tp [sec]											
3-4		0,16	0,04	0,00	0,00	0,00	0,00	0,00	0,00	0,00	0,00
4-5		51,47	105,37	0,00	0,00	0,00	0,00	0,00	0,00	0,00	0,00
5-6		1272,16	10103,67	428,81	0,00	0,00	0,00	0,00	0,00	0,00	0,00
6-7		3566,75	70426,07	48135,10	1576,17	0,00	0,00	0,00	0,00	0,00	0,00
7-8		3799,73	88050,72	215416,07	83891,98	2209,98	0,00	0,00	0,00	0,00	0,00
8-9		4531,02	83672,45	249123,45	**326164,40**	96431,59	3952,33	0,00	0,00	0,00	0,00
9-10		3496,28	77205,90	138891,83	275528,33	281760,80	85544,98	4880,43	0,00	0,00	0,00
10-11		1998,62	54809,52	112579,35	121903,47	185131,66	166570,58	68981,82	5059,66	0,00	0,00
11-12		1081,52	31404,99	83614,00	72092,72	64462,87	80391,30	66780,86	30812,52	2370,30	0,00
12-13		457,03	16209,24	38392,86	43555,80	28392,32	30228,20	27356,72	23519,20	11986,33	4737,19
13-14		106,71	6787,59	14378,20	20294,06	12012,58	11598,41	13142,94	10523,04	4581,06	1251,70
14-15		8,37	2139,75	5190,33	5660,81	5560,35	4862,17	2546,61	2637,02	482,61	587,67
15-16		1,54	652,86	2160,76	529,39	1000,12	373,50	0,00	0,00	0,00	0,00
16-17		1,42	230,12	781,25	556,82	345,17	0,00	0,00	0,00	0,00	0,00
17-18		0,00	0,00	163,43	704,69	0,00	0,00	0,00	0,00	0,00	0,00

Table 78. Final results achieved by using trapezoidal integration for angle of incident wave 0 degrees

Final Absorbed Power per year [kWh/year]											
	Hs [m]	0-1	1-2	2-3	3-4	4-5	5-6	6-7	7-8	8-9	9-10
Tp [sec]											
3-4		0,14	0,03	0,00	0,00	0,00	0,00	0,00	0,00	0,00	0,00
4-5		68,30	126,57	0,00	0,00	0,00	0,00	0,00	0,00	0,00	0,00
5-6		1215,96	10263,03	486,39	0,00	0,00	0,00	0,00	0,00	0,00	0,00
6-7		3130,93	61820,63	41513,61	1365,12	0,00	0,00	0,00	0,00	0,00	0,00
7-8		3383,93	78415,40	189873,65	72391,01	1894,78	0,00	0,00	0,00	0,00	0,00
8-9		4119,05	76064,81	226472,74	**300403,12**	89604,23	3676,46	0,00	0,00	0,00	0,00
9-10		3231,24	71353,22	128362,98	254641,59	260279,35	78736,05	4470,36	0,00	0,00	0,00
10-11		1871,04	51310,79	105392,91	114121,83	173456,08	157762,51	66143,15	4911,48	0,00	0,00
11-12		1022,83	29700,59	79076,12	68180,12	60964,36	76045,67	63073,51	28968,18	2214,35	0,00
12-13		436,02	15464,04	36627,78	41553,36	27087,01	28838,49	26156,23	22709,68	11699,95	4675,59
13-14		102,51	6520,40	13812,19	19495,17	11539,69	11141,83	12625,56	10111,69	4405,95	1204,13
14-15		8,08	2065,46	5010,10	5464,25	5367,28	4693,34	2458,18	2545,46	465,78	565,65
15-16		1,50	632,70	2094,03	513,04	969,24	361,97	0,00	0,00	0,00	0,00
16-17		1,38	223,99	760,45	542,00	335,98	0,00	0,00	0,00	0,00	0,00
17-18		0,00	0,00	159,83	689,17	0,00	0,00	0,00	0,00	0,00	0,00

Table 79. Final results achieved by using Simpson's code for angle of incident wave 30 degrees

Final Absorbed Power per year [kWh/year]											
	Hs [m]	0-1	1-2	2-3	3-4	4-5	5-6	6-7	7-8	8-9	9-10
Tp [sec]											
3-4		0,14	0,03	0,00	0,00	0,00	0,00	0,00	0,00	0,00	0,00
4-5		69,76	128,73	0,00	0,00	0,00	0,00	0,00	0,00	0,00	0,00
5-6		1239,36	10473,71	496,78	0,00	0,00	0,00	0,00	0,00	0,00	0,00
6-7		3149,11	62179,64	42140,00	1394,60	0,00	0,00	0,00	0,00	0,00	0,00
7-8		3382,84	78390,21	189453,16	71955,94	1883,29	0,00	0,00	0,00	0,00	0,00
8-9		4111,84	75931,64	226076,23	**299638,30**	89698,81	3702,69	0,00	0,00	0,00	0,00
9-10		3225,16	71219,00	128121,53	254162,62	261083,17	79510,45	4544,83	0,00	0,00	0,00
10-11		1868,05	51228,69	105224,28	113939,23	173127,83	156570,85	65098,46	4789,58	0,00	0,00
11-12		1021,62	29665,64	78983,08	68099,90	60892,63	76026,40	63467,62	29404,19	2269,65	0,00
12-13		435,44	15443,25	36578,54	41497,50	27050,59	28799,72	26092,18	22522,12	11518,38	4566,04
13-14		102,37	6512,06	13794,54	19470,26	11524,95	11127,60	12609,43	10102,71	4411,45	1208,64
14-15		8,08	2064,64	5008,12	5462,08	5365,15	4691,47	2457,21	2544,45	465,77	568,43
15-16		1,50	632,90	2094,72	513,21	969,56	362,09	0,00	0,00	0,00	0,00
16-17		1,38	223,95	760,33	541,91	335,93	0,00	0,00	0,00	0,00	0,00
17-18		0,00	0,00	159,57	688,06	0,00	0,00	0,00	0,00	0,00	0,00

Table 80. Final results achieved by using trapezoidal integration for angle of incident wave 30 degrees

Final Absorbed Power per year [kWh/year]											
	Hs [m]	0-1	1-2	2-3	3-4	4-5	5-6	6-7	7-8	8-9	9-10
Tp [sec]											
3-4		0,13	0,03	0,00	0,00	0,00	0,00	0,00	0,00	0,00	0,00
4-5		42,69	91,47	0,00	0,00	0,00	0,00	0,00	0,00	0,00	0,00
5-6		1553,64	11641,96	424,14	0,00	0,00	0,00	0,00	0,00	0,00	0,00
6-7		4505,70	88965,86	62238,74	2046,73	0,00	0,00	0,00	0,00	0,00	0,00
7-8		4513,72	104595,97	261122,88	106729,14	2867,15	0,00	0,00	0,00	0,00	0,00
8-9		5050,80	93271,05	277702,00	**356148,18**	102347,89	4101,20	0,00	0,00	0,00	0,00
9-10		3727,41	82309,82	148073,69	293742,94	289067,88	84863,41	4717,66	0,00	0,00	0,00
10-11		2072,53	56836,44	116742,67	126411,61	191660,52	170198,26	70067,69	5131,21	0,00	0,00
11-12		1103,12	32032,20	85283,91	73532,53	65750,31	81785,45	67043,18	30502,71	2313,97	0,00
12-13		461,89	16381,50	38800,87	44018,68	28694,05	30549,44	27655,57	23844,02	12210,14	4854,23
13-14		107,25	6822,38	14451,89	20398,07	12074,14	11657,86	13210,30	10570,57	4587,63	1249,36
14-15		8,38	2142,26	5196,40	5667,43	5566,86	4867,86	2549,59	2640,11	482,99	585,14
15-16		1,54	652,02	2157,98	528,71	998,84	373,02	0,00	0,00	0,00	0,00
16-17		1,42	229,71	779,87	555,84	344,56	0,00	0,00	0,00	0,00	0,00
17-18		0,00	0,00	163,29	704,11	0,00	0,00	0,00	0,00	0,00	0,00

Table 81. Final results achieved by using Simpson's code for angle of incident wave 60 degrees

Final Absorbed Power per year [kWh/year]											
	Hs [m]	**0-1**	**1-2**	**2-3**	**3-4**	**4-5**	**5-6**	**6-7**	**7-8**	**8-9**	**9-10**
Tp [sec]											
3-4		0,12	0,03	0,00	0,00	0,00	0,00	0,00	0,00	0,00	0,00
4-5		41,41	87,06	0,00	0,00	0,00	0,00	0,00	0,00	0,00	0,00
5-6		1423,97	10734,25	397,08	0,00	0,00	0,00	0,00	0,00	0,00	0,00
6-7		4150,26	81947,53	57162,16	1888,27	0,00	0,00	0,00	0,00	0,00	0,00
7-8		4235,12	98139,95	244027,15	99074,42	2661,16	0,00	0,00	0,00	0,00	0,00
8-9		4817,92	88970,46	264897,56	**342288,77**	99583,73	4036,15	0,00	0,00	0,00	0,00
9-10		3598,46	79462,29	142951,03	283580,81	282175,78	83795,40	4705,60	0,00	0,00	0,00
10-11		2017,77	55334,62	113657,90	123071,35	186625,78	165544,99	67835,99	4936,31	0,00	0,00
11-12		1080,44	31373,65	83530,57	72020,78	64398,55	80218,82	66322,08	30486,95	2338,37	0,00
12-13		454,12	16105,86	38148,00	43278,01	28211,24	30035,41	27173,02	23333,55	11880,38	4691,72
13-14		105,76	6727,33	14250,54	20113,88	11905,93	11495,44	13026,25	10429,59	4540,45	1240,65
14-15		8,29	2118,76	5139,40	5605,26	5505,79	4814,45	2521,62	2611,15	477,89	582,14
15-16		1,53	646,39	2139,34	524,14	990,21	369,80	0,00	0,00	0,00	0,00
16-17		1,41	227,91	773,77	551,49	341,87	0,00	0,00	0,00	0,00	0,00
17-18		0,00	0,00	161,95	698,32	0,00	0,00	0,00	0,00	0,00	0,00

Table 82. Final results achieved by using trapezoidal integration for angle of incident wave 60 degrees

Final Absorbed Power per year [kWh/year]											
	Hs [m]	**0-1**	**1-2**	**2-3**	**3-4**	**4-5**	**5-6**	**6-7**	**7-8**	**8-9**	**9-10**
Tp [sec]											
3,50		0,14	0,03	0,00	0,00	0,00	0,00	0,00	0,00	0,00	0,00
4,50		67,61	123,79	0,00	0,00	0,00	0,00	0,00	0,00	0,00	0,00
5,50		1212,82	10235,38	484,98	0,00	0,00	0,00	0,00	0,00	0,00	0,00
6,50		3125,53	61714,08	41466,06	1363,96	0,00	0,00	0,00	0,00	0,00	0,00
7,50		3377,63	78269,53	189527,62	72266,01	1891,59	0,00	0,00	0,00	0,00	0,00
8,50		4110,60	75908,73	226008,03	**299772,34**	89411,49	3668,43	0,00	0,00	0,00	0,00
9,50		3224,22	71198,26	128084,21	254088,58	259689,50	78551,79	4459,66	0,00	0,00	0,00
10,50		1866,89	51196,86	105158,91	113868,45	173069,75	157400,70	65988,15	4899,78	0,00	0,00
11,50		1020,56	29634,81	78901,01	68029,13	60829,36	75876,86	62932,08	28902,71	2209,31	0,00
12,50		435,08	15430,48	36548,31	41463,20	27028,23	28775,91	26099,52	22660,57	11674,73	4665,54
13,50		102,29	6506,70	13783,17	19454,21	11515,45	11118,43	12599,03	10090,49	4396,79	1201,64
14,50		8,06	2061,29	5000,00	5453,22	5356,45	4683,87	2453,22	2540,32	464,84	564,53
15,50		1,49	631,48	2090,01	512,05	967,37	361,27	0,00	0,00	0,00	0,00
16,50		1,38	223,58	759,07	541,01	335,37	0,00	0,00	0,00	0,00	0,00
17,50		0,00	0,00	159,55	687,98	0,00	0,00	0,00	0,00	0,00	0,00

Table 83. Final results achieved by using Simpson's code for angle of incident wave 90 degrees

Final Absorbed Power per year [kWh/year]											
	Hs [m]	0-1	1-2	2-3	3-4	4-5	5-6	6-7	7-8	8-9	9-10
Tp [sec]											
3-4		0,14	0,03	0,00	0,00	0,00	0,00	0,00	0,00	0,00	0,00
4-5		69,09	125,93	0,00	0,00	0,00	0,00	0,00	0,00	0,00	0,00
5-6		1236,44	10448,22	495,49	0,00	0,00	0,00	0,00	0,00	0,00	0,00
6-7		3144,07	62080,23	42097,10	1393,58	0,00	0,00	0,00	0,00	0,00	0,00
7-8		3376,81	78250,34	189122,16	71837,28	1880,27	0,00	0,00	0,00	0,00	0,00
8-9		4103,60	75779,56	225623,44	**299021,78**	89508,96	3694,72	0,00	0,00	0,00	0,00
9-10		3218,26	71066,72	127847,58	253619,16	260497,89	79325,73	4534,01	0,00	0,00	0,00
10-11		1863,95	51116,20	104993,22	113689,04	172746,43	156215,16	64947,22	4778,26	0,00	0,00
11-12		1019,38	29600,50	78809,66	67950,37	60758,93	75859,00	63326,23	29338,07	2264,51	0,00
12-13		434,50	15409,95	36499,68	41408,04	26992,27	28737,63	26035,95	22473,64	11493,62	4556,23
13-14		102,16	6498,46	13765,72	19429,58	11500,87	11104,35	12583,08	10081,65	4402,34	1206,16
14-15		8,06	2060,49	4998,07	5451,12	5354,38	4682,06	2452,28	2539,34	464,84	567,31
15-16		1,49	631,69	2090,71	512,22	967,70	361,39	0,00	0,00	0,00	0,00
16-17		1,38	223,55	758,95	540,93	335,32	0,00	0,00	0,00	0,00	0,00
17-18		0,00	0,00	159,29	686,87	0,00	0,00	0,00	0,00	0,00	0,00

Table 84. Final results achieved by using trapezoidal integration for angle of incident wave 90 degrees

Final Absorbed Power per year [kWh/year]											
	Hs [m]	0-1	1-2	2-3	3-4	4-5	5-6	6-7	7-8	8-9	9-10
Tp [sec]											
3-4		0,15	0,04	0,00	0,00	0,00	0,00	0,00	0,00	0,00	0,00
4-5		52,15	106,76	0,00	0,00	0,00	0,00	0,00	0,00	0,00	0,00
5-6		1380,65	10867,40	451,77	0,00	0,00	0,00	0,00	0,00	0,00	0,00
6-7		3859,76	76211,62	52386,83	1711,12	0,00	0,00	0,00	0,00	0,00	0,00
7-8		4025,92	93292,19	229379,06	90310,62	2386,19	0,00	0,00	0,00	0,00	0,00
8-9		4716,99	87106,73	259348,56	**336937,40**	98358,85	3984,52	0,00	0,00	0,00	0,00
9-10		3597,27	79436,14	142904,00	283487,51	286798,78	86122,34	4866,39	0,00	0,00	0,00
10-11		2040,51	55958,24	114938,83	124458,37	188988,49	170311,08	70894,40	5235,20	0,00	0,00
11-12		1098,38	31894,34	84916,86	73216,06	65467,33	81533,74	67177,54	30686,84	2335,39	0,00
12-13		462,69	16409,74	38867,76	44094,57	28743,52	30602,11	27714,24	23928,04	12267,07	4881,33
13-14		107,77	6855,01	14521,01	20495,63	12131,89	11713,62	13273,48	10621,70	4610,86	1255,92
14-15		8,43	2155,50	5228,51	5702,45	5601,25	4897,93	2565,34	2656,42	485,96	588,63
15-16		1,55	656,36	2172,35	532,22	1005,49	375,51	0,00	0,00	0,00	0,00
16-17		1,43	231,23	785,04	559,52	346,85	0,00	0,00	0,00	0,00	0,00
17-18		0,00	0,00	164,33	708,58	0,00	0,00	0,00	0,00	0,00	0,00

Table 85. Final results achieved by using Simpson's code for angle of incident wave 120 degrees

Final Absorbed Power per year [kWh/year]											
	Hs [m]	0-1	1-2	2-3	3-4	4-5	5-6	6-7	7-8	8-9	9-10
Tp [sec]											
3-4		0,15	0,04	0,00	0,00	0,00	0,00	0,00	0,00	0,00	0,00
4-5		50,82	103,21	0,00	0,00	0,00	0,00	0,00	0,00	0,00	0,00
5-6		1267,91	10065,47	426,75	0,00	0,00	0,00	0,00	0,00	0,00	0,00
6-7		3559,25	70277,90	48046,46	1573,44	0,00	0,00	0,00	0,00	0,00	0,00
7-8		3792,58	87885,10	215015,98	83739,19	2205,96	0,00	0,00	0,00	0,00	0,00
8-9		4522,72	83519,20	248667,17	**325568,56**	96256,49	3945,19	0,00	0,00	0,00	0,00
9-10		3489,89	77064,86	138638,10	275025,00	281251,82	85391,85	4871,75	0,00	0,00	0,00
10-11		1994,97	54709,36	112373,62	121680,70	184793,10	166263,81	68853,99	5050,24	0,00	0,00
11-12		1079,56	31347,91	83462,04	71961,69	64345,72	80244,87	66658,02	30755,36	2365,88	0,00
12-13		456,22	16180,20	38324,08	43477,77	28341,45	30174,05	27307,65	23476,83	11964,66	4728,59
13-14		106,52	6775,71	14353,03	20258,54	11991,55	11578,11	13119,94	10504,63	4573,07	1249,52
14-15		8,36	2136,13	5181,52	5651,20	5550,92	4853,92	2542,29	2632,55	481,80	586,69
15-16		1,54	651,79	2157,23	528,52	998,49	372,89	0,00	0,00	0,00	0,00
16-17		1,42	229,76	780,03	555,95	344,63	0,00	0,00	0,00	0,00	0,00
17-18		0,00	0,00	163,18	703,64	0,00	0,00	0,00	0,00	0,00	0,00

Table 86. Final results achieved by using trapezoidal integration for angle of incident wave 120 degrees

Final Absorbed Power per year [kWh/year]											
	Hs [m]	0-1	1-2	2-3	3-4	4-5	5-6	6-7	7-8	8-9	9-10
Tp [sec]											
3-4		0,14	0,03	0,00	0,00	0,00	0,00	0,00	0,00	0,00	0,00
4-5		67,67	123,95	0,00	0,00	0,00	0,00	0,00	0,00	0,00	0,00
5-6		1214,22	10246,97	485,53	0,00	0,00	0,00	0,00	0,00	0,00	0,00
6-7		3128,68	61776,33	41514,33	1365,64	0,00	0,00	0,00	0,00	0,00	0,00
7-8		3380,57	78337,66	189691,15	72325,98	1893,12	0,00	0,00	0,00	0,00	0,00
8-9		4113,82	75968,26	226185,28	**299997,99**	89476,12	3671,03	0,00	0,00	0,00	0,00
9-10		3226,52	71249,02	128175,53	254269,74	259876,01	78608,70	4462,92	0,00	0,00	0,00
10-11		1868,09	51229,87	105226,70	113941,86	173181,09	157499,71	66028,89	4902,76	0,00	0,00
11-12		1021,15	29651,97	78946,70	68068,53	60864,58	75920,38	62966,71	28918,06	2210,45	0,00
12-13		435,30	15438,47	36567,22	41484,66	27042,22	28790,81	26112,82	22671,44	11680,02	4667,55
13-14		102,34	6509,70	13789,54	19463,19	11520,77	11123,56	12604,85	10095,10	4398,69	1202,14
14-15		8,07	2062,14	5002,06	5455,47	5358,66	4685,80	2454,24	2541,37	465,03	564,75
15-16		1,49	631,71	2090,78	512,24	967,73	361,41	0,00	0,00	0,00	0,00
16-17		1,38	223,65	759,32	541,19	335,48	0,00	0,00	0,00	0,00	0,00
17-18		0,00	0,00	159,60	688,19	0,00	0,00	0,00	0,00	0,00	0,00

Table 87. Final results achieved by using Simpson's code for angle of incident wave 150 degrees

Final Absorbed Power per year [kWh/year]											
	Hs [m]	0-1	1-2	2-3	3-4	4-5	5-6	6-7	7-8	8-9	9-10
Tp [sec]											
3-4		0,14	0,03	0,00	0,00	0,00	0,00	0,00	0,00	0,00	0,00
4-5		69,13	126,08	0,00	0,00	0,00	0,00	0,00	0,00	0,00	0,00
5-6		1237,71	10458,40	495,94	0,00	0,00	0,00	0,00	0,00	0,00	0,00
6-7		3147,02	62138,40	42143,89	1395,25	0,00	0,00	0,00	0,00	0,00	0,00
7-8		3379,61	78315,24	189277,05	71893,07	1881,68	0,00	0,00	0,00	0,00	0,00
8-9		4106,72	75837,05	225794,62	**299241,36**	89572,67	3697,30	0,00	0,00	0,00	0,00
9-10		3220,50	71116,17	127936,53	253795,63	260681,23	79382,19	4537,27	0,00	0,00	0,00
10-11		1865,13	51148,52	105059,61	113760,92	172855,46	156312,09	64986,96	4781,15	0,00	0,00
11-12		1019,96	29617,36	78854,54	67989,07	60793,53	75901,78	63360,43	29353,33	2265,65	0,00
12-13		434,72	15417,82	36518,30	41429,16	27006,05	28752,29	26049,05	22484,35	11498,82	4558,20
13-14		102,21	6501,42	13772,00	19438,44	11506,11	11109,41	12588,82	10086,19	4404,22	1206,65
14-15		8,06	2061,33	5000,10	5453,34	5356,56	4683,97	2453,28	2540,38	465,02	567,53
15-16		1,49	631,92	2091,47	512,41	968,05	361,53	0,00	0,00	0,00	0,00
16-17		1,38	223,62	759,20	541,10	335,43	0,00	0,00	0,00	0,00	0,00
17-18		0,00	0,00	159,34	687,07	0,00	0,00	0,00	0,00	0,00	0,00

Table 88. Final results achieved by using trapezoidal integration for angle of incident wave 150 degrees

Final Absorbed Power per year [kWh/year]											
	Hs [m]	**0-1**	**1-2**	**2-3**	**3-4**	**4-5**	**5-6**	**6-7**	**7-8**	**8-9**	**9-10**
Tp [sec]											
3-4		0,13	0,03	0,00	0,00	0,00	0,00	0,00	0,00	0,00	0,00
4-5		43,21	93,01	0,00	0,00	0,00	0,00	0,00	0,00	0,00	0,00
5-6		1557,93	11681,03	426,29	0,00	0,00	0,00	0,00	0,00	0,00	0,00
6-7		4511,04	89071,14	62325,47	2049,83	0,00	0,00	0,00	0,00	0,00	0,00
7-8		4515,41	104634,98	261226,36	106777,52	2868,52	0,00	0,00	0,00	0,00	0,00
8-9		5049,66	93250,07	277639,54	**356015,23**	102292,42	4098,52	0,00	0,00	0,00	0,00
9-10		3724,94	82255,22	147975,46	293548,09	288808,24	84770,83	4711,85	0,00	0,00	0,00
10-11		2070,53	56781,48	116629,76	126289,35	191471,41	169997,44	69974,32	5123,76	0,00	0,00
11-12		1101,84	31994,90	85184,59	73446,90	65673,74	81688,10	66956,09	30460,37	2310,58	0,00
12-13		461,30	16360,49	38751,10	43962,22	28657,24	30510,26	27619,60	23811,43	12192,75	4847,07
13-14		107,11	6813,21	14432,47	20370,66	12057,92	11642,19	13192,55	10556,29	4581,28	1247,60
14-15		8,37	2139,33	5189,31	5659,70	5559,26	4861,21	2546,11	2636,50	482,33	584,34
15-16		1,54	651,13	2155,05	527,99	997,48	372,52	0,00	0,00	0,00	0,00
16-17		1,42	229,40	778,83	555,10	344,10	0,00	0,00	0,00	0,00	0,00
17-18		0,00	0,00	163,08	703,20	0,00	0,00	0,00	0,00	0,00	0,00

Table 89. Final results achieved by using Simpson's code for angle of incident wave 180 degrees

Final Absorbed Power per year [kWh/year]											
	Hs [m]	**0-1**	**1-2**	**2-3**	**3-4**	**4-5**	**5-6**	**6-7**	**7-8**	**8-9**	**9-10**
Tp [sec]											
3-4		0,13	0,03	0,00	0,00	0,00	0,00	0,00	0,00	0,00	0,00
4-5		41,92	88,60	0,00	0,00	0,00	0,00	0,00	0,00	0,00	0,00
5-6		1428,18	10772,25	399,16	0,00	0,00	0,00	0,00	0,00	0,00	0,00
6-7		4155,53	82051,54	57248,83	1891,41	0,00	0,00	0,00	0,00	0,00	0,00
7-8		4236,80	98178,83	244131,44	99124,83	2662,62	0,00	0,00	0,00	0,00	0,00
8-9		4816,79	88949,73	264835,86	**342157,61**	99528,56	4033,46	0,00	0,00	0,00	0,00
9-10		3596,00	79407,97	142853,32	283386,98	281914,43	83701,10	4699,62	0,00	0,00	0,00
10-11		2015,77	55279,84	113545,40	122949,53	186437,45	165346,89	67744,96	4929,13	0,00	0,00
11-12		1079,16	31336,44	83431,49	71935,35	64322,16	80121,54	66234,15	30443,68	2334,87	0,00
12-13		453,53	16084,89	38098,32	43221,66	28174,50	29996,31	27137,18	23301,30	11863,31	4684,76
13-14		105,61	6718,18	14231,16	20086,52	11889,73	11479,80	13008,53	10415,34	4534,11	1238,89
14-15		8,28	2115,84	5132,31	5597,53	5498,20	4807,82	2518,14	2607,55	477,23	581,33
15-16		1,53	645,50	2136,41	523,42	988,85	369,29	0,00	0,00	0,00	0,00
16-17		1,40	227,60	772,73	550,75	341,41	0,00	0,00	0,00	0,00	0,00
17-18		0,00	0,00	161,74	697,41	0,00	0,00	0,00	0,00	0,00	0,00

Table 90. Final results achieved by using trapezoidal integration for angle of incident wave 180 degrees

Furthermore, the sum of all the cells that corresponds to the total final power per year depending on the angle of incidence of Location 3, if we apply Simpson's code is:

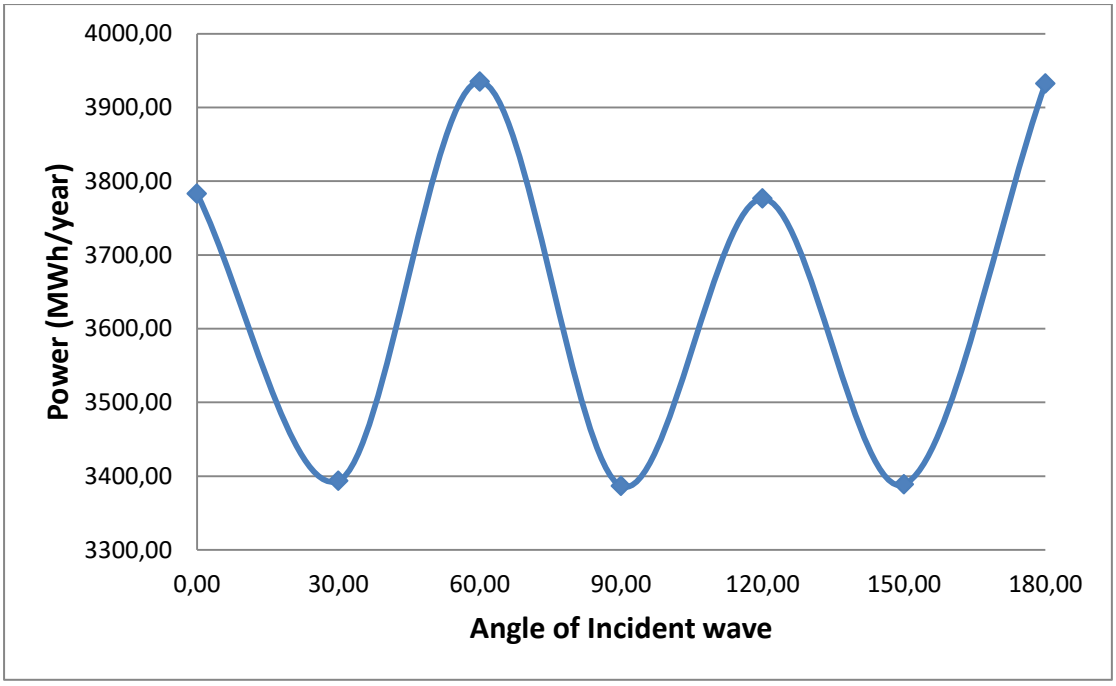

Figure 71. Total amount of Power per year for Location 3 depending on the angle of incidence achieved by using Simpson's code

Respectively, the sum of all the cells that corresponds to the total final power per year depending on the angle of incidence of Location 3, if we apply trapezoidal integration is:

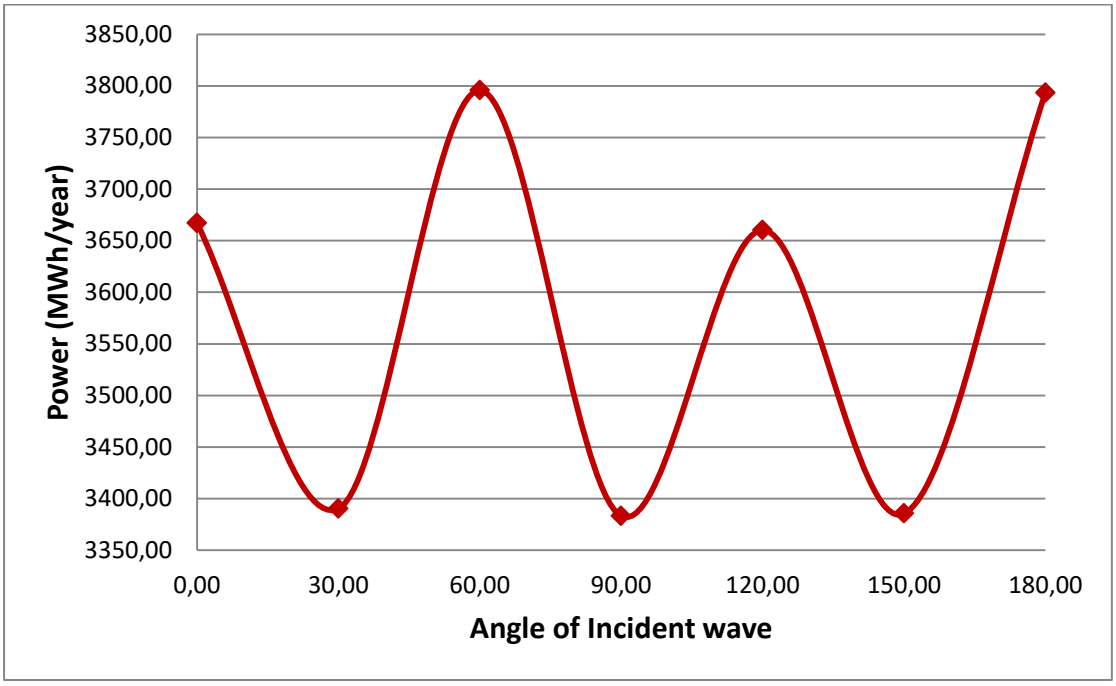

Figure 72. Total amount of Power per year for Location 3 depending on the angle of incidence achieved by using trapezoidal integration

Finally, if we compare the two integration methods, we have the following diagram:

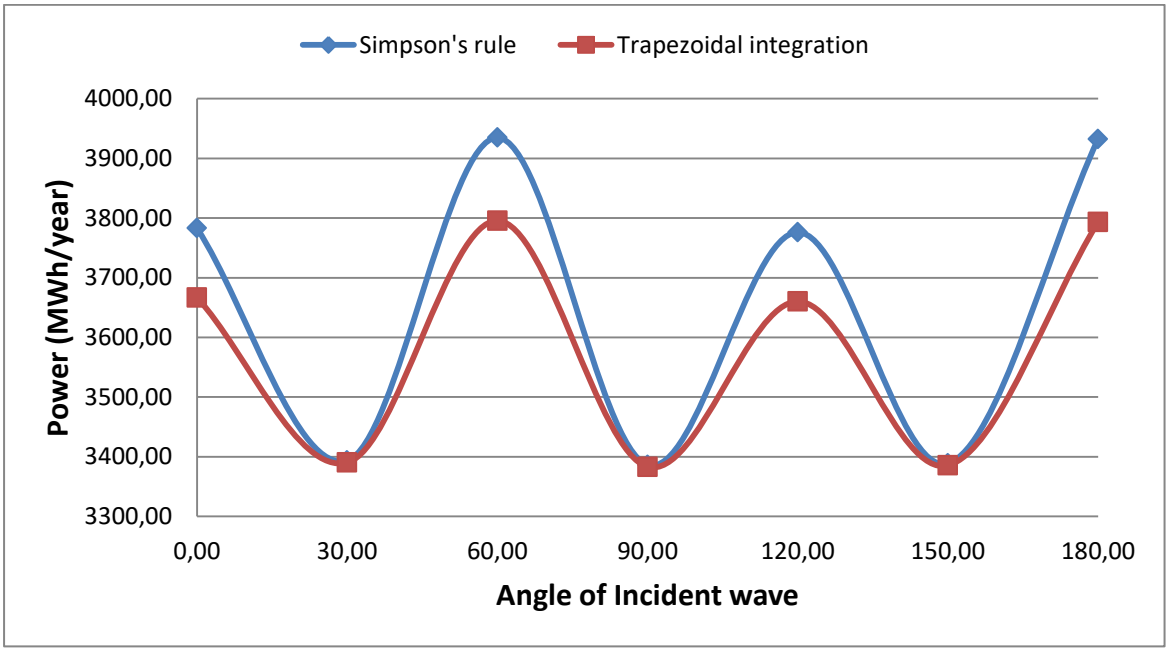

Figure 73. Comparison of two Integration methods

7.4 Integration Methods

For the Simpson's rule we used the following formula (Mpakopoulos et al., 1988):

$$\int_a^b f(x)dx = \frac{h}{3}\left[f(a) + 4f\left(\frac{a+b}{2}\right) + f(b)\right] \quad (37)$$

Where:

$h = (b-a)/2$

a,b : end points

The numerical approximation error of the above equation is:

$$-\frac{1}{90}\left(\frac{b-a}{2}\right)^5 f^{(4)}(\xi)$$

where ξ is some number between a and b

As far as the trapezoidal integration we have (Mpakopoulos et al., 1988):

$$\int_a^b f(x)dx = (b-a)\left[\frac{f(a)+f(b)}{2}\right] \quad (38)$$

With numerical approximation error:

$$-\frac{1}{12}\left(\frac{b-a}{2}\right)^3 f^{(2)}(\xi)$$

Where:

a,b : end points

ξ : some number between a and b

7.5 Matlab code

In order to calculate the spectrum for each sea state and the corresponding integration of the multiplication 2*S*Eabs, we created a code in Matlab. More specifically, the code computes for all the pairs H_S-T_P the corresponding JONSWAP spectrum. Furthermore, it loads all the needed data by HAMVAB and multiplies the absorbed power of the device (RAO) with the spectrum. The multiplication of these two values corresponds to a specific range of frequencies ω. This range begins from zero and finishes at 3 rad/s. Finally, the code calculates the integration either with Simpson's Rule or with the trapezoidal integration. This integration corresponds to the absorbed power that the device produces in a specific sea state. The whole procedure is repeated for angles of incident wave 0, 30, 60, 90, 120, 150 and 180 degrees.

7.6 Absorbed Power from the WT and the OWC devices for specific ranges of wind speeds

According the green line of Figure 62. we found the absorbed power of the WT and after that we calculated the annual MWh by multiplying with the number of frequency of occurrence, dividing with 31 that are the total years and multiplying with 3 because of the repeated three-hour measurements that we had during the day.

Wind Speed(Table 3)	2-4	4-6	6-8	8-10	10-12	12-14	14-16	16-18.62
Frequency of Occurrence(Table3)	17292	24182	24565	15133	6527	2175	621	89
Wind Power (Figure 62)	0,35	0,7	2,3	4,9	8,9	9,95	9,9	10
Final Absorbed Power from the WT in MWh/year	585,70	1638,14	5467,69	7175,97	5621,64	2094,31	594,96	86,13

Table 91. Calculation of absorbed power from the WT at Location 1

Hs(Table 3)	0,548	0,709	0,944	1,576	1,886	2,488	3,116	3,994
Tp(Table 3)	3,777	3,792	4,906	4,906	6,256	6,914	7,573	8,331
Wave Power(Matlab)	0,04	0,06	3,71	7,42	124,77	411,92	769,81	1233,89
Final Absorbed Power from the OWC Devices in MWh/year	0,06	0,14	8,82	10,87	78,81	86,70	46,26	10,63

Table 92. Calculation of absorbed power from the OWC devices at Location 1

Wind Speed(Table 3)	2-4	4-6	6-8	8-10	10-12	12-14	14-16	16-18	18-20,13
Frequency of Occurrence(Table3)	30024	22419	17505	11100	6040	2479	806	184	27
Wind Power (Figure 62)	0,35	0,70	2,30	4,90	8,90	9,95	9,90	10,00	10,05
Final Absorbed Power from the WT in MWh/year	1016,94	1518,71	3896,27	5263,55	5202,19	2387,04	772,20	178,06	26,26

Table 93. Calculation of absorbed power from the WT at Location 2

Hs(Table 3)	0,335	0,756	0,865	1,335	1,982	2,83	3,824	4,897	6,186
Tp(Table 3)	2,821	3,61	4,542	5,404	6,596	6,396	8,556	8,848	10,282
Wave Power(Matlab)	0,00	0,03	1,02	20,40	187,00	342,61	1077,31	1789,08	2314,51
Final Absorbed Power from the OWC Devices in MWh/year	0,00	0,07	1,74	21,91	109,30	82,19	84,03	31,86	6,05

Table 94. Calculation of absorbed power from the OWC devices at Location 2

Wind Speed(Table 5)	2-4	4-6	6-8	8-10	10-12	12-14	14-16	16-18	18-20	20-23,19
Frequency of Occurrence(Table 5)	14199	16965	18597	16083	12134	7256	3691	1304	305	50
Wind Power (Figure 62)	0,35	0,7	2,3	4,9	8,9	9,95	9,9	10	10,05	10,1
Final Absorbed Power from the WT in MWh/year	480,93	1149,24	4139,33	7626,45	10450,90	6986,83	3536,22	1261,94	296,64	48,87

Table 95. Calculation of absorbed power from the WT at Location 3

Hs(Table 5)	1,43	0,98	1,80	2,16	2,47	2,88	3,49	5,10	6,35	7,25
Tp(Table 5)	5,81	5,68	5,58	5,55	7,13	7,74	8,30	9,70	10,44	11,10
Wave Power(Matlab)	41,72	17,30	45,02	57,71	382,44	619,83	1020,50	2423,57	3795,39	4637,66
Final Absorbed Power from the OWC Devices in MWh/year	57,33	28,40	81,02	89,83	449,09	435,24	364,52	305,84	112,03	22,44

Table 96. Calculation of absorbed power from the OWC devices at Location 3

Following, one can find the figures with the comparisons of the two different absorbed powers:

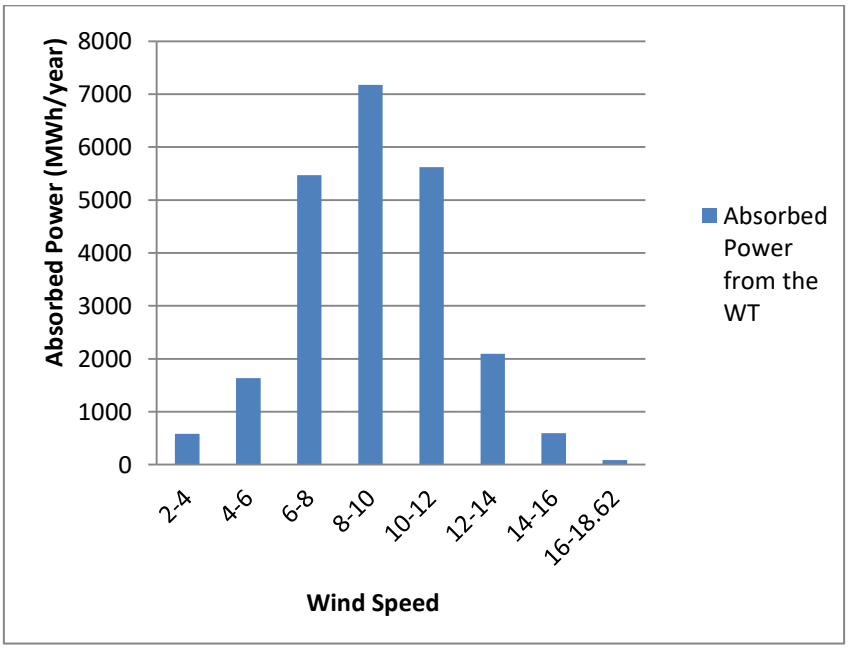

Figure 74. Absorbed Power from the WT at Location 1

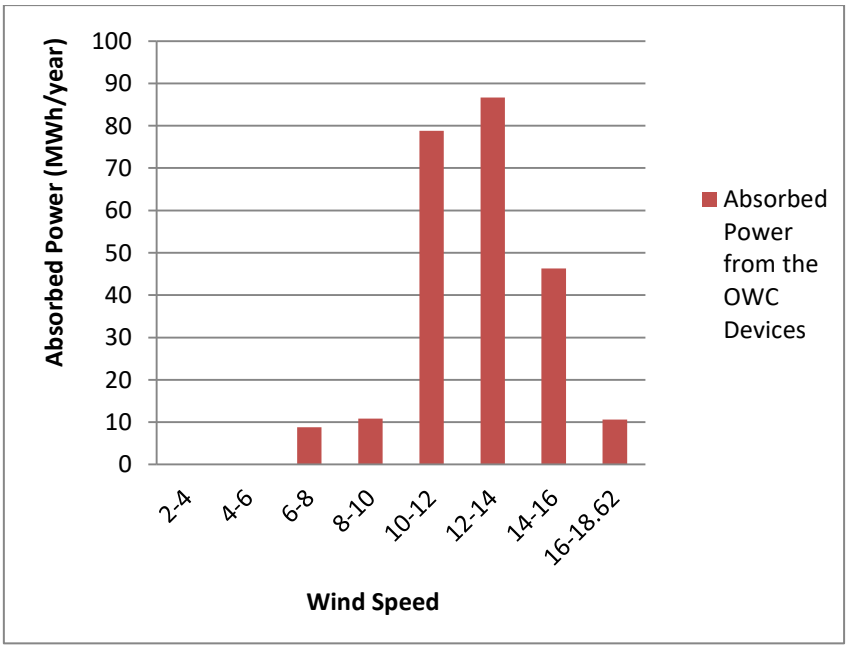

Figure 75. Absorbed Power from the OWC Devices at Location 1

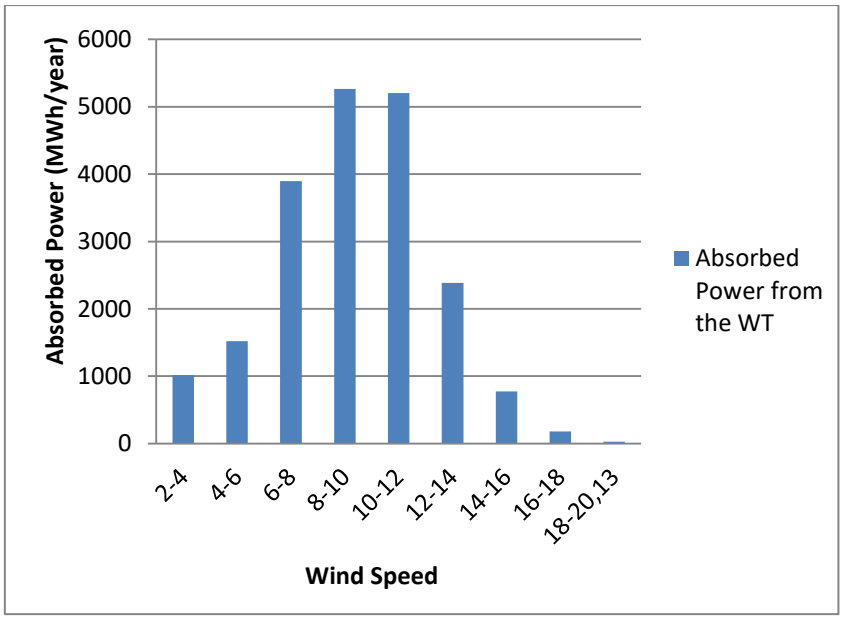

Figure 76. Absorbed Power from the WT at Location 2

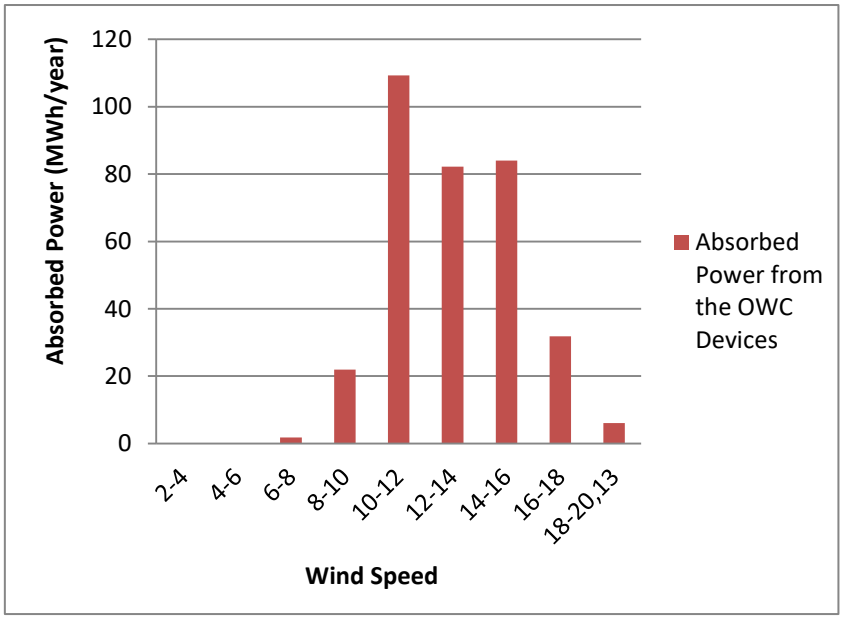

Figure 77. Absorbed Power from the OWC Devices at Location 2

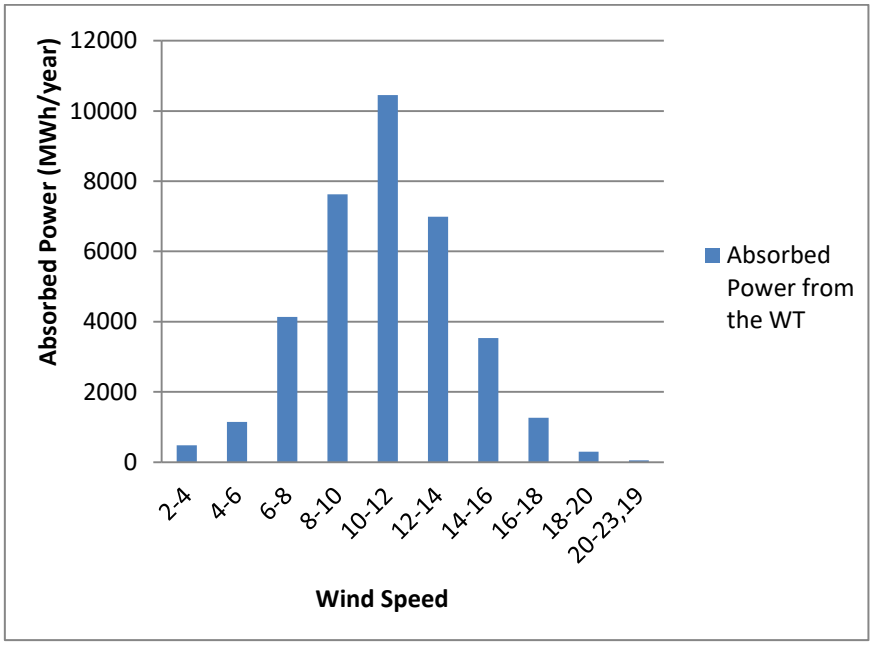

Figure 78. Absorbed Power from the WT at Location 3

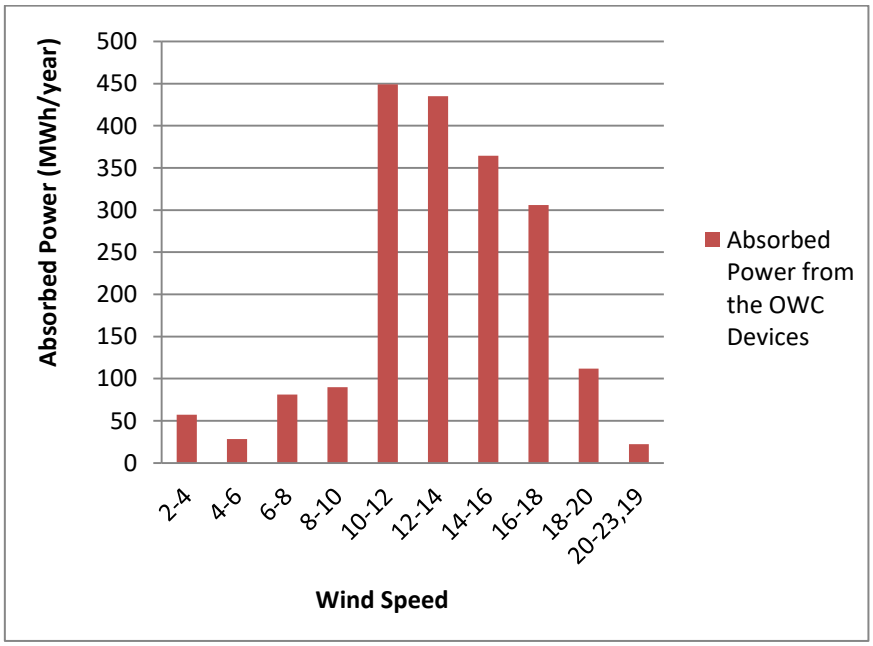

Figure 79. Absorbed Power from the OWC Devices at Location 3

8.Conclusions

A validation of the program HAMVAB was made. As we can see from the Fig. 39-48 the experimental results follow the curve of the HAMVAB results at most of the cases. However, at the first order line tension for Line No. 1 and at the pressure in chamber No. 1 there is a dispersion between the numerical and the experimental prices.

Moreover, a second check was made concerning the angles of incident wave. More specifically, we examined the exciting forces and moments of a the configuration in x, y and z-axis for 0, 30, 60, 90, 120, 150 and 180 degrees. Following the Fig. 49-54, we notice that for the exciting forces Fx and Fy there is similarity at the following pairs of angles: 0 and 180 degrees, 30 and 150 degrees, 60 and 120 degrees. The exciting force Fz is similar for all the angles and it is very close to zero for high values of frequency ω. As far as the exciting moments are concerned, we can see that Mx and My have similarities for the same pairs of angles as the exciting forces Fx and Fy. The exciting moment Mz is similar for all the examined angles apart from the 30, 90 and 150 degrees.

After that check, we made one more, related to the different speeds of the wind that the WT is exposed to. The conclusion from that check (Fig. 60) was that the absorbed wave powers of the configuration are equal irrespective of the different wind speeds, and the divergence is minimal.

Regarding the absorbed wave power of the investigated in the framework of the present Diploma Thesis floating energy platform in several real sea states, we examined 3 different locations and we calculated the final absorbed wave power per year at each of these locations. Firstly, we received the frequency of occurrence of Hs - Tp of the three locations as a data of forecasting calculations that lasted 31 years. A first notice is that the most frequently occurred sea state is characterized by the pair Hs= 0-1 m and Tp=4-5 s in location 1 and 2 and by the pair Hs= 1-2 m and Tp=6-7 s in location 3. Although, the highest absorbed wave power for Location 1 and 2 appears for the pair Hs= 2-3 m and Tp=7-8 sec and for Location 3 for the pair Hs= 3-4 m and Tp=8-9 sec. For the production of the Spectrum, we used the JONSWAP Spectrum, noticing that when the γ factor equals to 1, the JONSWAP Spectrum gives the same results with the Bretschneider Spectrum. Furthermore, as far as the results of the final annual absorbed wave power are concerned, they differ between the Simpson's Rule and the trapezoidal integration as well as among the different angles of incident wave. More specifically, according to the Fig. 65-73 we can see that the maximum annual absorbed wave power in all the locations appears when the angle of incident wave is 60 or 180 degrees; second highest absorbed power occurs for the angle 0 and 120 degrees and finally, the lowest absorbed power is for 30, 90 and 150 degrees. In addition, we notice that in all the locations, the Simpson's Rule gives higher absorbed power than the trapezoidal integration, especially for the angles 0, 60,

120 and 180 degrees. We consider the results from Simpson's rule more accurate as far as this method is more detailed and takes under consideration more points in the curve of the S*Eabs as a function of the wave frequency. This difference between the two integration methods is 8.6 % higher in 0, 60, 120 and 180 degrees for Simpson's Rule for Location 1, 7.75% for Location 2 and 3.4 % for Location 3. The last conclusion, refers to the location where a multi-purpose device, like the one we study, is more efficient and can produce more power. This location is the North Sea (Location 3), reaching the amount of 3934.73 MWh per year for angle of incident wave 60 degrees. The above conclusion can be explained logically, if we consider that the North Sea has more intensive weather conditions.

Furthermore, regarding the brief study for the absorbed power from the WT and the corresponding absorbed wave power for the same ranges of wind speeds, we notice that the first contributes almost 96% at the total absorbed power. This result maximize the importance of WT and its efficiency at the examined device.

To sum up, we remind the need of renewable energy sources nowadays and a device like the multi-purpose platform that we studied could definitely work efficiently and be part of the solution for the high demand of energy of the whole planet. The research and study concerning the design and optimization of devices and configurations like this continually increases. The present thesis helped in the calculation of the accurate absorbed power that a multi-purpose device can produce annually in these three locations in Europe and further research could take place about the fatigue problems and the cost analysis of a project like that in these specific locations.

9. Bibliography

9.1 Hardcopy Sources

1. Abdul Khalique Talpur, 2016, Types of Wave Energy Devices, BE – Mechatronics, Szabist, Karachi
2. Babarit A., Hals J., 2011, On the maximum and actual capture width ratio of wave energy converters, 9th EWTEC, Southampton.
3. Bachynski E.E., Moan T., 2012, Design considerations for tension leg platform wind turbines, J. Mar. Struct. 29, 89-114.
4. Cruz Joao, 2010, Estimating the Loads and Energy Yield of Arrays of Wave Energy Converters under Realistic Seas, Research Paper.
5. DNV, 2007, Enviromental Conditions and Enviromental Loads, Recommended Practice DNV-RP-C205.
6. DNV, 2011, Structural Design of Offshore Units(WSD Method), DNV-OS-C201.
7. Drew B., Plummer A. R., Sahinkaya M.N., A review of wave energy converter technology, 2009, Proceedings of the Institution of Mechanical Engineers, Part A: Journal of Power and Energy 2009 223: 887
8. Evans D.V., Porter R., 1996, Efficient calculation of hydrodynamic properties of OWC type devices, OMAE, Volume I , Part B, 123-132.
9. Falcão A., 2005, Frequency domain, time domain and stochastic modeling of wave energy converters,CA-OE Workshop 1, Aalborg, Denmark, 5 - 6 April.
10. Falnes J., 2002, Ocean waves and oscillating systems: linear interactions including wave-energy extraction; Cambridge University Press.
11. Heath T. V., 2012, A review of oscillating water columns Philosophical Transactions of The Royal Society A (2012) 370, 235-245.

12. Hervé Martins-Rivas, Chiang C. Mei, 2009, Wave power extraction from an oscillating water column along a straight coast.

13. Konispoliatis D.N, 2014, Hydrodynamic Analysis of Floating Oscillating Water Column devices for Wave Energy Absorption, PhD Thesis, National Technical University of Athens, School of Naval Architecture and Marine Engineering.

14. Konispoliatis, D.N, Mavrakos, S.A, 2014, Mean Drift Loads on arrays of free floating OWC Devices consisting of concentric cylinders, Proceedings, 29th IWWWFB, Osaka, Japan, March 30 – April 02.

15. Konispoliatis D.N, Mavrakos S.A., 2015, Hydrodynamic analysis of an array of interacting free-floating oscillating water column (OWC's) devices, Ocean Engineering Volume 111, 1 January 2016, 179-197.

16. Konispoliatis D.N, Mazarakos T.P., Mavrakos S.A., 2016, Hydrodynamic analysis of three-unit arrays of floating annular oscillating-water-column wave energy converters, Applied Ocean Research 61, 42 - 64.

17. Konispoliatis D.N, Mavrakos S.A., 2013, Hydrodynamics of arrays of OWC's devices consisting of concentric cylinders restrained in waves, Proceedings, 10th European Wave and Tidal Energy Conference (EWTEC 2013), International Conference Ocean, Aalborg, Denmark.

18. Manolas D., Riziotis V., Voutsinas S.. 2012, Assessment of 3D aerodynamic effects on the behaviour of floating wind turbines, The science of making torque from Wind, TORQUE 2012, Oldenbourg, Germany.

19. Mavrakos S.A, PROGRAM : H.A.M.V.A.B. A description of the Program and its Use, 1996, School of Naval Architecture and Marine Engineering, Division

of Marine Structures, Laboratory for Floating Structures and Mooring Systems.

20. Mavrakos S.A., Koumoutsakos P., 1987, Hydrodynamic interaction among vertical axisymmetric bodies restrained in waves, Applied Ocean Research, Vol. 9, No. 3.
21. Mavrakos S.A., 1991, Hydrodynamic coefficients for groups of interacting vertical axisymmetric bodies, Ocean Engineering, Vol. 18, No. 5, 485-515.
22. Mavrakos S.A., 1999, "Design and Construction of Ships and Offshore Structures", University Publications of the National Technical University of Athens.
23. Mavrakos S.A., 1999, "Mooring of Offshore Structures", University Publications of the National Technical University of Athens.
24. Mavrakos S. A., 2018, Life-Cycle Assessment of a Renewable Energy Multi-Purpose Floating Offshore System, project supported by the European Union, Research Fund for Cool & Steel(RFCS), Mid-Team Report
25. Mazarakos T.P., Konispoliatis D.N., Mavrakos S.A., Manolas D., Voutsinas S., 2015, Coupled Hydro - Aero - Elastic Analysis of a Multi – Purpose Floating Structure for Offshore Wind and Wave Energy Sources Exploitation, 13th International Conference on the Stability of Ships and Ocean Vehicles, 14 – 19 June 2015, Glasgow, UK.
26. Mazarakos T.P., 2016, Ship design and scientific platforms, Part I - Ships, 7th FerryBox Workshop, 7 - 8 April, Heraklion - Crete, Greece.
27. Mazarakos T.P., Konispoliatis D.N., Mavrakos S.A, 2016, Parametric hydrodynamic analysis of a moored floating structure for combined wind and

wave energy exploitation, 12th International Conference on Hydrodynamics (ICHD 2016).

28. Mazarakos T.P., Konispoliatis D.N., Manolas D., Voutsinas S., Mavrakos S.A., 2015, Modelling of an Offshore Multi - Purpose Floating Structure Supporting a Wind Turbine Including Second - Order Wave Loads, 11th European Wave and Tidal Energy Conference Series (11th EWTEC), France.
29. Mazarakos T.P., Konispoliatis D.N., Katsaounis, S. Polyzos, D. Manolas, S. Voutsinas and S.A. Mavrakos, 2017, Numerical and experimental studies of an offshore multi - purpose floating structure supporting a wind turbine, 11th European Wave and Tidal Energy Conference Series (12th EWTEC), 27 August - 2 September, Cork, Ireland.
30. Mpakopoulos A., Chrysovergis I., 1988, Intoduction to Numerical Analysis.
31. National Commission on the BP Deepwater Horizon Oil Spill and Offshore Drilling, 2010, A Brief History of Offshore Oil Drilling Staff, Working Paper No. 11.
32. Newman J.N. 1977, The motions of a floating slender torus; J. Fluid Mech, Vol. 83, pp. 721-735.
33. Okhusu M., 1974, Hydrodynamic forceson multiple cylinders in waves, Int. Symp. on the Dynamics of Marine Vehicles and structures in Waves, University College London, London.
34. Papadakis G., Riziotis V., Voutsinas S., Mavrakos S.A. 2014, WT's reduced order aeroelastic models (in Greek). Technical Report No. D3.2, Program POSEIDON (2014), Greek General Secretariat for Research and Technology.
35. Parker N.W., 2007, Extended Tension Leg Platform Design for Offshore Wind Turbine Systems, Massachusetts Institute of Technology.

36. Project POSEIDON: “Multi- purpose floating structures for offshore wind and wave energy sources exploitation” (Oct. 2012 – Sep. 2015), Supported by the Greek Secretarial for Research and Technology, http://aristeia-poseidon.naval.ntua.gr/
37. REFOS: “Life – Cycle Assessment of a Renewable Energy Multi – Purpose Floating Offshore System”, Funded by the EC, Research Fund for Coal and Steel, Grant Agreement No 709256 – REFOS - RFSR – 2015.
38. Riziotis V.A., Voutsinas S.G., 1997, GAST: A general aerodynamic and structural prediction tool for wind turbines. Procerdings of the EWEC’ 97, Dublín, Ireland.
39. Riziotis V.A., Voutsinas S.G., Politis E.S., Chaviaropoulos P.K., 2004, Aeroelastic Stability of Wind Turbines: the problem, the methods, the issues, Wind Energy, 7, 373-392.
40. Sarmento, A.J.N.A., Falcao, A.F. de O., 1985, Wave generation by an oscillating surface-pressure and its application in wave-energy extraction. J. Fluid Mech. 150, 467-485.
41. Senjanovic I., Hadzic N., Tomic M., 2011, On the linear stiffness of tension leg platforms, Sustainable Mar. Trans. Exp. Sea Res. 108 ,1081-1088.
42. Twersky V., 1952, Multiple scattering of radiation by an arbitrary configuration of parallel cylinders, J. Acoustical Soc. of America.
43. Vijfhuizen W., 2006 Design of wind and wave power barge, Master Thesis
44. Vlachou C., 2013, Experimental and numerical investigation of the loads at triangular floating platform supporting a wind turbine, Diploma Thesis.
45. Wang H.f. , Fam Y-h., 2013, Preliminary design of offshore turbine tension leg platform in the South China sea, J. Eng. Sci. Technol. Rev. 6 (3), 88-92.

9.2 Internet Sources

1. http://www.gatesheadmill.co.uk/path_head_water_mill.html (Accessed 26/9/2017)
2. http://ec.europa.eu/eurostat/statistics-explained/index.php/Renewable_energy_statistics (Accessed 2/6/2017)
3. https://urvishdave.wordpress.com/2013/03/21/charanka-solar-park-overview-pv-modules-inverter-technology-details-of-gujarat-solar-park-projects/ (Accessed 9/1/2018)
4. http://www.altenergy.org/renewables/renewables.html (Accessed 26/9/2017)
5. https://www.dlubal.com/en/solutions/industries/other/offshore-structural-analysis-software (Accessed 10/2/2018)
6. https://www.energyindustryonline.com/single-post/2017/01/23/BW-Offshore-have-Interim-extension-agreement-for-FPSO-Abo (Accessed 26/9/2017)
7. http://www.strukts.com/2012/05/types-of-offshore-platforms_70.html (Accessed 26/9/2017)
8. http://lshipdesign.blogspot.de/2015/09/types-of-offshore-structures.html (Accessed 9/1/2018)
9. https://aoghs.org/offshore-history/offshore-oil-history/ (Accessed 10/2/2018)
10. https://www.nov.com/Segments/Rig_Systems/Offshore/Offshore_Units/Fixed_Platforms/Fixed_Platforms.aspx (Accessed 9/1/2018)
11. http://www.marinetalk.com/articles-marine-companies/art/Spar-Alliance-Dissolved--AKE00414923IN.html (Accessed 26/9/2017)
12. http://northcoastcourier.co.za/32937/mystery-ship-keeps-residents-guessing/ (Accessed 26/9/2017)
13. http://www.writeopinions.com/compliant-tower (Accessed 26/9/2017)
14. http://www.maersk.com/en/hardware/xle-rigs (Accessed 26/9/2017)
15. http://www.drillingformulas.com/floating-offshore-structures-offshore-structure-series/ (Accessed 10/2/2018)
16. https://energy.gov/eere/water/marine-and-hydrokinetic-technology-glossary (Accessed 10/2/2018)
17. http://www.esru.strath.ac.uk/EandE/Web_sites/01-02/RE_info/wavecase.htm (Accessed 26/9/2017)
18. https://www.google.gr/maps/ (Accessed 26/9/2017)
19. https://www.openei.org/ (Accessed 26/9/2017)
20. https://www.researchgate.net/ (Accessed 26/9/2017)
21. https://tethys.pnnl.gov/ (Accessed 26/9/2017)

22. http://www.alternativeconsumer.com/2013/08/22/oceanlinx-wave-power-turbines-wave-energy-from-down-under/ (Accessed 26/9/2017)
23. https://rules.dnvgl.com/ (Accessed 26/9/2017)
24. http://www.wikiwaves.org/Ocean-Wave_Spectra (Accessed 26/9/2017)
25. https://www.mathworks.com/ (Accessed 26/9/2017)
26. http://www.codecogs.com/library/engineering/fluid_mechanics/waves/spectra/jonswap.php (Accessed 26/9/2017)
27. https://en.wikipedia.org/wiki/Wind_power_in_China (Accessed 26/9/2017)
28. http://www.beachapedia.org/Renewable_Ocean_Energy (Accessed 9/1/2018)
29. https://drprem.com/guide/aquamarine-s-oyster-wave-energy-converter-comes-into-action/ (Accessed 23/5/2018)
30. http://www.alternative-energy-tutorials.com/wave-energy/wave-energy-devices.html (Accessed 8/10/2017)
31. http://coastalenergyandenvironment.web.unc.edu/ocean-energy-generating-technologies/wave-energy/the-pelamis-wave-energy-converter/ (Accessed 8/10/2017)
32. http://www.awsocean.com/technology.html (Accessed 8/10/2017)
33. https://www.emaze.com/@AORWCZCRW/Wall-Street- (Accessed 8/12/2017)
34. https://www3.epa.gov/climatechange//kids/solutions/technologies/geothermal.html (Accessed 8/12/2017)
35. https://www.woodharbinger.com/tidal-energy-sustainable-resource/ (Accessed 8/12/2017)
36. http://cmheavyindustries.com/wave-energy (Accessed 8/12/2017)
37. http://takvera.blogspot.gr/2015/07/harnessing-ocean-temperature.html (Accessed 8/12/2017)
38. https://www.britannica.com/technology/energy-conversion (Accessed 10/2/2018)

39. https://stoprust.com/technical-library-items/02-corrosion-control/ (Accessed 14/3/2018)
40. https://www.offshore-mag.com/articles/print/volume-62/issue-11/news/general-interest/gom-yards-deal-with-competitors-tight-budgets.html (Accessed 14/3/2018)
41. http://aristeia-poseidon.naval.ntua.gr/(Accessed 23/5/2018)
42. www.refos-project.eu(Accessed 23/5/2018)

10. Appendix

Input file RE031 for ω from 0.05 rad/s until 1.5 rad/s for OWC with 10MW WT:

HYDRODYNAMIC ANALYSIS. ARISTEIA FLOATING W/T.

.TRUE. .TRUE. .TRUE. .TRUE. .TRUE.

200.0 4 30 7 00.000

3

1 1 1 1 1

1 1 1 1 1

1 1 1 1 1

1 1 1 1 1

15.50 15.50 15.50 6.000

14.00 14.00 14.00 0.000

7.000 7.000 7.000 0.000

-28.87 14.43 14.43 0.000

0.000 -25.00 25.00 0.000

0.000

7 39 7 1 1 3 0

015.50

0.050 0.100 0.150 0.200 0.250 0.300 0.350 0.400 0.450 0.500

0.550 0.600 0.650 0.700 0.750 0.800 0.850 0.900 0.950 1.000

1.050 1.100 1.150 1.200 1.250 1.300 1.350 1.400 1.450 1.500

2 1 1 1 2

0.0 0.0 -3.180 9.5501E3 6.385E6 6.385E6 1.170E7

1 -28.87 0.00 -20.00

104 104 173533 0 0 0

0 0 18838

2 14.43 25.00 -20.00

104 104 173533 0 0 0

0 0 18838

3 14.43 -25.00 -20.00

104 104 173533 0 0 0

0 0 18838

15.50 15.50 15.50 6.000

1

GEOMETRIC CHARACTERISTICS OF THE INDIVIDUAL BODY

15.50

.FALSE..TRUE. .TRUE. .false..TRUE.

2 0

1 0

180.0 200.0 192.0

79 39 79

7.000 14.00 15.50

200.0 -2.891 325961. 1967.

2

0.0

343.848

2

3

2

0

1

GEOMETRIC CHARACTERISTICS OF THE CYLINDER SUPPORTING THE W/

6.000

.FALSE..TRUE. .TRUE. .FALSE..TRUE.

0 0

180.0

79

6.000

200.0 -5.000 41732. 1118.

0

1

1

0.00 0.00 0.00 0.00 110080.00 0.00 13.37 0.00 0.00 -34.48
1569.90 -17.62 0.00 0.00 0.00 0.00 -0.01 0.01

0.00 0.00 0.00 -110080.00 0.00 -439.37 0.14 2.50 -0.03 -
292.68 -2696.60 -18.30 0.00 0.00 0.00 0.02 -0.29 -11.88

0.00 0.00 0.00 0.00 439.37 0.00 0.15 -0.03 2.48 9.53 35.31 -
2710.90 0.00 0.00 0.00 -0.01 11.64 0.29

0.00 -110080.00 0.00 10397000.00 0.00 56517.00 5407.50 -
292.72 9.51 68330.00 959020.00 2475.80 0.00 0.00 0.00 -
1042600.00 89.05 1378.80

110080.00 0.00 439.37 0.00 10337000.00 0.00 1568.90 16.97
17.29 -6081.10 200850.00 60737.00 0.00 0.00 0.00
0.00 -1042600.00 -27.35

0.00 -439.37 0.00 56517.00 0.00 97578.00 -13.77 -17.67
17.53 2048.60 -64646.00 16212.00 0.00 0.00 0.00 -
4308.80 35.57 -3.59